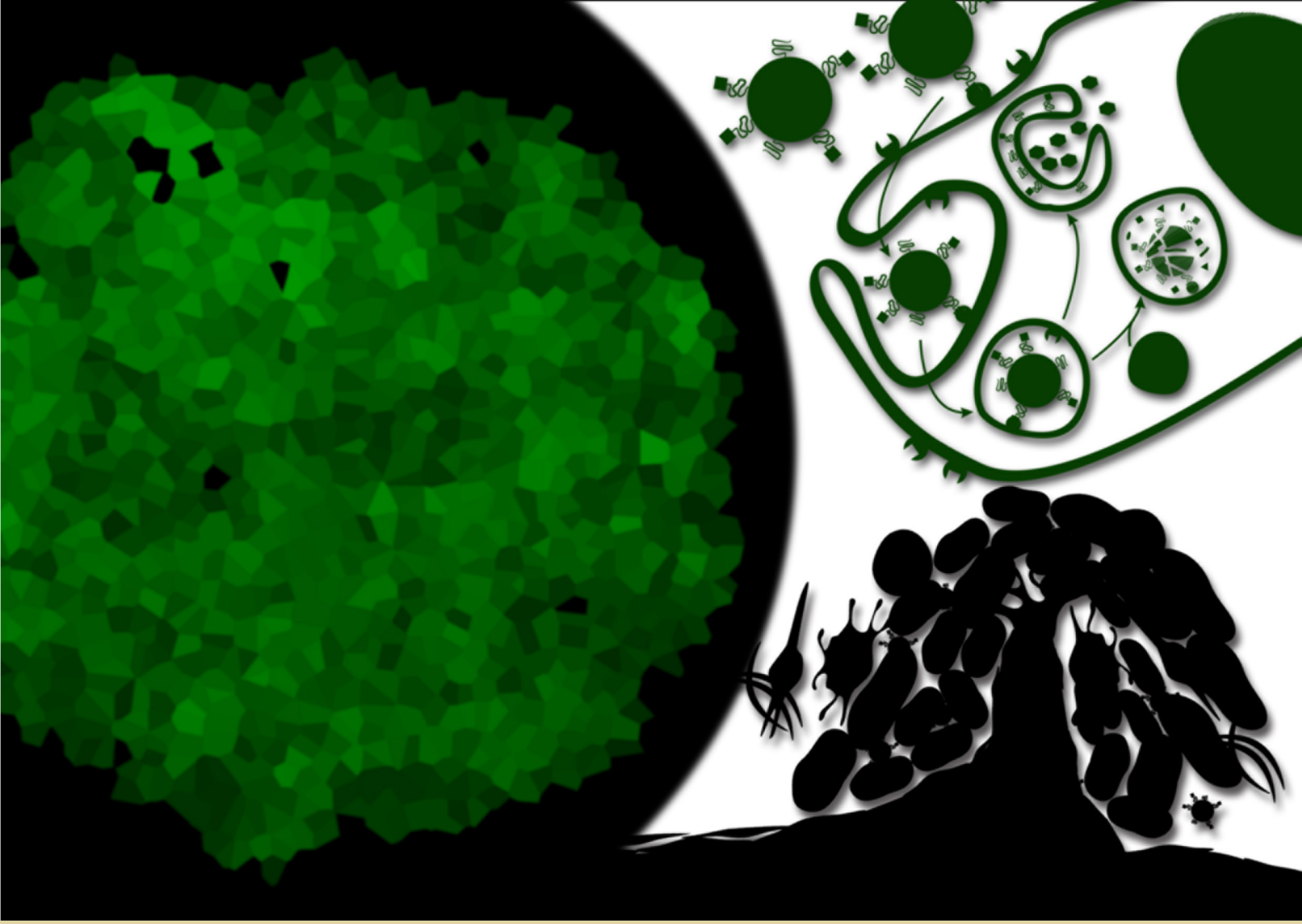

Nuno André Carvalho da Fonseca

Targeted intracellular delivery of synergistic drug combinations: tackling drug resistance in human breast cancer

Tese de Doutoramento em Ciências Farmacêuticas, área de especialização de Tecnologia Farmacêutica,
orientada pelos Professor Doutor João Nuno Moreira e Professor Doutor Sérgio Paulo de Magalhães Simões
e apresentada à Faculdade de Farmácia da Universidade de Coimbra.

Setembro de 2014

· U C ·

Universidade de Coimbra

Targeted intracellular delivery of synergistic drug combinations: tackling drug resistance in human breast cancer

Thesis submitted to the Faculty of Pharmacy of the University of Coimbra to apply for the degree of Doctor of Philosophy in the area of Pharmaceutical Sciences, specialization in Pharmaceutical Technology.

Nuno André Carvalho da Fonseca
2014

Universidade de Coimbra

The work described in this thesis was conducted at the Center for Neuroscience and Cell Biology (CNC) from the University of Coimbra, under the scientific supervision of Professor João Nuno Moreira and Professor Sérgio Simões.

Nuno André Carvalho da Fonseca was a student of the Pharmaceutical Sciences PhD program from the Faculty of Pharmacy, University of Coimbra and a recipient of the fellowship SFRH/BD/64243/2009 from the Portuguese Foundation for Science and Technology (FCT). The work was supported by the grants InovC/UC (2013), QREN/FEDER/COMPETE (Ref. 30248/IN0617) and PEst-C/SAU/LA0001/2011.

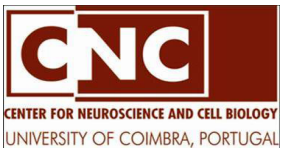

UNIÃO EUROPEIA
Fundo Europeu
de Desenvolvimento Regional

"We each exist for but a short time, and in that time explore but a small part of the whole universe. But humans are a curious species. We wonder, we seek answers. Living in this vast world that is by turn kind and cruel, and gazing at the immense heavens above, people have always asked a multitude of questions. How can we understand the world in which we find ourselves?"

Stephen Hawking, *"The grand design"*

To my family and friends

Acknowledgments

At the end of this journey, it is paramount to acknowledge those who made part of the work leading to this thesis.

To Professor João Nuno Moreira, my supervisor and Principal Investigator in this project, I would like to express my deepest gratitude for the mentorship and guidance, and for the incentive, opportunity, and for the extraordinary feeling of scientific freedom that ultimately enabled me to push forward beyond the scope of the original plans. This was only possible by the friendship and trust that he has laid on me, and for that I am truly grateful. To my co-supervisor Professor Sérgio Simões, I express my sincere gratefulness for the kindness and enthusiasm as well as the critical and insightful comments about the work.

To the Director of the Faculty of Pharmacy of the University of Coimbra, and to the President of the Center for Neuroscience and Cell Biology (CNC), Professor Catarina Resende de Oliveira, I manifest my gratitude for the welcoming in the respective institutions and for the conditions offered to develop this work, thanking also those who work in the mentioned institutions.

My thankfulness to the chair of the department of Vectors and Gene Therapy at the Center for Neuroscience and Cell Biology, Professor Maria Conceição Pedroso de Lima for having accepted me in the group to develop this work.

My genuine thanks to all the colleagues and friends working at the Vectors and Gene Therapy department, with a special and deepest gratitude to Lígia Silva, Vera Moura, Carla Gomes, Ana Gregório, Ângela Fernandes, Vanessa Monteiro, Ana Cruz, Susana Cecílio, Rui Lopes and Isabel Onofre for the support and scientific brainstorming, but above all for the companionship and friendship demonstrated along the journey. Without those, this work would not be possible.

I acknowledge Ana Sofia Rodrigues and Professor João Ramalho-Santos from the Biology of Reproduction and Stem Cell Group at CNC and Dr. Paulo Santos, Dr. Vera Alves and Professor Manuel Santos Rosa from the Immunology Institute of Faculty of Medicine, University of Coimbra for the extensive collaboration and cooperation in the cancer stem cell and embryonic stem cell studies.

I also thank all those working in the animal facilities at CNC/Faculty of Medicine for their support, help and guidance.

A special thanks to my friends for the support! They were (and still are...) also responsible for maintaining me in the right path.

However, my greatest and deepest gratitude is directed to my parents, Laurindo and Lúcia, to my sister Ana and all my family, for their love, patience, support, tenderness, care and comprehension throughout my life! They shaped myself as I am and led me to where I am today! For that I am truly grateful. Words will never be sufficient to describe you…

Finally, to you, Joana… We met early in the beginning of this journey and for some heavenly reason, fate decided to join us only in later times… Either way, to have met you, to receive your love and passion and attention is truly blessing. This meaningful journey culminates here, but for us, I suspect this is only the beginning…

Table of Contents

Thesis Abstract

Breast cancer remains a major public health care burden, with tremendous impact on society. Therapeutic intervention is often undermined by the intrinsic heterotypic nature of tumors, in which a multitude of cell types intertwine to foster new biological features that support tumor development. Among them, resistance to cornerstone chemotherapies remains pivotal. It has been postulated that cancer stem cells (CSC), a sub-population of stem-like cancer cells exhibiting self-renewal capability and high tumorigenic capacity, have a central role in tumor development, metastization, recurrence as well as drug resistance. In addition, the recent acknowledgement that CSC can originate from non-stem cancer cells (non-SCC) highlighted the need to develop strategies targeting both cell sub-populations.

It has been recognized that success requires the identification of compounds that, when combined, lead to synergistic tumor inhibition. However, *in vivo* application of such protocols is dependent on the ability to deliver the appropriate drug ratio at the tumor level. In this respect, nanotechnology-based delivery platforms, like liposomes, offer an elegant solution for the *in vivo* translation of such strategy. Modifying drugs' pharmacokinetics by the co-encapsulation into liposomes enables one to achieve the synchronous temporal and spatial delivery of a drug combination at tumor site. Additionally, the coating of nanoparticles with ligands targeting specific overexpressed receptors would enable the precise delivery of drug combinations into particular cellular sub-populations, such as the CSC, ultimately enabling a gain in terms of efficacy while simultaneously decreasing systemic toxicity.

In the present work, it is described the development of a PEGylated liposomal formulation co-encapsulating a combination of doxorubicin (inner aqueous core) and the pro-apoptotic C6-ceramide (liposomal membrane bilayer), capable to

target, by a ligand coupled at its surface, both putative breast CSC and non-SCC, besides other tumor cells. The ligand - F3 peptide - enables the specific binding to nucleolin (NCL), a protein overexpressed by cancer cells and endothelial cells of tumor angiogenic blood vessels, promoting active nanoparticle internalization. In addition, a pH-sensitive triggered release mechanism enabling burst release of the cargo upon intracellular delivery, upon endosomal acidification, has also been included.

Drug screening has demonstrated that a combination of doxorubicin (DXR):C6-ceramide (C6-Cer) at 1:2 molar ratio interacted synergistically against drug resistant/triple negative MDA-MB-231 breast cancer cells, as well as drug sensitive MDA-MB-435S melanoma cells. F3 peptide-targeted liposomes encapsulating the DXR:C6-Cer 1:2 molar ratio performed similarly as targeted liposomal DXR, encapsulating twice the amount of DXR. Importantly, F3-targeted liposomes encapsulating DXR:C6-Cer 1:2 molar ratio enabled a cell death above 90% at 24 h of incubation against both DXR-resistant and sensitive cells, unattainable by the F3 peptide-targeted liposomal doxorubicin. Furthermore, a F3-targeted formulation encapsulating a mildly additive/antagonistic DXR:C6-Cer 1:1 molar ratio enabled an effect above 90% for an incubation period as short as 4 h, suggesting that delivery route, at the cell level, may shift the nature of drug interaction. Such activity induced a marked cell and nucleus swelling at similar extent, consistent with necrotic cell death.

Moreover, it was demonstrated that F3 peptide-targeted liposomes associated with both breast non-SCC and putative CSC, but in higher extent with the latter (2.6- and 3.2-fold for triple negative MDA-MB-231 and luminal-like MCF-7 cells, respectively), in an energy-dependent process. Increased mRNA levels of NANOG and OCT4 transcription factors, paralleled by NCL, were found in putative breast CSC as compared to non-SCC, from triple negative breast cancer cells. Additionally, using mouse embryonic stem cells as stemness *bona fide* model, it was shown that

both NCL mRNA levels and cellular association of F3 peptide-targeted liposomes were dependent on stemness status. In addition, it was demonstrated that triple negative breast NCL^+ cells were more tumorigenic than NCL^- cells, paralleling putative breast CSC behavior. Furthermore, F3 peptide-targeted triggered-release liposomes promoted the efficient and simultaneous delivery of DXR:C6-Cer combinations into triple negative breast CSCs, enabling extensive cell death.

Altogether, the results presented in chapters 2 and 3 of this thesis demonstrated that F3 peptide-targeted intracellular delivery of different DXR:C6-Cer ratios, with diverse drug interactions, enabled a significant increase of efficacy against chemotherapy resistant cells. Additionally, the results suggested a clear link between NCL expression (including cell membrane NCL) and the stem cell-like phenotype, namely in triple negative breast cancer, enabling the simultaneous intracellular delivery of drug combinations-containing liposomes functionalized with the F3 peptide into both CSC and non-SCC.

Provided the necessary accessibility to the CSC niche, this technology, combined with the established NCL-mediated targeting of tumor angiogenic blood vessels, has the potential to simultaneously debulk multiple cellular compartments of the tumor microenvironment, while decreasing tumor recurrence and systemic toxicity, ultimately providing long-term disease free survival.

Resumo

O cancro da mama representa um enorme problema de saúde pública com grande impacto na sociedade. A abordagem terapêutica é muitas vezes comprometida pela natureza heterotípica intrínseca dos tumores nos quais diferentes tipos celulares interagem conduzindo o ganho de novas funções biológicas que suportam o desenvolvimento do tumor. Entre outras, a resistência a quimioterapia permanece uma questão central. As células estaminais cancerígenas (CSC) representam uma subpopulação celular com características estaminais, com elevada capacidade de renovação e elevado potencial tumorigénico. Estas têm um papel fundamental no desenvolvimento tumoral, metastatização, recorrência, assim como na resistência a fármacos. O facto reconhecido recentemente de que as células cancerígenas não-estaminais (non-SCC) podem dar origem a CSC sublinha a necessidade de se encontrarem estratégias terapêuticas direcionadas simultaneamente a estas subpopulações.

O sucesso de uma intervenção terapêutica eficaz poderá estar dependente da identificação de combinações de fármacos capazes de inibir sinergicamente o crescimento tumoral. No entanto, a aplicação de protocolos desta natureza *in vivo* é dependente da entrega, ao nível do tumor, do rácio de fármacos adequado. Nesse sentido, plataformas nanotecnológicas de entrega de fármacos, como os lipossomas, representam uma abordagem adequada para a translação *in vivo* daquela estratégia. A alteração da farmacocinética, através da co-encapsulação em lipossomas, permite a entrega da combinação de fármacos de forma sincronizada, espacial e temporalmente, ao nível do tumor. A funcionalização destas nanopartículas com ligandos direcionados a recetores específicos poderia permitir a entrega de uma combinação de fármacos a subpopulações celulares particulares, como as CSC, levando a um aumento da eficácia e, simultaneamente, a uma diminuição de toxicidade sistémica.

No âmbito do presente trabalho, é descrito o desenvolvimento de lipossomas PEGuilados, encapsulando uma combinação de doxorrubicina (núcleo aquoso) e C6-ceramida (bicamada lipídica) direcionados, através de um ligando à superfície, às CSC e non-SCC da mama, para além de outras células tumorais. O ligando – peptídeo F3 – reconhece especificamente a nucleolina (NCL), uma proteína abundante em células cancerígenas e células endoteliais de vasos angiogénicos de tumores, levando à internalização ativa da nanopartícula. Foi ainda incluindo um mecanismo de libertação de fármacos sensível ao pH, ativado após internalização seguida de acidificação dos endossomas.

Após *screening*, demonstrou-se que a combinação doxorrubicina (DXR):C6-ceramide (C6-Cer) no rácio molar de 1:2 interagiu sinergicamente contra células cancerígenas da mama MDA-MB-231 (resistentes/triplas negativas), assim como em células de melanoma (MDA-MB-435S) sensíveis a fármacos. Os lipossomas direcionados pelo peptídeo F3, co-encapsulando o rácio molar 1:2 da combinação DXR:C6-Cer foram semelhantes, em termos de eficácia, à DXR lipossomal direcionada pelo mesmo peptídeo e encapsulando o dobro da quantidade desta. Não menos importante, os lipossomas direcionados pelo peptídeo F3 contendo a combinação DXR:C6-Cer 1:2 levaram a uma morte celular acima de 90% após 24 h de incubação em ambas a linhas, o que não se verificou para a lipossomas direcionados contendo apenas DXR. Por outro lado, lipossomas direcionados pelo peptídeo F3, encapsulando a combinação DXR:C6-Cer no ratio molar 1:1 (aditivo/antagonista) conduziram a uma morte celular superior a 90% para um período de incubação de 4 h, sugerindo que a natureza da interação entre fármacos pode mudar com a via de entrada na célula. Tal atividade levou a um aumento do tamanho celular e nuclear, consistente com morte celular por necrose.

Adicionalmente foi demonstrado que os lipossomas direcionados pelo peptídeo F3 associavam ativamente com ambas non-SCC e CSC da mama, em maior extensão com estas últimas (2,6 e 3,6 vezes para as linhas MDA-MB-231 e MCF-7

(tipo luminal), respetivamente). Também foram encontrados níveis de mRNA dos fatores de transcrição NANOG e OCT4 aumentados, à semelhança da NCL, nas CSC triplas negativas quando comparadas com non-SCC. Usando células estaminais embrionárias de murganho como modelo *bona fide* de propriedades estaminais, foi demonstrado que o nível de mRNA da NCL assim como a associação celular de lipossomas direcionados pelo peptídeo F3 era dependente do estado estaminal. Demonstrou-se ainda que células cancerígenas da mama NCL^+, triplas negativas, eram mais tumorigénicas do que células NCL^-, um comportamento semelhante às CSC. Em paralelo, mostrou-se que os lipossomas direcionados pelo peptídeo F3 promoveram uma entrega eficiente da combinação DXR:C6-Cer em CSC da mama triplas negativas, levando a uma extensa morte celular.

Em suma, os resultados apresentados nos capítulos 2 e 3 desta tese demonstraram que a entrega intracelular, direcionada pelo peptídeo F3, de diferentes ratios DXR:C6-Cer conduziu a um aumento relevante da eficácia contra células resistentes à quimioterapia. Ainda, os dados sugeriram uma ligação clara entre a expressão de NCL e o fenótipo estaminal, nomeadamente em cancro da mama triplo negativo, permitindo a entrega intracelular de lipossomas direcionados pelo peptídeo F3 encapsulando combinações de fármacos, a ambas CSC e non-SCC.

Assegurada a acessibilidade ao nicho das CSC, esta tecnologia, aliada ao direcionamento para os vasos angiogénicos dos tumores mediado pela NCL já descrito, tem o potencial de atacar múltiplos compartimentos celulares do microambiente tumoral, levando a uma diminuição da recorrência e da toxicidade, potencialmente providenciando um aumento da esperança de sobrevivência a longo termo de doentes com tumores de mama.

Abreviations list

Akt (PKB)	Protein kinase B
ALDH	Aldehyde dehydrogenase
ALL	Acute lymphoblastic leukemia
AML	Acute myeloid leukemia
Ang2	Angiopoietin 2
APC	Adenomatous polyposis coli gene
BAX	BCL2-associated X protein
Bcl-2	B-cell Lymphoma 2 protains
Bmi-1	BMI1 polycomb ring finger oncogene
BRCA1	Breast cancer susceptibility gene 1
BRCA2	Breast cancer susceptibility gene 2
C6-Ceramide	N-hexanoyl-D-erythro-sphingosine
CD24	Cluster of differentiation 24
CD44	Cluster of differentiation 44
CHEMS	3β-hydroxy-5-cholestene-3-hemisuccinate
CI	Combination index
c-Myc	v-myc avian myelocytomatosis viral oncogene homolog
CSC	Cancer stem cells
CXCL7	Pro-platelet basic protein (chemokine (C-X-C motif) ligand 7)
CXCR1	Chemokine (C-X-C motif) receptor 1
CXCR2	Chemokine (C-X-C motif) receptor 2
DLL	Delta-like ligands
DNA	Deoxyribonucleic Acid
DOPE	2-dioleoyl-sn-glycero-3-phosphoethanolamine
DRI	Dose-reduction index
DSH	Dishevelled
DSPC	1,2-distearoyl-sn-glycero-3-phosphocholine
DSPE-PEG_{2k}	1,2-distearoyl-sn-glycero-3-phosphoethanolamine-N-[methoxy(polyethylene glycol)-2000]
DSPE-PEG_{2k}-mal	1,2-distearoyl-sn-glycero-3-phosphoethanolamine-N-[maleimide(polyethylene glycol)-2000]
DXR	Doxorrubicin

EGF	Epidermal growth factor
EGFR	Epidermal Growth Factor Receptor
EMT	Epithelial-to-mesenchymal transition
EPR	Enhanced permeability and retention effect
ER	Estrogen receptors
F3	Fragment 3 of the human high mobility group protein 2
FACS	Fluorescence-activated cell sorting
FBS	Fetal Bovine Serum
FDA	Food and Drug Administration
GCS	Glucosylceramide synthase
GDF3	Growth differentiation factor 3
GLI	GLI family zinc finger
GSK3β	Glycogen synthase kinase 3 beta
HBS	HEPES buffer saline
HCC	Hepatcellular carcinoma
HER	Human epidermal growth factor receptor
HH	Hedgehog ligand
HIF-1α	Hypoxia inducible factors 1 alpha
HIF-2α	Hypoxia inducible factors 2 alpha
IC_{50}	Inhibitory concentration at 50% effect
IC_{70}	Inhibitory concentration at 70% effect
IC_{90}	Inhibitory concentration at 90% effect
Il-6	Interleukin 6
IL-8	Interleukine 8
iPS	Induced pluripotent stem cells
JAG	Jagged ligands
JAK	Janus Kinase
KLF4	Kruppel-like factor 4
Lgr5	Leucine-rich repeat-containing heterotrimeric guanine nucleotide-binding protein-coupled receptor 5
LIF	Leukemia inducible factor
LRP	Low-density lipoprotein receptor-related protein
MAPK	Mitogen activated protein kinases

MaSC	Mammary stem cells
MCF-7	Luminal-type breast cancer cells (adenocarcinoma)
MDA-MB-231	Triple negative breast cancer cells (adenocarcinoma)
MDA-MB-435S	Melanoma cells
MDR1	Gene encoding P-glycoprotein
mESC	Mouse embryonic stem cells
MMP	Matrix metalloproteinase
MPC	Mesenchymal progenitor cells
MPS	Mononuclear phagocytic system
mRNA	Messenger RNA
MTD	Maximum tolerated dose
mTOR	Mammalian target of rapamycin
MTT	2H-Tetrazolium, 2-(4,5-dimethyl-2-thiazolyl)-3,5-diphenyl-, bromide
NCL	Nucleolin
NICD	Notch intracellular domain
non-SCC	Non-Stem cancer cells
NSG	NOD scid gamma mice
OCT4 (POU5F1)	POU class 5 homeobox 1
OKSM	OCT4, KLF4, SOX2 and c-MYC gene
PBS	Phosphate buffer saline
PDI	Polidispersion Index
PEG	Poly(ethylene)glycol
PI3K	Phosphoinositide 3-Kinase
PTCH	Patched proteins
RNA	Ribonucleic acid
RTK	Receptor Tyrosine Kinase
S1P	Sphingosine-1-phosphate
SEM	Standard error of mean
siRNA	small interfering RNA
SMase	Sphingomyelinase
SMO	Smoothened, frizzled class receptor
SOX2	SRY (sex determining region Y)-box 2
Src	Src kinase

STAT	Signal Transducers and Activators of Transcription
TDGF	Teratocarcinoma-derived growth factor
Tf	Transferrin
TGFβ	Tumor growth factor beta
TIC	Tumor initiating cells
VEGF	Vascular endothelial growth factor
VEGFR1	Vascular endothelial growth factor receptor 1
VEGFR2	Vascular endothelial growth factor receptor 2
Wnt	Wingless protein
ZEB1	Zinc finger E-box binding homeobox 1

Drawings

List of figures

List of tables

Preface

The present thesis describes the development of a F3 peptide-targeted liposomal triggered release nanoparticle for the simultaneous and intracellular delivery of doxorubicin and C6-ceramide combinations into breast cancer stem cells. The thesis is organized in four chapters according to the established publication strategy.

The ***first chapter*** addresses the importance of the tumor microenvironment in cancer development, from which new molecular and cellular targets emerge. In this respect, a special focus is given to cancer stem cells (CSC), which play a pivotal role in drug resistance and tumor relapse. These concepts are instrumental for the understanding of the use of nanotechnology-based drug delivery as a form of therapeutic intervention in oncology, including the one presented in this thesis.

The ***second chapter*** describes the development and physico-chemical characterization of F3 peptide-targeted triggered release liposomes for the simultaneous delivery of doxorubicin and C6-ceramide into breast cancer cells. *In vitro* screening studies were performed in order to establish the nature of interaction between these two drugs. *In vitro* cellular cytotoxicity studies, cell viability and morphology assessment were performed to evaluate efficacy gains and characterize the cell death mechanism.

The ***third chapter*** addresses the application of F3 peptide-targeted liposomes for the intracellular delivery of a combination of doxorubicin and C6-ceramide into putative breast CSC, based on the overexpression of cell surface nucleolin. Cellular association with breast cancer cell lines was performed to study the interaction of F3 peptide-targeted liposomes with putative CSC and non-SCC (non-stem cancer cells). Cell sorted sub-populations were functionally characterized *in vitro*

upon assessing stem-like status by mammosphere assay and evaluation of mRNA levels of nucleolin and pluripotency markers. Further confirmation was obtained from experiments with embryonic stem cells. Moreover, tumorigenic potential of sorted putative CSC, non-SCC and nucleolin-overexpressing cells was also evaluated. Finally, cytotoxicity studies were performed to evaluate the efficacy of the developed F3 peptide-targeted liposomes encapsulating a synergistic combination of doxorubicin and C6-ceramide against mammosphere-derived cells.

The ***fourth chapter*** summarizes the relevant findings of the preceding chapters, and contextualizes them in future work.

Chapter 1

Bridging cancer biology and the patients' needs with nanotechnology-based approaches

Part of this chapter was published in:

Fonseca, N. A., Gregorio, A. C., Valerio-Fernandes, A., Simoes, S. and Moreira, J. N. **(2014)**

Bridging cancer biology and the patients' needs with nanotechnology-based approaches

Cancer Treat Rev 40(5): 626-635.

2

1.1. Cancer disease: a heavy burden claiming for innovative therapeutic intervention

Cancer remains a stressful condition in the western world, having surpassed heart diseases in 1999 as the leading cause of death (Jemal *et al.* 2006; Siegel *et al.* 2013). Globally, lung cancer stands as the leading cause of death amongst the respiratory system tumors, whereas colon cancer stands out in digestive diseases (Jemal *et al.* 2011). If one accounts for gender, a substantially different reality emerges, revealing breast cancer as the leading cause of death, accounting for 23% of all cancer cases among women (Jemal *et al.* 2011). Epidemiologic data from the United States of America suggest that 1 in 8 women will develop breast cancer over their life-time (Desantis *et al.* 2013; Siegel *et al.* 2013). Among those, some will derive from familial inheritance. In this respect, *BRCA1* and *BRCA2* mutations confer high risk of breast cancer development, accounting for 40% of the familial cases (Shuen *et al.* 2011). Over the years, such scenarios have unleashed a tremendous effort from the scientific community in order to address this disturbing health problem. Such efforts have been unraveling novel insights about tumor biology, namely new potential molecular and cellular targets while, simultaneously, setting forth better disease models and innovative therapeutic tools.

1.2. Tumor microenvironment as a key player in cancer development

Before the introduction of the microenvironment concept, tumors were thought as a collection of uncontrolled actively-dividing cells, generated from several oncogenic hits or activating mutations, and sharing similar proliferation and tumorigenic potential. It was believed that those cells had the same capacity to generate tumors when implanted in mouse models (Hanahan *et al.* 2000; Hanahan *et al.* 2011). Though simplistic compared to actual disease theoretical models, this concept enabled the development of a vast set of molecules capable

to tackle the disease, from which some still remain as the cornerstone treatment of several cancer conditions (Jordan *et al.* 1991; Miller *et al.* 2001; Minotti *et al.* 2004). Such simplistic approach has greatly evolved with the newly found roles of cellular and molecular players already existing within the tumor microenvironment.

In fact, a multitude of different cell types, including cancer cells, fibroblasts, endothelial cells or cells from the immune system, may be found within the tumor microenvironment. They carry dissimilar roles, thus contributing to the heterotypic nature of tumors (Hanahan *et al.* 2011). This layout suggests an intrinsic interaction between those cells, which ultimately provides a fostering ground for the acquisition of several features that support tumor development. Indeed, such features were rationally summarized by Douglas Hanahan and Robert Weinberg in a seminal manuscript from 2000 (Hanahan *et al.* 2000), and included originally six important hallmarks of the disease, which were further upgraded in a new article (Hanahan *et al.* 2011): (I) sustained proliferative signaling, (II) evading growth suppressors, (III) enabling replicative immortality, (IV) resisting cell death, (V) angiogenesis induction, (VI) activation of invasion and metastasis, (VII) immune system evasion, (VIII) deregulation of cellular energetics, and also enabling characteristics as (IX) genome instability and mutation and (X) tumor-promoting inflammation.

As main drivers of tumor development, the aforementioned features account for the major known deregulated pathways in cancer/tumor cells, which control metabolism, including nucleic acid turnover, cellular proliferation and fate, and cell signaling, which eventually intertwine with the recruitment of essential biological capabilities. One of the most common triggered processes for promoting and supporting tumor development is angiogenesis, regardless the histological origin of the tumor (Hanahan *et al.* 2011).

1.2.1 Angiogenesis: fueling tumor development

Angiogenesis, understood as the formation of new vascular vessels from pre-existing ones, represents an essential mechanism for homeostasis maintenance, contributing to phenomena like wound healing (Tonnesen *et al.* 2000). However, cancer shifts the intrinsic beneficial nature of those processes, subverting them for the benefit of tumor growth and development.

Tumor growth is highly dependent on a constant flow of nutrients. However, uncontrolled growth in the case of solid tumors renders the development of a central mass which lacks a properly functional blood vessel network to encompass the delivery of oxygen and nutrients, as well as to remove carbon dioxide. Additionally, lymphatic drainage is also compromised, leading to the accumulation of metabolic waste (Hanahan *et al.* 2011). To cope with such condition, tumors expand to the vicinity of existing vessels. Nonetheless, overtime, this condition reveals itself insufficient to sustain tumor development, leading tumor cells to induce angiogenesis as an attempt to cope with nutrient scarcity as tumor grows (Ferrara *et al.* 2005; Hanahan *et al.* 2011; Welti *et al.* 2013).

Several cellular and molecular signaling components are involved in the tumor angiogenic process. VEGF, a potent pro-angiogenic factor, is central for vessel development, with cancer cells and mesenchymal progenitor cells (MPCs) functioning as main secretion drivers (Carmeliet *et al.* 2011a; Melero-Martin *et al.* 2011; Welti *et al.* 2013). In part, and concomitantly with pro-angiogenic Ang2 and MMP activity, VEGF signaling enables the selection, formation and migration of the tip cell from endothelial cells (ECs), the leading driver of vessel sprouting (Carmeliet *et al.* 2011a; Welti *et al.* 2013). It is the ratio VEGFR1/VEGFR2, expressed by ECs, that dictates the tip cell positioning in detriment of proliferating stalk cell formation (Carmeliet *et al.* 2011a). As stalk elongates, pericyte recruitment occurs to stabilize new vessels (Duda *et al.* 2006; Le Bourhis *et al.* 2010; Carmeliet *et al.* 2011a; Melero-Martin *et al.* 2011; Welti *et al.* 2013). During angiogenesis, which

also occurs in response to hypoxia, where HIF-1α and HIF-2α activation leads to pro-angiogenic VEGF expression in an attempt to increase oxygen supplies (Carmeliet *et al.* 2011a), new vessel formation is far from ideal. Despite capable of nourishing the tumor in large extent, the newly formed vessel network is highly dysfunctional due to unregulated angiogenic stimulation (Welti *et al.* 2013). Structurally, tumor angiogenic vessels present high tortuosity and fenestrae with a size up to 600 nm wide, depending on the tumor type, thus impairing perfusion capacity as well as limiting the counteract of the tumor hydrostatic pressure, both stringent steps blighting nutrient and drug perfusion (Yuan *et al.* 1995; Carmeliet *et al.* 2011b). Ultimately, angiogenesis enters a vicious cycle where poor vessel assembly compromises nourishment which leads to hypoxia that, in turn, guides tumor cells to increase pro-angiogenic factor secretion, like VEGF, for stimulation of the angiogenic process (Carmeliet *et al.* 2011a).

Overall, angiogenesis involves several molecular and cellular elements, each one playing a central role in tumor vessel network formation, enabling tumors to adapt and evolve according to environmental conditions.

Impairing tumor angiogenesis has proven to be a promising strategy for antitumor therapies (Ferrara *et al.* 2005; Carmeliet *et al.* 2011a). Some have been more successful than others, which demonstrate the need for new and more effective solutions (Welti *et al.* 2013).

1.2.2 Cancer stem cells and tumor initiation

Along with instrumental processes for drug resistance and tumor survival, such as angiogenesis, new research has unveiled the role of a rather illusive cell type, resembling cells from embryonic development. The acknowledgement of common signaling pathways between stem cells and subpopulations of tumor cells, set developmental biology and cancer closer than one would think, and gave rise to the cancer stem cell concept (Reya *et al.* 2001).

1.2.2.1 Lessons from stem cells: cellular reprogramming

Pluripotent stem cells have the potential to differentiate into any type of cells of the three germ layers (endoderm, mesoderm and ectoderm) (De Miguel *et al.* 2010), and they also display self-renewal capability (Evans *et al.* 1981; Thomson *et al.* 1998; De Miguel *et al.* 2010). In the attempt to identify pluripotent cells, such as embryonic stem cells (ESC), several markers have been established, including high levels of *NANOG*, *OCT4* (a.k.a. *POU5F1*), *TDGF* and *GDF3*, which are strongly regulated developmental genes (Adewumi *et al.* 2007; De Miguel *et al.* 2010). Nanog and Oct4, as well as Sox2, are regulatory transcription factors essential for self-renewal and pluripotency maintenance of stem cells (Pan *et al.* 2007; Stadtfeld *et al.* 2010). They control several downstream gene targets, including *STAT3*, essential for self-renewal (Niwa *et al.* 1998; Boyer *et al.* 2005; Stuart *et al.* 2014). Tight levels of Oct4 control the transition between pluripotency and differentiation (Radzisheuskaya *et al.* 2013). Takahashi *et al.* demonstrated that it is possible to reprogram somatic cells such as adult fibroblasts, first from mouse, and later from human, into a state of pluripotency. Upon promoting the expression of four key transcription factors - Oct4, Sox2, c-Myc and Klf4 (OSKM) -, induced pluripotent stem cells (iPS) were generated (Takahashi *et al.* 2006; Takahashi *et al.* 2007). These cells closely resembled ESC, showing similar expression patterns of stem cell markers, like *NANOG* or *GDF3*, and demonstrating oriented differentiation capacity (Takahashi *et al.* 2007).

Overall, this suggests that cells with self-renewal potential can be generated from terminally differentiated somatic cells, thus reverting hierarchical developmental organization. This guided reintroduction of stemness in somatic cells somewhat represents a gain of function, a feature often occurring during cancer development.

1.2.2.2 The stemness concept in cancer

Tumors are biological entities that can be interpreted as an aberrant dysfunctional organ initiated by a tumorigenic cancer cell with the capacity to proliferate indefinitely by acquired mutations (Reya *et al.* 2001; Visvader 2011). Viewed as an organ, tumors present functional heterogeneity in the microenvironment demonstrated by the existence of different populations of cells, including different cancer cells. In order to accommodate that functional heterogeneity, a hierarchical organization model of tumor development, known as the cancer stem cell model, was proposed. This model postulates the existence of a sub-population of stem-like cells (the "cancer stem cells" - CSC) within the tumor microenvironment, responsible for sustained tumor growth (Reya *et al.* 2001; Visvader *et al.* 2008; Visvader 2011; Visvader *et al.* 2012; Kreso *et al.* 2014). CSC have been defined operationally by their capacity to form new tumors in immunocompromised mice upon isolation of an established tumor (Scheel *et al.* 2012). However, the observation that not all cells of a putative CSC population are able to seed tumors, led to the introduction of Tumor Initiating Cells (TIC) as reflective of the CSC operational definition (Figure 1.1) (Scheel *et al.* 2012).

Conceptually and in the absence of pre-established disease, a TIC might either be a normal adult stem cell, which has acquired several abnormal transformations; or a partially differentiated cell, like a common progenitor; or a differentiated cell which has gone through a series of oncogenic hits, thus acquiring a stem-like character (Reya *et al.* 2001; Hanahan *et al.* 2011; Visvader *et al.* 2012). As these cells expand, acquired mutations during neoplastic progression may result in the development of cancer stem cells (CSC), which are responsible for sustained tumor growth and maintenance, as well as in an enrichment of cells capable of tumor initiation (Figure 1.1) (Visvader 2011). Despite abnormal, CSC share features of normal stem cells such as self-renewal and differentiation capacity (Reya *et al.* 2001; Vallier *et al.* 2009; Visvader *et al.* 2012).

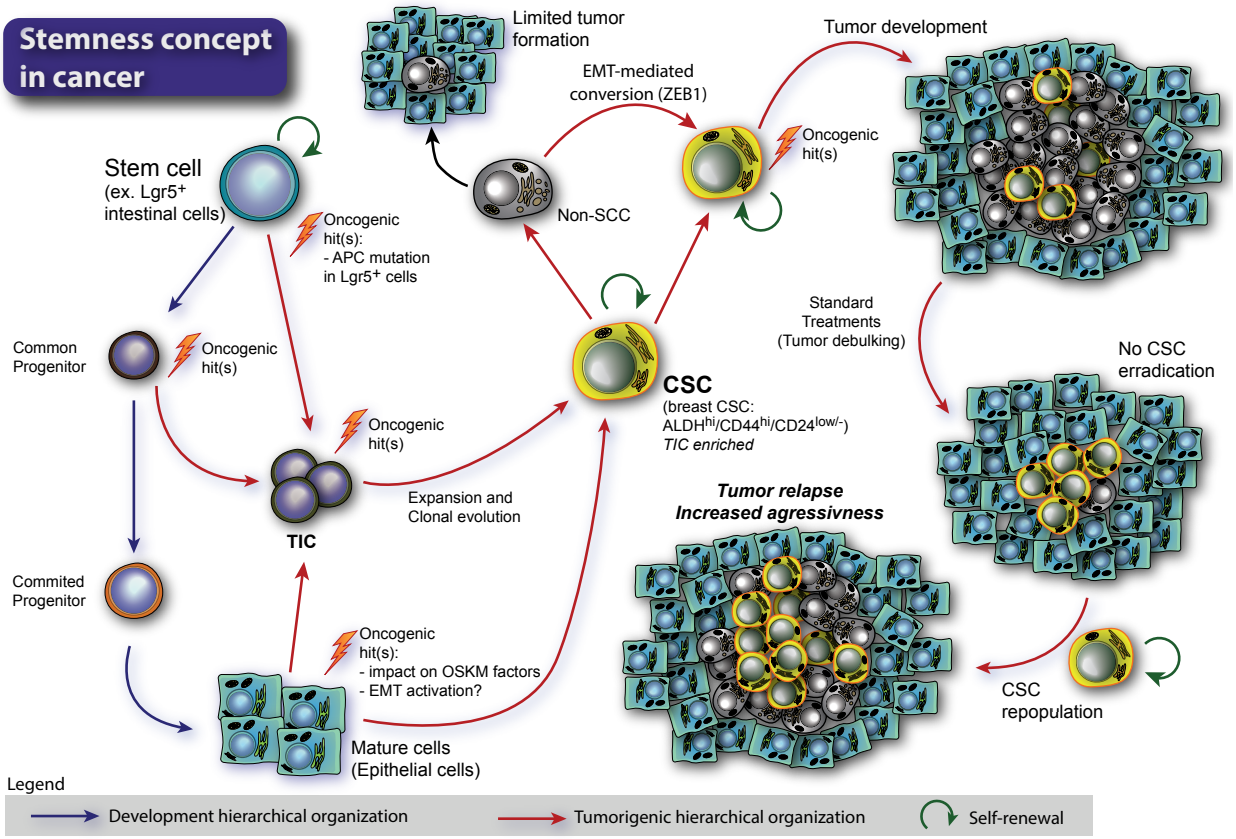

Figure 1.1 - From stem cells to tumor initiating cells and cancer stem cells.

In normal developmental cellular hierarchy, **stem cells** originate **progenitor cells**, which generate progressively more committed progeny, culminating in the establishment of **mature cells** composing the different tissues. In tumor development, either one of those cells (stem, progenitor or mature cells) may suffer different oncogenic hits, eventually turning them into **Tumor Initiating Cells (TICs)**. As these cells expand, subsequent oncogenic hits (occurring epigenetically, for example) lead to the generation of **Cancer Stem Cells (CSCs)**. CSCs are therefore the drivers sustaining tumorigenesis, a role that cannot be undertaken by any other tumor cell (like **non-SCC**) unless they convert into a CSC phenotype. Either way, standard treatments are many times only capable to debulk tumor mass, but cannot eliminate the drug resistant CSCs. Residual CSCs are in turn capable of repopulating the tumor area, often leading to tumor resistance and increased disease aggressiveness.

The cancer stem cell existence was firstly reported by Bonnet *et al.* (Bonnet *et al.* 1997) in acute myeloid leukemia, by implicating aberrant hematopoietic cells expressing the $CD34^{+}/CD38^{-}$ phenotype (a.k.a. SCID leukemia initiating cells – SL-IC) in disease development, which were also able to differentiate into leukemic blasts. Later on, cancer stem cells were also implicated in solid tumor development

by Al-Hajj *et al*. (Al-Hajj *et al.* 2003). Since then, putative CSC have been unveiled in different tumor types using a series of different surface markers (Stuelten *et al.* 2010; Visvader *et al.* 2012). Nonetheless, the evolving landscape is highly complex, since tumors of different histological origins may present different densities of putative CSC (understood as tumorigenic) rising from acquired mutations. These cells may further clonally evolve under genetic and epigenetic control, presenting different degrees of hierarchical organization (Kreso *et al.* 2014). This poses an enormous challenge for the identification of markers, which is often supported by functional characterization using *in vivo* tumorigenic assays or *in vitro* sphere suspension cultures (Kreso *et al.* 2014). Another relevant work supporting the CSC concept, with direct stem cell involvement in cancer initiation and development, was established in a mouse model of intestinal cancer and involved a specific APC mutation in $Lgr5^{+}$ crypt intestinal stem cells (Barker *et al.* 2009; Snippert *et al.* 2010; Schepers *et al.* 2012; Schuijers *et al.* 2012). That work enabled one to clearly perceive stem cell or stem cell-like phenotype involvement in cancer initiation and progression. The Lgr5 marker has also been suggested for breast cancer patient stratification (Chen *et al.* 2013a). In addition, recent evidence suggests the existence of bipotent mammary stem cells (MaSC) in postnatal gland capable of giving raise to both myoepithelial and luminal cell lineages, thus highly contributing to physiological ductal tree homeostasis (Rios *et al.* 2014). The existence of MaSC in adult gland may support breast cancer development in light of CSC theory, owing to loss of physiological regulation of those cells, either by spontaneous or extrinsically acquired mutations (Rios *et al.* 2014).

1.2.2.3 The CSC role in breast cancer

In 2003, a first clue for the existence of putative breast CSC was found by functional comparison of breast cancer cells expressing different levels of surface markers CD44 (receptor for hyaluronic acid and extracellular changes monitor)

and CD24 (cell-cell and matrix interaction) (Al-Hajj *et al.* 2003; Jaggupilli *et al.* 2012). Later on, aldehyde dehydrogenase (ALDH) levels and/or activity (also present in normal adult breast stem cells), was correlated with poor clinical outcome, metastasis, tumor relapse and drug resistance (Ginestier *et al.* 2007; Liu *et al.* 2010a; Croker *et al.* 2011; Marcato *et al.* 2011). Those three markers (CD44, CD24, and ALDH) remain as consensual for identification of putative breast CSC (Badve *et al.* 2012). Nevertheless, such consensus is cautiously maintained since those markers may, in fact, identify breast CSC with different degrees of differentiation according to tumor histologic origin (Ricardo *et al.* 2011). Regardless their origin, it is clear that putative CSC have a significant role in reshaping tumor microenvironment, a feature supported by aberrant pathway activation, like Wnt signaling, or activated epithelial-to-mesenchymal transition, a cornerstone in cancer metastasis (Takebe *et al.* 2011; Scheel *et al.* 2012).

1.2.2.3.1 Cancer stem cell traits and microenvironmental regulation

Breast CSC are considered as instrumental for disease development and progression, as well as therapy evasion, leading to recurrence. Their origin is yet unknown. Nevertheless, recent data suggests that cells with stem-like properties – breast CSCs – were generated by defined reprograming factors (OSKM cocktail) from non-tumorigenic human mammary epithelial cells (Nishi *et al.* 2013). Additionally, it has been reported that radiation concomitantly with steroid hormones (high proliferative effects in progenitor cells) leads to an increase in $ALDH^+$ cell population (putative breast CSC) (Vares *et al.* 2013). Both works suggest that cancer cells with stem-like traits could be generated through acquired mutations leading to uncontrolled reactivation of pluripotency-associated programs in adult somatic cells (or even MaSC). This is a process that could be, in part, initiated/modulated by environmental stimulus like xenobiotics or radiation. Indeed, Sox2 seems to be highly expressed in early stage breast tumors,

controlling xenograft tumor initiation (Leis *et al.* 2012). This is in accordance with the generation of Sox2-overexpressing cancer stem-like cells from luminal breast cancer cells upon nuclear reprogramming using OSKM factors (Corominas-Faja *et al.* 2013). Interestingly though, despite expressing high levels of Sox2, those cells expressed low levels of Oct4 and Nanog, which are also absent in early stage breast tumors (Leis *et al.* 2012; Corominas-Faja *et al.* 2013). Additionally, breast cancer cells from different histological origins (such as luminal or basal) express different levels of the pluripotency markers Oct4, Nanog and Sox2 (Ling *et al.* 2012). Upon analysis of a series of human breast tumors, Nanog has been associated with poor prognosis, correlating with highly proliferative early stage tumors (Nagata *et al.* 2014). Therefore, it is plausible that nuclear reprogramming, with the consequent involvement of potency markers, could in fact play a central role in cancer development, notwithstanding that cells may rely on this process to different extents (Nanog and Oct4 not expressed in early stage tumor), leading to different phenotypic signatures among breast or even other histological tumors.

Indeed, the expression of current CSC markers, such as ALDH, CD44 or CD24, differs among breast cancer molecular subtypes. ALDH has a scattered distribution in each subtype, and basal-like tumors enclose higher percentage of $CD44^{+}$/$CD24^{-/low}$ than the luminal type (Ricardo *et al.* 2011). This suggests that the referred markers may identify cells with several degrees of differentiation (Ricardo *et al.* 2011), thus potentially representing different pools of putative CSC.

Nevertheless, those markers convey an important prognostic value for the disease. In fact, ALDH1 overexpression has been related to poor clinical outcome for breast cancer (Ginestier *et al.* 2007). That could be related to the fact that ALDH1 activity allows the selection of cells with increased metastatic potential, in accordance to the predictive value of ALDH1A3 for metastasis development (Croker *et al.* 2009; Marcato *et al.* 2011). Additionally, $CD44^{+}$/$CD24^{-/low}$ phenotypic cells are predominant in triple-negative invasive breast carcinomas, an

aggressive molecular subtype associated with poor clinical outcome (Idowu *et al.* 2012). Considering special histological types of breast cancer, medullary and metaplastic carcinomas (associated with high grade basal-like and claudin-low molecular subtypes) are enriched with $CD44^{+}/CD24^{-/low}/ALDH1^{+}$ cells (de Beca *et al.* 2013). Interestingly though, this picture does not always hold true since there are indications that $CD44^{-}/CD24^{+}$ phenotype is related to poor prognosis in early invasive breast carcinoma (Ahmed *et al.* 2012). Thus, although important, their relevance may vary according to the histologic type and/or tumor stage as well as to the degree of differentiation of tumor cells, which highlights the heterogeneity of the tumor microenvironment. In fact, the diverse cellular components of microenvironment unlock many regulatory restraints of CSC, providing the soil for those to proliferate and evolve (Korkaya *et al.* 2011).

Microenvironment cells, such as fibroblasts, endothelial cells or even mesenchymal stem cells (MSC), have been shown to regulate breast CSC through production of different signaling molecules associated with survival, proliferation or differentiation (Liu *et al.* 2011). Among these, the cytokine regulatory network has been shown to be essential, upon demonstration that CXCR1 is necessary for breast CSC self-renewal and survival (Figure 1.2) (Ginestier *et al.* 2010). In addition, endothelial cell signaling has also been suggested to regulate CSC self-renewal in breast cancer (Korkaya *et al.* 2011). Although important in physiological conditions in diverse cellular functions, these signals may translate into activation of fundamental signaling pathways, often deregulated in CSC, like Notch, Hedgehog and Wnt/β-Catenin (Takebe *et al.* 2011; Bolos *et al.* 2013; Cai *et al.* 2013; Karamboulas *et al.* 2013; Lamb *et al.* 2013; Nagamatsu *et al.* 2014) or the canonical JAK/STAT or PI3k/Akt pathways (Korkaya *et al.* 2009; Ithimakin *et al.* 2013; Lin *et al.* 2013) (summarized in Figure 1.2), supporting survival and self-renewal of those.

Altogether, feature overlap between embryonic development and cancer is rapidly accumulating, setting forth a hierarchical organization of tumor cells where

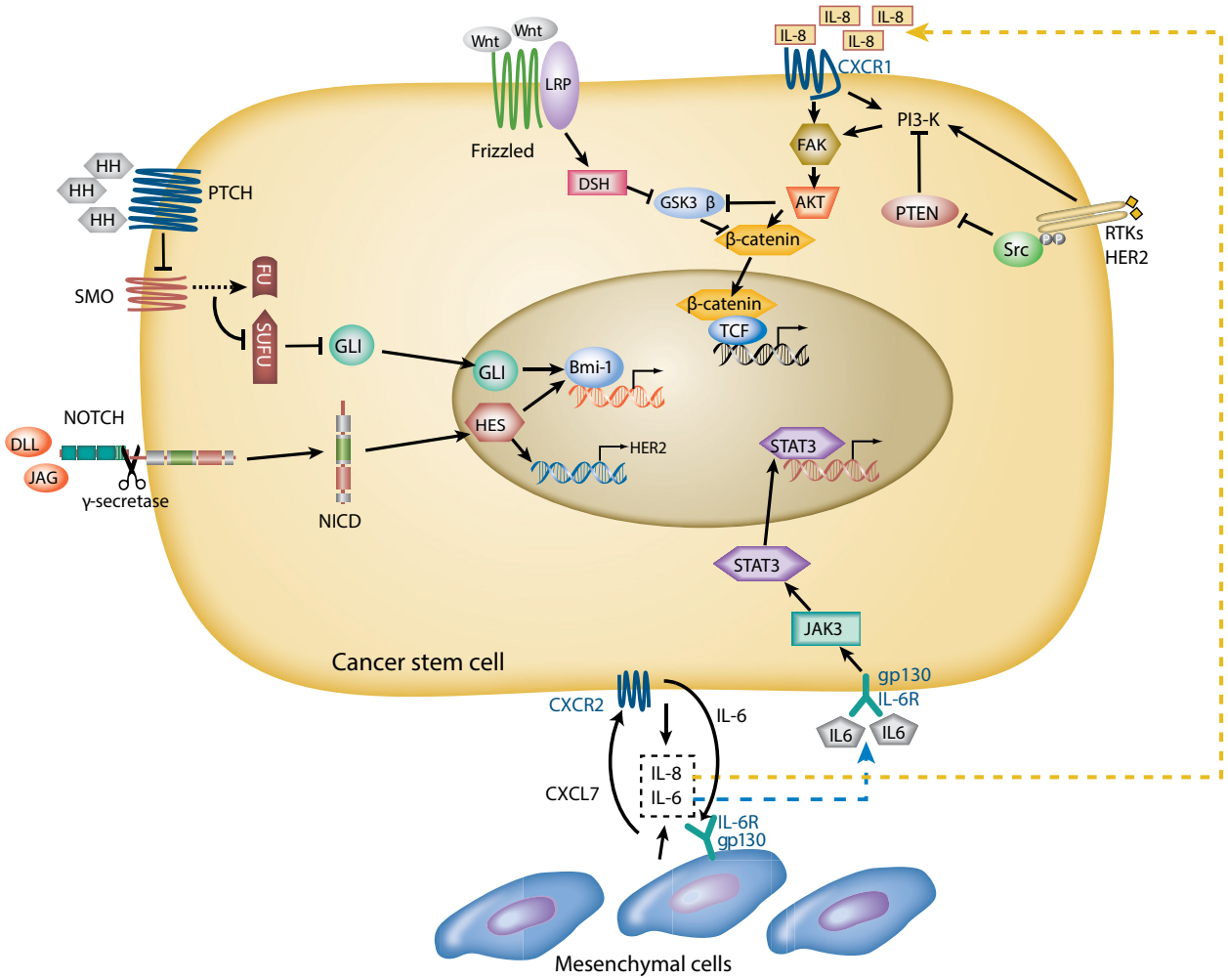

Figure 1.2 - Fundamental pathways deregulated in cancer stem cells.
Developmental signal transduction pathways, including Notch, Wnt and Hedgehog are highly associated with CSC phenotype. Additional signal transduction is mediated by receptor tyrosine kinases (RTK), like HER2, and PI3k/Akt pathway or JAK/STAT pathway. Mesenchymal-cell mediated regulation of CSC through interleukins adds an additional layer to the regulatory network. *Adapted and edited from (Liu et al. 2010a).*

an intricate interaction between embryonic and classical signaling networks modulates CSC behavior and properties, and reshape tumor landscape.

1.2.2.3.2 Epithelial-to-mesenchymal transition and breast CSC

From the aforementioned, cancer could be understood as a derailed disease setting its roots in part on the uncontrolled activation/reactivation of embryonic programs by cancer cells. Epithelial-to-mesenchymal transition (EMT) may

represent the "gain-of-function" process enabling stem-like features in cancer cells. EMT (initially a concept developed in embryology as a mean of tissue remodeling) is the program by which epithelial cells acquire the ability to invade adjacent and/or distant tissues, enabling their dissemination and further metastization (Hanahan *et al.* 2011; Scheel *et al.* 2012). Its main manifestation is related to the loss of the epithelial adhesion molecules, among which E-cadherin stands out, under the control of transcription repressors Snail, Slug, Zeb1 and Twist (Hanahan *et al.* 2011; Scheel *et al.* 2012). Indeed, it was recently shown that ZEB1 promoter enables a swift shift from a non-SCC status to a CSC state in response to environmental stimulus like TGFβ (Chaffer *et al.* 2013). This challenges the unidirectional hierarchical CSC concept, demonstrating that non-SCC and CSC can readily convert in each other upon environmental stimuli, a process governed, in part, by EMT (Marjanovic *et al.* 2013). In addition, the conversion seems to be common to both normal epithelial cells as well as cancer cells (Chaffer *et al.* 2011). Thus, this suggests that cancer cells may rely on physiological occurring programs to acquire highly aggressive phenotypic traits, which include motility and invasiveness, central to metastasis (Scheel *et al.* 2012).

Ultimately, the interconversion between non-SCC and CSC may underlie drug resistance, enabling cells to switch to a more drug resistant phenotype, as well as CSC-mediated metastasis (Geng *et al.* 2014).

1.2.2.4 Nucleolin: is it a target in CSC?

From a biological perspective, it is becoming clear that tumors and all their cellular components seem to rely on the aberrant acquisition of features that enable them to thrive (Hanahan *et al.* 2011). Those features are many times present in physiological processes that owing to impaired information flow, through oncogenic hits, became aberrantly activated. Nonetheless, such transformations are followed by the expression of specific markers which enable one to follow

many traits of those processes.

Alongside the above-mentioned markers, nucleolin (NCL) has been associated with breast cancer. Nucleolin is a nucleolar protein involved in chromatin structure as well as transcription, ribosome assembly and nucleous-cytoplasm transport, playing a central role in cell cycle and nucleolus structure (Ginisty *et al.* 1999; Srivastava *et al.* 1999; Ugrinova *et al.* 2007). Notwithstanding, in cancer, NCL has also been described as highly overexpressed in cellular membranes of cancer cells and endothelial cells of tumor angiogenic vessels (Ginisty *et al.* 1999; Christian *et al.* 2003; Hovanessian *et al.* 2010). It has been also demonstrated that NCL mediates the antiangiogenic and antilymphangiogenic properties of endostatin and that synergizes with EGFR and mutant Ras to promote tumor growth (Shi *et al.* 2007; Fogal *et al.* 2009; Zhuo *et al.* 2010; Farin *et al.* 2011).

Concomitantly to its role in cancer, NCL has also been described as important in embryonic stem cell biology. Indeed, its interaction with Oct4 was documented during cell cycle progression upon phosphorylation in ESC (Johansson *et al.* 2010). Of utmost importance, NCL expression was described to be essential for maintenance of embryonic stem cell homeostasis and self-renewal through p53 pathway suppression (Yang *et al.* 2011; Cinghu *et al.* 2014). As such, it is evident that NCL is supporting functions in cells both physiologically at developmental stage as well as in cancer. Therefore, as stemness functions are many times translated to cancer in the figure of CSC, nucleolin overexpression could provide a mean to target these cells.

1.2.3 The entwined advantages of targeting emerging molecular and cellular targets

Cancer can be understood as an intricate cascade of aberrantly activated physiological processes. Even though this provides several levels for therapeutic intervention, it also represents a colossal challenge, since most processes are

gateways to circumvent treatment and often lead to drug resistance (Singh *et al.* 2010). Nevertheless, targeting emerging molecular and cellular components of the tumor microenvironment has shed some light in the paths to follow.

Angiogenesis and its cellular and molecular components have been, in some cases, successfully targeted using anti-angiogenic therapies, based on the knowledge that cutting off tumor nourishment impairs tumor growth (Ferrara *et al.* 2005; Welti *et al.* 2013). This is the case of VEGF and bevacizumab. However, anti-angiogenic therapy is highly affected by poor efficiency and development of resistance (Carmeliet *et al.* 2011a). Moreover, it has been postulated that instead of impairing an already poor functional vessel network, vessel normalization could be a potential benefit by favoring oxygenation, which in turn would increase the efficacy of many treatments relying on oxygen radicals formation, such as radiotherapy (Carmeliet *et al.* 2011a). Indeed, vessel normalization can ameliorate tumor perfusion, enabling better drug delivery and limiting tumor cell dissemination and metastasis (Carmeliet *et al.* 2011b). Double targeting strategies have also been developed for simultaneous targeting of different cellular populations. A small drug delivery system targeting both cancer cells and angiogenic endothelial cells enabled the reduction of the viable rim area of breast tumor models, essential for surgical tumor removal (Moura *et al.* 2012).

Other important emerging therapeutic targets are CSC, owing to their association with drug resistance, disease recurrence and metastasis. Therefore, multiple approaches to eradicate CSC are under development, including the design of inhibitors to embryonic signaling pathways, such as Wnt, Notch and Hedgedhog, which control stemness features like CSC self-renewal and expansion (Vazquez-Martin *et al.* 2011). Indeed, through Notch silencing, breast cancer stem cell expansion was arrested (Suman *et al.* 2013). Tackling a downstream effector of Notch, γ-secretase, using GSIXII inhibitor, led to breast cancer cell death (Seveno *et al.* 2012). Another strategy for CSC targeting relies on modulation of their

markers, like CD44. In fact, short-hairpin mediated silencing of CD44 combined with doxorubicin suppressed the growth of breast tumor models (Van Pham *et al.* 2012).

Overall, one can infer that cancer disease complexity demands simultaneous targeting of different cellular and molecular components from the tumor microenvironment (like multiple signaling pathways) for successful therapeutic intervention. In order to accomplish this premise, one has to be able to simultaneously deliver combinations of drugs (or gene silencing tools) at the tumor site. Fulfilling that requirement, nanotechnology-based platforms are at the forefront of drug delivery due to the different levels of versatility they can provide: targeting diverse tumor cells with more than one drug, of various natures.

1.3. Advanced drug delivery for cancer treatment: from tumor biology to nanotechnology

Drug development has led the way by delivering a vast set of molecules capable to tackle the disease, from which some still remain as the cornerstone treatment of several cancer conditions. They act upon interfering with cell cycle progression by impairing correct DNA synthesis or repair (like alkylating agents), inhibiting mitotic spindle formation (as vinca alkaloids) (Jordan *et al.* 1991), stabilizing microtubule (like taxanes) (Miller *et al.* 2001) or inhibiting topoisomerase II (typical of anthracyclines) (Minotti *et al.* 2004). Ultimately, each of the mentioned examples triggers cell death, either programmed or not. Supporting such rationale is tumor biology and the intrinsic features of tumor cells - the *hallmarks of cancer* (Hanahan *et al.* 2011). Drugs of the aforementioned classes interfere with DNA processing, inducing cell cycle arrest, an event that ultimately prompts for apoptosis in highly proliferating cells, including neoplastic and healthy (Gottesman 2002). This is the reason why these drugs are not devoided of severe side effects, which arise from the accumulation of chemotherapeutics in cells of the bone marrow, gastro-intestinal tract or hair follicles (Minotti *et al.* 2004), which represent a

true limitation for their clinical use. In order to overcome this bottleneck, many research groups, both from academia and industry, have dedicated their efforts to develop strategies to simultaneously circumvent side effects and increase the efficacy of chemotherapeutic agents.

The advent of nanotechnology introduced the possibility to manipulate different materials at the nanoscale level, rendering a variety of structures with different applications in areas such as cell-based therapies or cancer therapy and diagnosis. At the nanoscale level (between 1 and 100 nm), materials present unique physical, chemical and biological features which differ significantly from bulk materials (Ranganathan *et al.* 2012). In particular, several biocompatible nanocarriers have been long-making their way through the nanotechnology field, holding the promise to keep revolutionizing cancer treatment (Peer *et al.* 2007; Duncan *et al.* 2011).

Several nanomedicines have been developed over the years as drug delivery entities, including carbon nanotubes, polymer therapeutics, dendrimers, liposomes, metal particles, among others, many of them going into clinical trials (Peer *et al.* 2007; Wang *et al.* 2012). Based on the intrinsic properties of the tumor microenvironment, such nanoparticles are being developed to provide increased stability of the entrapped drug, by preventing early degradation, and modify and control the pharmacokinetics, an essential feature to circumvent toxicity and favoring the biodistribution profile towards the tumor (Peer *et al.* 2007). In this respect, liposomes stand in the leading edge of nanocarrier development.

1.3.1 Enhanced Permeability and Retention effect – the foundation of nanopharmaceutical tissue targeting

1.3.1.1 Liposomes: the 1st generation

The development of innovative systems for drug delivery started long ago as a means to solve the toxicity profile of a leading edge antitumor agent, doxorubicin

(DXR). This potent drug has a broad spectrum activity against many solid tumors, as well as leukemias (Minotti *et al.* 2004). However, its clinical use in humans is associated with severe dose-limiting cardiotoxicity (Minotti *et al.* 2004). In the early days, the "first generation" of liposomes viewed their most successful iteration with the encapsulation of doxorubicin by Gabizon *et al.* in 1982. The authors demonstrated that neutral and negatively charged liposomes (termed OLV-DOX) were able to retain doxorubicin and decrease the accumulation in cardiac tissues, thus minimizing cardiotoxicity (Gabizon *et al.* 1982). However, a series of drawbacks culminated with the demonstration that the OLV-DOX liposome technology had poor pharmacokinetic parameters in humans, setting forth extended drug leakage from the particle, which potentially could result in undesired cardiotoxicity (Gabizon *et al.* 1991). In addition, classical (without surface hydrophilic polymers) liposomes faced extensive clearance by the mononuclear phagocytic system (MPS) (Wang *et al.* 2012), following adsorption of opsonins (Immordino *et al.* 2006). Such shortcomings diminished the expectations of the successful application of liposomes into the clinics at that time (Barenholz 2012). Nonetheless, several years later, confidence was once regained upon the introduction of a technological innovation that would change that scenario.

1.3.1.2 PEGylated liposomes: enhancing EPR-driven tumor accumulation

Nanotechnology-based drug delivery studies, namely with liposomes, established that longer blood circulation times translate into an increased drug accumulation of nanoparticles in solid tumors. This associated with altered pharmacokinetics and biodistribution profiles of the latter, which are closely related to the physico-chemical properties of the nanotechnology. Such improvements render an increase in safety for the clinical use of otherwise extremely toxic chemotherapeutics. This rationale was supported by the technological development protagonized by PEG [poly(ethylene) glycol polymer]

and translated into the concomitant approval of Doxil® by the Food and Drug Administration (FDA) in 1995. This was a revolutionary accomplishment, which brought a boost of confidence into liposome technology for medical applications.

Doxil® belongs to the "second generation" of liposomes, featuring long blood circulation times, a feature attained by modulation of the lipid composition, especially by engraftment of a PEG-derived lipid. It was reasoned that the hydrophilic cloud around the liposomes enabled by PEG, minimized opsonization and blood clearance by the MPS system (Lasic *et al.* 1991; Papahadjopoulos *et al.* 1991; Sapra *et al.* 2003). The resulting extended blood half-lives led to increased drug accumulation in solid tumors while reducing toxicity in non-target organs. This passive tumor targeting was conceptualized by Maeda as the *enhanced permeability and retention* (EPR) effect (Figure 1.3).

The specific tumor structure presents an extensive network of dysfunctional and leaky blood vessels, resulting from persistently activated angiogenesis. The leaky vessel structure (with fenestrae up to 600 nm) combined with poor tumor lymphatic drainage originates the EPR effect, enabling the passive accumulation of nanosystems (either lipid-based or polymeric) at the tumor site (Matsumura *et al.* 1986; Maeda 2010; Maeda *et al.* 2011). Additionally, those modifications led to dose-independent drug blood clearance, contrary to classical liposomes, enabling accurate *in vivo* prediction of drug levels (Allen *et al.* 1991b; Papahadjopoulos *et al.* 1991; Gabizon *et al.* 1994; Sapra *et al.* 2003). Many of the existing nanomedicines explore the features above described and are considered the basis of drug delivery development (Peer *et al.* 2007; Schroeder *et al.* 2012; Wang *et al.* 2012).

Doxil® entered a "first in man" study revealing similar pharmacokinetics to preclinical studies, with extended half-lives, slow plasma clearance and efficient drug retention (Gabizon *et al.* 1994), culminating with the approval by FDA in 1995 for Kaposi's sarcoma, then followed by recurrent ovarian cancer, metastatic breast cancer and multiple myeloma (Barenholz 2012). Indeed, Doxil®

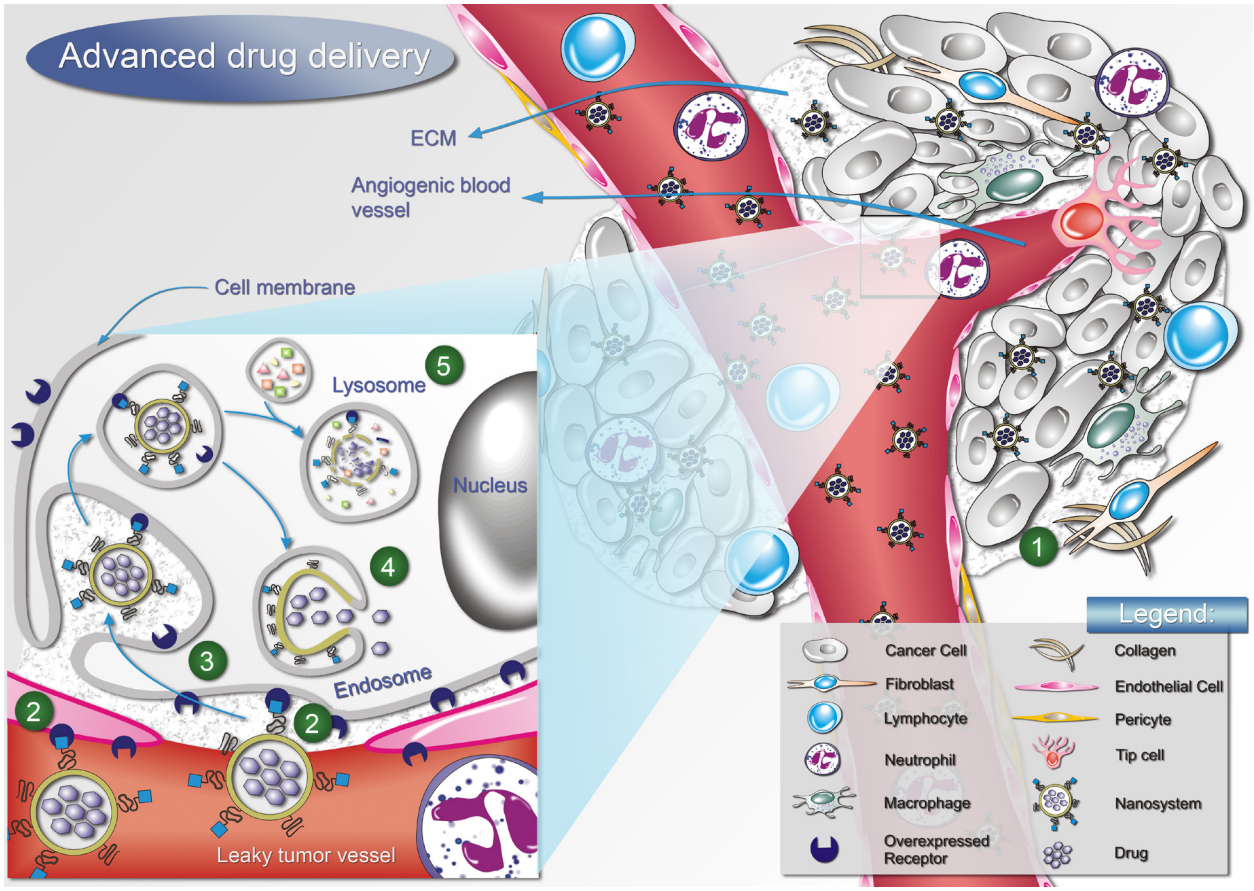

Figure 1.3 – Advanced drug delivery systems and their interaction with tumor microenvironment.

(1) Passive Targeting. Upon systemic administration, the long circulating nanoparticles, either liposomes or polymeric particles, accumulate at the tumor site mainly due to the EPR effect, a contribution of blood vessel leakiness derived from sustained angiogenesis activation and poor lymphatic drainage. **(2) Active Targeting.** Active targeting using different moieties to recognize overexpressed receptors in tumor cells (either cancer cells, or even cells from the tumor stroma), represents an approach with great potential to cope with unspecific toxicity and increased therapeutic efficacy. **(3) Nanosystem internalization.** To allow a successful intracellular delivery of the payload, nanosystems should employ a targeting moiety able to promote ligand specific cell internalization and act as a controlled release depot in the target cells. **(4) Endosomal escape.** Cell internalization *per se*, does not guarantee the increased efficacy. The system should be engineered to promote drug release from the endosomal compartment, therefore increasing drug intracellular bioavailability, while avoiding or limiting **drug degradation in the lysosomes (5)**, an important aspect for siRNA intracellular delivery.

demonstrated similar efficacy against metastatic breast cancer when compared to free doxorubicin, but with significantly lower cardiotoxicity (O'Brien *et al.* 2004).

The combined use of PEGylated liposomal doxorubicin with other drugs is also being explored as a mean to increase treatment efficacy. Recently, Doxil® combined with carboplatin demonstrated better therapeutic index with less toxicity than the combination of paclitaxel and carboplatin for the treatment of ovarian cancer in the elderly (Kurtz *et al.* 2011). In another trial, a modified combination of bortezomib, dexamethasone and PEGylated liposomal doxorubicin demonstrated improved tolerability, while maintaining a good response in the treatment of multiple myeloma compared to standard therapy (Berenson *et al.* 2011).

Recently developed, a PEGylated formulation employing an innovative irinotecan stabilization strategy based on highly negatively charged sucrose octasulfate (Nanoliposomal CPT-11) demonstrated increased efficacy against intracranial glioblastoma xenografts (Drummond *et al.* 2006; Chen *et al.* 2013b). These results supported a phase 1 clinical trial evaluation in patients with recurrent high-grade gliomas, to which patient recruitment is ongoing (NCT00734682).

However, applications of PEGylated liposomes extend beyond the delivery of small drugs. Efforts have been made in order to use such nanoparticles for the delivery of siRNA for gene silencing therapy (recently reviewed by Gomes-da-Silva *et al.* (Gomes-da-Silva *et al.* 2012a; Gomes-da-Silva *et al.* 2013c)).

1.3.1.3 Liposomes: the 1st generation strikes back

Doxil® marketing created the opportunity for the approval of other formulations, including classical liposomal formulations (Barenholz 2012), as Myocet™ and Daunoxome®, containing doxorubicin and daunorubicin, respectively (Immordino *et al.* 2006). These formulations have in common the presence of cholesterol in their composition, in an attempt to modulate their fluidity and lipid packing, as it influences the type of proteins that opsonize liposomes upon intravenous administration (Chonn *et al.* 1992). The increased rigidity introduced by cholesterol in Daunoxome® or Myocet™ decreased the extent of uptake by the

MPS, either *in vitro* or *in vivo*, decreasing drug accumulation in the heart, despite the demonstration of dose-dependent blood clearance when compared to PEGylated doxorubicin, which renders delivered-dose prediction more difficult (Gabizon *et al.* 1989; Allen *et al.* 1991a; Gabizon *et al.* 1994).

Myocet™ has been approved as first line treatment for metastatic breast cancer, in combination with cyclophosphamide (Leonard *et al.* 2009). In patients with metastatic breast cancer, the levels of doxorubicin in plasma were higher for Myocet™ than for free doxorubicin, which translated to lower of both blood clearance and volume of distribution (Swenson *et al.* 2003). Such profile contributed to lower cardiotoxicity of doxorubicin, without significantly compromising efficacy relative to the free drug (Batist *et al.* 2001; Harris *et al.* 2002).

As Doxil®, Daunoxome® is currently approved for HIV-related Kaposi's sarcoma (Petre *et al.* 2007). Its lipid formulation, incorporating only distearoylphosphatidylcholine and cholesterol, presents an approximately neutral charge and small size (45 nm) which are essential to MPS avoidance and longer blood circulation times (Petre *et al.* 2007). Clinically, Daunoxome® demonstrated improved pharmacokinetics when compared to daunorubicin with significant antitumor activity (Gill *et al.* 1995). Importantly, Daunoxome® combined with granulocyte colony-stimulating factor (FLAG) has demonstrated improved treatment response in pediatric relapse acute myeloid leukemia (AML) (Kaspers *et al.* 2013).

More recently, Marqibo®, a liposomal formulation of vincristine received FDA approval under the agency's accelerated approval program (APP). Its referenced indication includes a rare subtype of acute lymphoblastic leukemia (ALL), the Philadelphia chromosome (Ph) negative ALL (clinical trial NCT00495079). Two previous studies confirmed the reduced toxicity profile and efficacy of Marqibo®, either alone or in combination with dexamethasone (Thomas *et al.* 2006; Thomas *et al.* 2009). A phase 3 trial is ongoing to assess its use in the elderly for the

treatment of newly diagnosed ALL (clinical trial NCT01439347).

In Table 1.1, examples of some of the most relevant EPR-based nanosystems are presented, including for polymer-protein and polymer-drug conjugates, as well as polymeric micelles.

1.3.1.4 Limitations of EPR-based strategies

All stated examples have represented a huge benefit for patients, mainly by minimizing severe free chemotherapeutics-associated side effects. However, some hurdles need still to be addressed as the described EPR-based strategies present their own toxicity profile. One classical example is the Palmar Plantar Erythrodysthesia associated with the use of PEGylated liposomes containing doxorubicin, with a dose-dependent severity (Lorusso *et al.* 2007). Additionally, the heterogeneity of EPR in solid tumors of diverse histological origin, as well as within the same tumor, limits a broader implementation of nanomedicines (Prabhakar *et al.* 2013). This evidences the need for other principles to modulate drug delivery (Kamaly *et al.* 2012; Duncan *et al.* 2013).

1.3.2 Modeling intracellular and extracellular drug release: improving biovailability

Aiming at enhancing safety and efficacy by improving drug specificity of action at the tumor level, technologies that enhance drug release from PEGylated liposomes are being developed, including pH-sensitive and thermosensitive liposomes (Karanth *et al.* 2007; Li *et al.* 2013) as well as targeted and/or drug combinatorial approaches (discussed in sections *1.3.3* and *1.3.4*, respectively).

pH-sensitive liposomes have been engineered in such way that they are stable at physiological pH, but undergo destabilization and acquire fusogenic properties under acidic conditions, following receptor-mediated endocytosis, thus releasing their aqueous contents (Simoes *et al.* 2004). Numerous studies have reported applications of pH-sensitive liposomes for transport and intracellular delivery of

Table 1.1 – Nanotechnological platforms based on EPR effect.

Type	Mechanism	Brand/code name	Company	Formulation	Indication	Clinical Status	Trial/ref
Passive targeting							
Liposome	EPR	DOXIL®	Johnson&Johnson	PEGylated liposomal doxorubicin	Kaposi's Sarcoma	Approved	
					Recurrent ovarian cancer		
					Metastatic brest cancer		
					Multiple myeloma		
		MYOCET™	Cephalon	Liposomal Doxorubicin	Metastatic brest cancer	Approved	
		DAUNOXOME®	Galen	Liposomal Daunorubicin	Kaposi's Sarcoma	Approved	
		MARQIBO®	Talon Therapeutics Inc	Liposomal vincristine	Ph chromosome negative ALL	AAP	NCT00495079
					ALL in elderly	Phase 3	NCT01439347
		TKM-PLK1	Tekmira Pharmaceuticals	Liposomal siRNA against PLK1	Solid tumors	Phase 1	NCT01262235
		Nanoliposomal CPT-11		Liposomal Camptothecin-sucrose octusulte complex	High-grade glioma	Phase 1	NCT00734682
	Modeled release (EPR driven)	THERMODOX®	Celsion	Thermosensitive liposomes (Doxorubicin)	Breast cancer recurrence	Phase 1/2	NCT00826085
					Hepatocellular carcinoma	Phase 3	NCT00617981
					Primary/metastatic liver cancer	Phase 1	NCT00441376
	Drug combination (EPR driven)	CPX-351	Celator Pharmaceuticals	Liposomal combination cytarabine and daunorubicin (5:1)	AML in elderly	Phase 2	NCT00788892
					AML relapse		NCT00822094
Polymeric nanomedicines	Mainly EPR	ZINOSTATIN STIMALER®	Yamanuchi	Neocarzinostatin SMANCS	Hepatocellular carcinoma	Approved	
		ONCASPAR®	Sigma-Tau Pharmaceuticals, Inc.	PEG-L-asparaginase construct	Acute lymphoblastic leukemia	Approved	
		NEULASTA®	Amgen	PEGylated-recombinant methionyl human granulocyte colony-stimulating factor	Severe cancer chemotherapy-induced neutropaenia	Approved	
		PEGASYS®	Genentech	PEGylated interferon (IFN)-alfa(α)-2a	Chronic myeloid leukemia	Phase 2	NCT01392170
					Kidney cancer	Phase 1/2 (completed)	NCT00003542
		PEGINTRON®	Merck & Co., Inc	PEGylated interferon (IFN)-alfa(α)-2b	Unresectable or Metastatic Kidney Cancer	Phase 2 (completed)	NCT00467077
					Recurrent Ovarian Cancer	Phase 1/2	NCT01637532
					Head and Neck Cancer	Phase 2 (completed)	NCT00276523
		PK1	CRC/Pharmacia	Doxorubicin-HPMA-galactosamine conjugate	Advanced breast cancer	Phase 2	NCT00003165
		PK2	CRC/Pharmacia	Doxorubicin-HPMA conjugate	Liver Hepatoma	Phase 1	
		PNU166945	Pharmacia	Paclitaxel-HPMA copolymer	Refractory solid tumors	Phase 1	
		MAG-CPT	Pharmacia	Camptothecin-HPMA copolymer	Solid tumors	Phase 1	NCT00004076
		AP5280	Access Pharmaceuticals Inc	Platinate-HPMA copolymer	Solid tumors	Phase 1	(Rademaker-Lakhai, Terret et al. 2004)
		PROLINDAC®	Access Pharmaceuticals Inc	DACH-platinum-HPMA copolymer	Solid tumors	Phase 1	NCT00415298
		OPAXIO™	Cell Therapeutics Inc	polyglutamate-paclitaxel	Non-small cell lung cancer in Women	Phase 3	NCT00576225
					Advanced Ovarian or Primary Peritoneal or Fallopian Tube Cancer	Phase 3	NCT00108745
					Head and Neck Cancer	Phase 1/2	NCT00660218
					Glioblastoma multiforme	Phase 2	NCT01402063
		CRLX101	Cerulean Pharma Inc.	Camptothecin conjugated to Polymeric cyclodextrin(PEG) copolymer	Solid tumors	Phase 1/2	NCT00333502
					Non-small cell lung cancer	Phase 2	NCT01380769
					Renal cell carcinoma	Phase 1	NCT01625936
					Gastric cancers		NCT01612546
		GENEXOL-PM	Samyan Corp	Paclitaxel-loaded Polymeric micelle	Breast cancer	Phase 3	NCT00876486
					Ovarian cancer	Phase 1/2	NCT00886717
					Head and neck cancer	Phase 2	NCT01689194
		NK105	Nippon Kayaku Co.,Ltd.	paclitaxel-incorporating micellar nanoparticle	Breast Cancer	Phase 3	NCT01644890
		NK 911	Nippon Kayaku Co.,Ltd.	PEG–poly(aspartic acid) block copolymer-DXR	Solid tumors	Phase 1	(Matsumura, Hamaguchi et al. 2004)
		SP1049C	Supratek Pharma Inc.	Pluronics micellar formulation of DXR	Esophagus and gastroesophageal adenocarcinoma	Phase 2	(Valle, Armstrong et al. 2011)

AAP – FDA accelerated approval program; AML – acute myeloid leukemia; ALL – acute lymphoblastic leukemia

agents for cancer treatment (Simoes *et al.* 2004; Karanth *et al.* 2007). However, to date no pH-sensitive formulation has reached clinical trials, mainly owing to pH-sensitive liposomes inferior blood circulation profiles as well as lower drug retention capacity relative to non-pH-sensitive counterparts (Ishida *et al.* 2006). This could therefore represent a safety issue, in the sense that free drug would be available in circulation, which potentially would lead to undesired toxicity, besides limiting therapeutic efficacy. Nonetheless, the hidden potential of this type of liposomes could be unlocked if further modifications are introduced, like ligand-mediated targeting towards the tumor vasculature (discussed in section *1.3.3.2*).

Another promising strategy for the extracellular triggered drug release is based on nanosystems with thermosensitive properties. Needham and colleagues formulated a PEGylated thermosensitive drug delivery system containing doxorubicin and a lysolipid optimized for mild hyperthermic temperatures (39 to 40ºC) that are easily achievable in a clinical setting (Needham *et al.* 2000; Needham *et al.* 2001). This novel thermosensitive liposome (marketed as Thermodox®) was significantly more effective than the free drug or the non-thermosensitive counterpart, at reducing tumor growth in a mouse xenograft of a human squamous cell carcinoma line (Gaber *et al.* 1995; Gaber *et al.* 1996).

Two main clinical trials are being performed combining Thermodox® with radiofrequency ablation (RFA) for the treatment of hepatocellular carcinoma (HCC) (Phase 3 clinical trial: NCT00617981), and Thermodox® with hyperthermia in patients with breast cancer recurrences at the chest wall (clinical trial NCT00826085). A case report from the ongoing Phase 3 trial, demonstrated that Thermodox®/RFA combined therapy led to the complete treatment of a HCC patient, thus enabling to envisage the potential of such strategy (Hong *et al.* 2013). Additionally, a phase 1 trial involving Thermodox ® and RFA in patients with primary or metastatic liver cancer has now been completed, demonstrating

a dose-dependent median time to treatment failure (clinical trial NCT00441376) (Poon *et al.* 2011). Other thermal ablative modalities, such as high-intensity focused ultrasound, are also being considered for future combinations with the lyso-thermosensitive liposomal doxorubicin (Poon *et al.* 2011).

1.3.3 Receptor-mediated targeting: "binding" two worlds

Endowing nanotechnology-based delivery systems with the ability to release their payload intracellularly, upon functionalization of their surface with internalizing targeting ligands (Figure 1.3) is a strategy that, after overcoming several biological barriers at the tumor level, might greatly impact therapeutic efficacy (and safety as well) of nanomedicines.

1.3.3.1 Targeting cancer cells

MCC-465 is a PEGylated immunoliposome encapsulating doxorubicin and functionalized with $F(ab')_2$ fragment of human monoclonal antibody GAH (Hamaguchi *et al.* 2004; Matsumura *et al.* 2004). Preclinical studies showed increased antitumor activity against mouse xenografts of several human gastric cancers, relative to DXR alone or its non-targeted counterpart, propelling a phase 1 clinical trial. Results demonstrated that MCC-465 was well tolerated and a phase 2 trial was recommended (Matsumura *et al.* 2004). No recent data supporting this technology was made available to this date.

Two transferrin-targeted liposomal formulations encapsulating oxaliplatin (MBP-426) (Suzuki *et al.* 2008) and p53 gene (SGT53-01) (Xu *et al.* 2001) are also under clinical investigation. MBP-426, developed by Mebiopharm Co., Ltd., is in phase 2 clinical trial (NCT00964080) to assess its efficacy in combination with Leucovorin (water soluble form of folate) and/or 5-FU in patients with metastatic gastric, gastro-esophageal junction or esophageal adenocarcinoma. SGT53-01, of SynerGene Therapeutics, is under phase 1 trial for safety evaluation in combination

with docetaxel (clinical trial NCT00470613) (Wang *et al.* 2012).

Merrimack Pharmaceuticals has under phase 1 clinical trial a novel HER2-targeted liposomal formulation encapsulating doxorubicin, MM-302 (clinical trial NCT01304797). Supporting this decision was the demonstration of increased anti-tumorigenic effects against breast cancer models, with reduced cardiotoxicity, evaluated through cardiomyocyte platform derived from human stem cells (Reynolds *et al.* 2012).

Additionally, in 2008, CALAA-01, a Tf (AD-PEG-Tf)-modified cyclodextrin-containing polymeric nanoparticles, was the first nanoparticle to enter in clinical development (clinical trial NCT00689065) for targeted siRNA delivery in humans (Davis 2009; Davis *et al.* 2010). Despite its potential, the development of CALAA-01 has been recently withdrawn. Nevertheless, this formulation was able to deliver high amounts of siRNA payload with endosomal release of siRNA, following receptor-mediated endocytosis, enabling the iRNA-mediated silencing of M2 subunit of ribonucleotide reductase (RRM2) in humans (Davis 2009; Davis *et al.* 2010). This demonstrates that similar systems should be further explored aiming at optimizing their *in vivo* performance for siRNA delivery.

Common to all these technologies is the targeting component to cancer cells. While in the case of hematological cancers this does not represent a limitation, the same does not hold true regarding solid tumors, since the restricted diffusion within the tumor interstitial space, limits the access to cancer cells in the near vicinity of tumor blood vessels. If, in some cases, that strategy would suffice, in other scenarios a different approach is needed. Thus, more accessible targets or even multi-target approaches are under development.

1.3.3.2 Targeting tumor vasculature and multiple cell subpopulations

Tumor vasculature has a predominant role in tumor development and progression (Hanahan *et al.* 2011). Due to such importance, and given its readily

accessible nature, tumor vasculature targeting has gained notorious interest.

Exploring the differences between mature and tumor angiogenic blood vessels, vasculature targeting is defined as a key strategy against cancer by providing a means to overrule the supporting framework for tumor growth and metastasis. Additionally, tumor vasculature presents itself as a more accessible target than cancer cells, enabling even nanosystems with less favorable kinetics, like pH-sensitive liposomes, to succeed as delivery agents towards solid tumors.

Recently, Moura *et al.* proposed a dual targeted pH-sensitive lipid-based nanoparticle for efficient delivery of chemotherapeutic agents, upon functionalization with the F3 peptide (a.k.a. PEGASEMP™) (Moura *et al.* 2012). It specifically recognizes nucleolin, a membrane protein that is overexpressed in several cancer cells, including those from breast, as well as in cells from the tumor microenvironment, namely endothelial cells in tumor blood vessels (Christian *et al.* 2003; Hovanessian *et al.* 2010; Moura *et al.* 2012). This same strategy has been further applied for the delivery of siRNA (Gomes-da-Silva *et al.* 2012b; Gomes-da-Silva *et al.* 2013a; Gomes-da-Silva *et al.* 2013b).

Pastorino *et al.* have developed a similar dual targeting strategy against neuroblastoma (Loi *et al.* 2010; Pastorino *et al.* 2013). Doxorubicin-loaded liposomes functionalized with peptides containing either NGR or CPRECES motifs were able to target aminopeptidase-N expressing endothelial cells and aminopeptidase A expressing perivascular tumor cells, respectively, enabling increased efficacy against neuroblastoma when compared to non-targeted liposomes (Loi *et al.* 2010; Pastorino *et al.* 2013).

BIND Therapeutics combined ligand-mediated targeting and controlled-release in a polymer-based nanoparticle, BIND-014. BIND-014 is a prostate specific membrane antigen (PSMA)-targeted docetaxel-encapsulated polymeric nanoparticle, which entered phase 1 clinical trials (NCT01300533) in 2011 (Shi *et al.* 2011; Hrkach *et al.* 2012). This nanoparticle takes advantage of the overexpression

of PSMA in both prostate cancer and endothelial cells from tumor vasculature, enabling dual-targeting capacity (Chang *et al.* 1999; Wang *et al.* 2012). Initial clinical results from patients with advanced solid tumors indicate that BIND-014 displays a pharmacological profile distinct from docetaxel, including pharmacokinetic properties consistent with long circulation half-life in blood and retention of docetaxel in the vascular compartments. Two out of 3 patients exhibited tumor shrinkage using 20% to 40% of the free-docetaxel dosage typically administered in clinical practice (75mg/m^2) (Hrkach *et al.* 2012).

In 2005, Abraxane® (nab-paclitaxel) received FDA approval for the treatment of metastatic breast cancer (Gradishar *et al.* 2005). This paclitaxel albumin-bound (nab) nanoparticle is a particular case of active targeting in the absence of a defined ligand, enabling drug delivery through gp60-mediated endothelial transcytosis, a natural albumin-dependent process (Gradishar 2006). Abraxane®, in comparison with Taxol®, demonstrated significantly higher tumor response rates and longer times to tumor progression among metastatic breast cancer patients who did not respond to combination therapy (Gradishar 2005; Gradishar *et al.* 2005). Besides breast cancer, Abraxane® has also been evaluated in clinical trials involving non-small cell lung cancer (NSCLC) and non-hematologic malignancies (Montana *et al.* 2011).

Clinical translation of the aforementioned nanoparticles holds great promise as versatile nanocarriers for a wide range of therapeutics for various biomedical applications, notably in cancer treatment.

In Table 1.2, examples of some of the most relevant receptor-mediated targeting based nanosystems are presented.

1.3.4 Delivery of drug combinations: improving efficacy

Nanotechnology-based delivery systems also allow the delivery of drug combinations and significant improvements to their biodistribution. The

Table 1.2 – Nanotechnological platforms based on receptor-mediated targeting.

Type	Mechanism	Brand/code name	Company	Formulation	Indication	Clinical Status	Trial/ref
Active targeting							
Liposome	Cancer cell targeting	MCC-465	National Cancer Center, Japan	GAH[F(ab')2] immunoliposome (Doxorubicin)	Gastric cancer	Phase 1	(Matsumura, Gotohet al. 2004)
		MBP-426	Mebiopharm Co., Ltd	Transferrin-targeted liposomal oxiplatin	Gastric adenocarcinoma	Phase1/2	NCT00964080
		SGT53-01	SynerGene Therapeutics	Transferrin-targeted liposomal p53 gene	Neoplasm	Phase 1	NCT00470613
		MM-302	Merrimack Pharmaceuticals	Her2-targeted liposomal doxorubicin	Breast cancer	Phase 1	NCT01304797
Polymeric nanomedicines	Dual targeting (cancer and tumor vasculature cell)	BIND-014	BIND Therapeutics	(PSMA)-targeted docetaxel-encapsulated polymeric nanoparticle	Advanced or metastatic cancer	Phase 1	NCT01300533
					Prostate cancer	Phase 2	NCT01812746
					Non-small cell lung cancer	Phase 2	NCT01792479
	Cancer cell targeting	CALAA-01	Arrowhead Research Corp.	Transferrin targeted cyclodextrin formulation of siRNA	Solid tumors	Phase 1	NCT00689065 (Terminated)
Protein-based nanosystem	Tumor endothelial cell transcytosis	ABRAXANE®	Celgene Corp.	Albumin bound paclitaxel	Metastatic breast cancer	Approved	
					Recurrent and Refractory Lymphoma	Phase 1/2	NCT01555853
					Metastatic Pancreatic Cancer	Phase 2	NCT01461915

combination of different chemotherapeutics is a widely adopted strategy in cancer treatment, in order to overcome drug resistance (Pinto *et al.* 2011). When combined, anticancer drugs can lead to a synergistic, additive or antagonist effect against tumor cells *in vivo*, depending on the molar ratios of each individual agent at the tumor site (Mayer *et al.* 2006). However, the translation of their interaction from *in vitro* to an *in vivo* setting is impaired by the specific pharmacokinetic pattern of each of the agents in the combination, as it will subsequently compromise the needed (synergistic) drug ratio to reach the tumor (Mayer *et al.* 2006; Feldman *et al.* 2011). In this respect, the pharmacological properties of those combinations can be improved upon their encapsulation into nanotechnology-based delivery systems, such as liposomes, designed to alter the biodistribution of their associated drugs (Mayer *et al.* 2006; Tardi *et al.* 2009a).

CPX-351 is a liposomal formulation from Celator Pharmaceuticals, which retains, *in vivo*, the synergistic drug ratio of cytarabine and daunorubicin, at 5:1 molar ratio (Mayer *et al.* 2006; Tardi *et al.* 2009a). A phase 1 dose escalation trial of CPX-351 showed promising anti-leukemic activity through complete remission in patients with advanced previously treated hematological malignancies (Feldman *et al.* 2011). Celator Pharmaceuticals has now completed two randomized phase

2 clinical trials (clinical trials NCT00788892 and NCT00822094). Data from NCT00788892 study, for the treatment of AML in elderly, demonstrated that CPX-351 had increased response rate when compared to control group, with acceptable toxicity, supporting its entry in a phase 3 trial (Lancet *et al.* 2014). Data from the second study, suggested that CPX-351 may increase the outcome for first-relapse poor-risk AML patients (Cortes *et al.* 2014). Another promising candidate for clinical development is CPX-571. This liposomal formulation encapsulates irinotecan and cisplatin, a drug combination used in the treatment of small-cell lung cancer (Noda *et al.* 2002; Tardi *et al.* 2009b). The first studies on CPX-571 showed a superior antitumor activity of the liposome containing a 7:1 molar ratio of the doublet over the free drug cocktail in different tumor models. Furthermore, CPX-571 presented an overall efficacy, consistent with *in vivo* synergy, in a range of human tumor xenografts, including an irinotecan-resistant model (Tardi *et al.* 2009b).

1.3.5 Nanosystem development for targeted delivery of drug combinations

The success of Celator Pharmaceuticals technologies points out the fact that *in vivo* translation of ratiometrically designed drug combinations presents an enormous therapeutic potential (Dicko *et al.* 2010). Those strategies are based on the simultaneous encapsulation of both drugs in the inner aqueous core of liposomes. Though elegant, this strategy may limit the number of loaded drug molecules as well as the combined administration of hydrophobic drugs (Zucker *et al.* 2009). An alternative approach may be carried out upon allocating one of the drugs in the liposomal membrane and the second drug in the aqueous core, thus enabling the simultaneous delivery of hydrophobic and hydrophilic drugs (Khazanov *et al.* 2008). Additionally, the load capacity of each liposome could be stretched to its maximum at both system phases (aqueous core and membrane), enabling high loading of a ratiometric drug combination *per* single liposome.

Among others, sphingolipids are highly hydrophobic molecules that have been described as apoptotic (Khazanov *et al.* 2008; Hannun *et al.* 2011).

1.3.5.1 Combining ceramides and small drugs into nanosystems: towards targeted delivery

Ceramides are one family of bioactive sphingolipids involved in several metabolic and cellular processes, including apoptosis (Carpinteiro *et al.* 2008; Hannun *et al.* 2011). They can be *de novo* synthesized from palmitate and serine in the endoplasmic reticulum or can be derived from sphingomyelin upon phosphocoline removal by sphingomyelinase (SMase) (Hannun *et al.* 2008; Giussani *et al.* 2014). Ceramides might go through further modifications and enter in different signaling pathways as messengers (Hannun *et al.* 2008; Canals *et al.* 2011; Giussani *et al.* 2014). Examples of these modifications are glycosylation, upon the action of glucosylceramide synthase (GCS), leading to the production of glucosylceramides or the synthesis of sphingosine-1-phosphate (S1P) (Giussani *et al.* 2014). Both processes have been implicated in cancer cell death resistance, owing to depletion of pro-apoptotic ceramides and accumulation of pro-survival glucosylceramides and S1P (Giussani *et al.* 2014).

Indeed, ceramide deprivation followed by GCS elevation has been related to doxorubicin resistance, in part by GCS-promoted upregulation of MDR1 expression, the gene encoding P-glycoprotein (Gouaze-Andersson *et al.* 2007; Liu *et al.* 2008; Liu *et al.* 2010b). Interestingly, ceramide glycosylation mediated by GCS has been described to uphold breast CSC properties (Gupta *et al.* 2012). The pro-apoptotic nature of ceramides seems to be related to their action on PI3K/Akt pathway as well as at the mitochondria level. Ceramides have been described to inhibit Akt activation leading to $p27^{kip1}$ expression, activation of p38 MAPK and BAX-mediated apoptosis (Kim *et al.* 2008; Arboleda *et al.* 2010; Kim *et al.* 2010). Alternatively, ceramides induce channel opening in the mitochondria leading

to cytochrome c release, a process that can be reverted by anti-apoptotic Bcl-2 family proteins (Siskind *et al.* 2000; Siskind *et al.* 2002; Siskind *et al.* 2006; Siskind *et al.* 2008).

Regardless the mechanism of action, the pro-apoptotic nature of ceramides has been explored for therapeutic intervention either alone or in combination (Giussani *et al.* 2014). In fact, ceramides have been combined with either doxorubicin or tamoxifen increasing the efficacy and sensibility of cancer cells to those drugs (Ji *et al.* 2010; Morad *et al.* 2013). However, ceramides hydrophobic nature limits their application *in vivo*. As such, nanodelivery systems like liposomes represent an interesting approach to unlock their *in vivo* therapeutic potential. Liposomal delivery of short-chain ceramides, such as C6-ceramide, has been described to induce apoptosis and arrest tumor growth in breast cancer models (Stover *et al.* 2003; Stover *et al.* 2005). Liposomal apoptotic short-chain ceramides have been combined with sorafenib to synergistically increase melanoma and breast cancer cell death, thus halting tumor development (Tran *et al.* 2008). Additionally, co-encapsulation of C6-ceramide and doxorubicin has shown to increase the lifespan of colon tumor bearing mice (Khazanov *et al.* 2008). Notwithstanding, the described nanosystems lack specific cellular delivery. In this respect, Koshkaryev *et al.* have demonstrated that transferrin-modified liposomes encapsulating C6-ceramide induced increased apoptosis in an ovarian cancer model, an effect mediated by ceramide-induced lysosomal membrane permeabilization and catehpsin D release (Koshkaryev *et al.* 2012).

Overall, the above-mentioned studies have in common the demonstration of a successful pathway towards the development of targeted nanosystems for the specific cellular delivery of drug combinations, using ceramides as a common denominator.

1.4. State-of-the-art overview and project aims

From the current state-of-the-art aforementioned, it is clear that cancer treatment represents a massive challenge owing to intricate relationships established in the tumor microenvironment, where cells, signaling molecules and signaling cascades cooperate in an unstable genetic playground leading to constant variability and therapeutic evasion. As such, single targeting of one altered pathway or cell population is not sufficient. Instead, simultaneous and multi-targeting at several levels of tumor organization should be considered for successful therapeutic intervention. In a position to address this need, nanotechnology-based therapies are at the forefront for cancer treatment.

In the last decades, with the growing interest and advances in the nanotechnology field, there has been a progressive increase in the number of nanoparticle-based therapeutics approved for clinical use. Currently, there are approximately 250 nanomedicine agents in different stages of preclinical and clinical development, with two-thirds of the investigational applications related to cancer treatment (Etheridge *et al.* 2012). These numbers clearly demonstrate the impact of nanotechnology in the landscape of medicine and pharmaceutical industry. Particularly, the drug delivery field has been the one collecting more benefits from nanotechnology-driven research and development. It has enabled a renewed interest on drugs with a narrow therapeutic window or poor pharmacokinetics, left either as last choice or even completely abandoned.

In the context of the current state-of-the-art, and exploiting key features of the tumor microenvironment and combining them into a unique nanoliposomal formulation, the current project aimed at:

- the establishment of synergistic ratios between doxorubicin, a cornerstone drug for the treatment of breast cancer, and the pro-apoptotic sphingolipid C6-ceramide;

- the development of F3 peptide-targeted and triggered release liposomes that could enable nucleolin-mediated endocytosis of the developed synergistic drug combination into putative breast CSC, besides other tumor cells, ultimately envisaging increased anti-tumor efficacy.

Chapter 2

Simultaneous active intracellular delivery of doxorubicin and C6-ceramide shifts the additive/antagonistic drug interaction of non-encapsulated combination

This chapter has been accepted for publication in:

Fonseca, N. A., Gomes-da-Silva, L.C., Moura, V., Simoes, S. and Moreira, J. N. **(2014)** *Simultaneous active intracellular delivery of doxorubicin and C6-ceramide shifts the additive/antagonistic drug interaction of non-encapsulated combination.* J Control Release

Abstract

Drug resistance remains the Achilles tendon undermining the success of chemotherapy. It has been recognized that success requires the identification of compounds that, when combined, lead to synergistic tumor inhibition while simultaneously minimizing systemic toxicity. However, *in vivo* application of such protocols is dependent on the ability to deliver the appropriate drug ratio at the tumor level. In this respect, nanotechnology-based delivery platforms, like liposomes, offer an elegant solution for the *in vivo* translation of such strategy.

In this work, we propose the active intracellular delivery of combinations of doxorubicin and the pro-apoptotic sphingolipid, C6-ceramide, using our previously described cytosolic triggered release-enabling liposomes, targeting nucleolin with the F3 peptide.

Combination of doxorubicin (DXR):C6-ceramide (C6-Cer) at 1:2 molar ratio interacted synergistically against drug resistant/triple negative MDA-MB-231 breast cancer cells, as well as drug sensitive MDA-MB-435S melanoma cells. Cell viability studies indicated that F3-targeted liposomes encapsulating DXR:C6-Cer 1:2 molar ratio (p[F3]DC12) performed similarly as targeted liposomal DXR (p[F3]SL), encapsulating twice the amount of DXR, at the IC_{50}, for an incubation time of 24 h. Importantly, F3-targeted liposomes encapsulating DXR:C6-Cer 1:2 molar ratio (p[F3]DC12) enabled a cell death above 90% at 24 h of treatment against both DXR-resistant and sensitive cells, unattainable by the F3-targeted liposomal doxorubicin. Furthermore, a F3-targeted formulation encapsulating a mildly additive/antagonistic DXR:C6-Cer 1:1 molar ratio (p[F3]DC11) enabled an effect above 90% for an incubation period as short as 4 h, suggesting that delivery route at the cell level may shift the nature of drug interaction. Such activity, including the one for p[F3]DC12, induced a marked cell and nucleus swelling at similar extent, consistent with necrotic cell death.

Overall, these results demonstrated that F3-targeted intracellular delivery of different DXR/C6-Cer ratios, with diversed drug interactions, enabled a highly relevant increased efficacy against chemotherapy resistant cells.

2.1. Introduction

As global cancer burden continues to increase, 1.6 million new cancer cases were expected in 2013, from which approximately 0.58 million deaths were estimated only in US (Jemal *et al.* 2011; Siegel *et al.* 2013). Chemotherapy still represents the cornerstone treatment of disseminated malignancies. Nonetheless, drug resistance remains as the Achilles tendon undermining the success of chemotherapy, mainly owing to molecular and cellular heterogeneity within the tumor microenvironment (Saeki *et al.* 2005; Hanahan *et al.* 2011). One of the attempts to solve this problem is the combination of drugs near to their maximum tolerated dose (MTD), often exposing patients to unacceptable toxicity. Alternatively, it has been recognized that success requires the identification of compounds that, when combined, lead to synergistic tumor inhibition while simultaneously minimizing systemic toxicity (Ramaswamy 2007; Dicko *et al.* 2010).

One of the most important pathways deregulated in cancer is the PI3K/Akt signaling cascade (Baselga 2011). In several murine models of cancer, inhibition of PI3K/Akt signaling retards tumorigenesis by restoring the apoptotic sensitivity of cancer cells to chemotherapeutic agents (Courtney *et al.* 2010). In this respect, ceramides are one of the most promising drugs, which have been described to inhibit the PI3K/Akt pathway both in HL-60 leukemia cells (Kim *et al.* 2008) and in PC-3 prostate cancer cells (Kim *et al.* 2010). However, the intracellular activity of ceramides is challenged by glucosylceramide synthase (GCS), an enzyme that converts pro-apoptotic ceramides into inactive glucosylceramides (Uchida *et al.* 2004; Gouaze *et al.* 2005; Liu *et al.* 2010b). In addition, GCS has been related with doxorubicin (DXR) resistance, by modulation and depletion of doxorubicin-induced ceramide levels (Uchida *et al.* 2004; Liu *et al.* 2008). This intrinsic relation, supports the addition of exogenous ceramides concomitantly with doxorubicin, to counteract GCS-mediated pro-apoptotic sphingolipid depletion, which along

with ceramide-mediated PI3K/Akt modulation could enable increased efficacy at lower chemotherapeutic doses (Ji *et al.* 2010). Additionally, it has been demonstrated that ceramides impair angiogenesis, the formation of new blood vessels from pre-existing ones, an important component in the tumor microenvironment dynamics which supports tumor growth (Bansode 2011; Hanahan *et al.* 2011; Bocci *et al.* 2012). Therefore, impairing cellular and biological functions of tumors using synergistic combinations of drugs like ceramides and doxorubicin, could translate into an increased gain in efficacy upon acting at different levels of the tumor microenvironment. However, *in vivo* application of such protocols is highly dependent on the ability to synchronize the pharmacokinetics of each individual drug present in the combination, thus enabling the tumor accumulation of a synergistic drug cocktail (Mayer *et al.* 2006), namely at the intracellular level of targeted tumor cells. Nanotechnology-based delivery platforms, such as liposomes, upon the extracellular release of a encapsulated drug combination, have shown increased efficacy in murine models of cancer (Mayer *et al.* 2006; Tardi *et al.* 2009a) as well as in a first-in-man study against acute myeloid leukemia (Lim *et al.* 2010; Feldman *et al.* 2011).

Considering the state-of-the-art, the present work aims at selecting a synergistic drug combination between C6-ceramide and doxorubicin and assessing the impact of its intracellular delivery using the F3 peptide-targeted pH-sensitive lipid-based nanoparticle, developed by our group (Moura *et al.* 2012). The F3 peptide enables specific recognition of nucleolin, a protein highly expressed in cancer cells and endothelial cells of tumor angiogenic blood vessels (Srivastava *et al.* 1999; Christian *et al.* 2003; Shi *et al.* 2007; Hovanessian *et al.* 2010). Synergy will be established using the median-effect analysis proposed by Chou and Talalay (Chou *et al.* 1984; Chou 2006; Chou 2011), against cancer cell models, including a drug resistant breast cancer triple negative model and a drug sensitive melanoma model.

2.2. Results

2.2.1 Cytotoxicity of individual drugs against cancer cell lines of diverse histological origin

Assessment of single cytotoxicity of the drugs in study is a requirement for the establishment of their nature of interaction using the median-effect analysis (Chou 2006). Fulfilling that requisite, triple negative breast cancer MDA-MB-231 and melanoma MDA-MB-435S (Rae et al. 2007) cell lines were incubated with serial dilutions of either DXR or C6-ceramide for 24 h at 37°C, in an atmosphere of 5% CO_2. The former was clearly more resistant to DXR than the latter (IC_{50} = 1.66 μM versus IC_{50} = 0.40 μM; Figure 2.1, A versus C), in contrast to the higher sensitivity to C6-Ceramide (IC_{50} = 6.15 μM versus IC_{50} = 11.5 μM; Figure 2.1, B versus D, respectively). Expectedly, the described inactive analogue, C6-dihydroceramide, presented a significantly lower activity than C6-Ceramide (corresponding to a 10-fold higher IC_{50}), rendering it unconsidered for subsequent studies (data not shown).

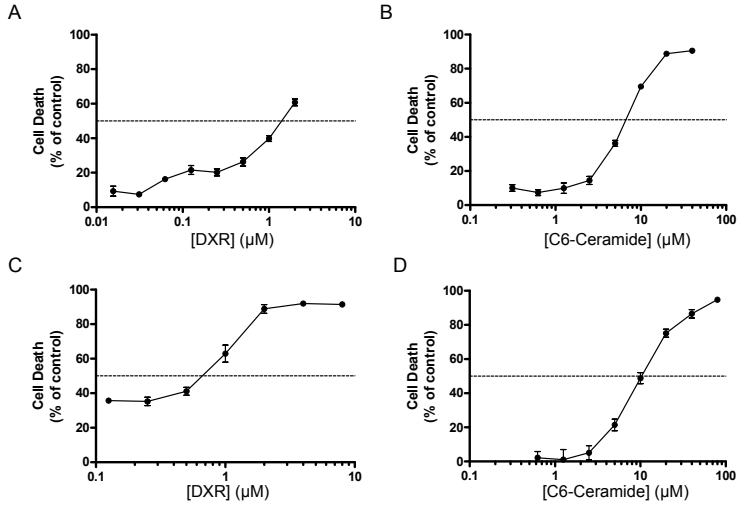

Figure 2.1 – Cytotoxicity of free doxorubicin (DXR) and C6-ceramide (C6-Cer) against breast and melanoma cancer cell lines. DXR or C6- ceramide (in serially diluted concentrations) were incubated for 24 h at 37ºC with either MDA-MB-231 (A and B, respectively) or MDA-MB-435 (C and D, respectively) breast cancer or melanoma cell lines respectively, and the experiment was further prolonged for 72 h after which cell death was assessed by the MTT assay. Dose-response curves represent the mean ± SEM for each concentration tested. Doted-line: 50% of cell death.

2.2.2 Establishment of synergistic combinations of doxorubicin and C6-ceramide

In order to assess the nature of interaction between the two drugs, different doxorubicin (DXR):C6-ceramide (C6-Cer) ratios, from 1:40 to 5:1, were tested, using the MDA-MB-231 breast cancer and MDA-MB-435S melanoma cell lines. Data generated from the *in vitro* screening were analyzed using the median-effect method described by Chou and Talalay (Chou 2006; Chou 2011). With this method, the combination index (CI), a measurement of the nature of interaction between the two drugs, has been determined. A combination index of <1, ≈1 or >1, corresponds to a synergistic, additive or antagonistic interaction, respectively.

The results indicated that the combination of doxorubicin and C6-ceramide exhibited synergistic activity (Figure 2.2). Interestingly, the nature of the interaction

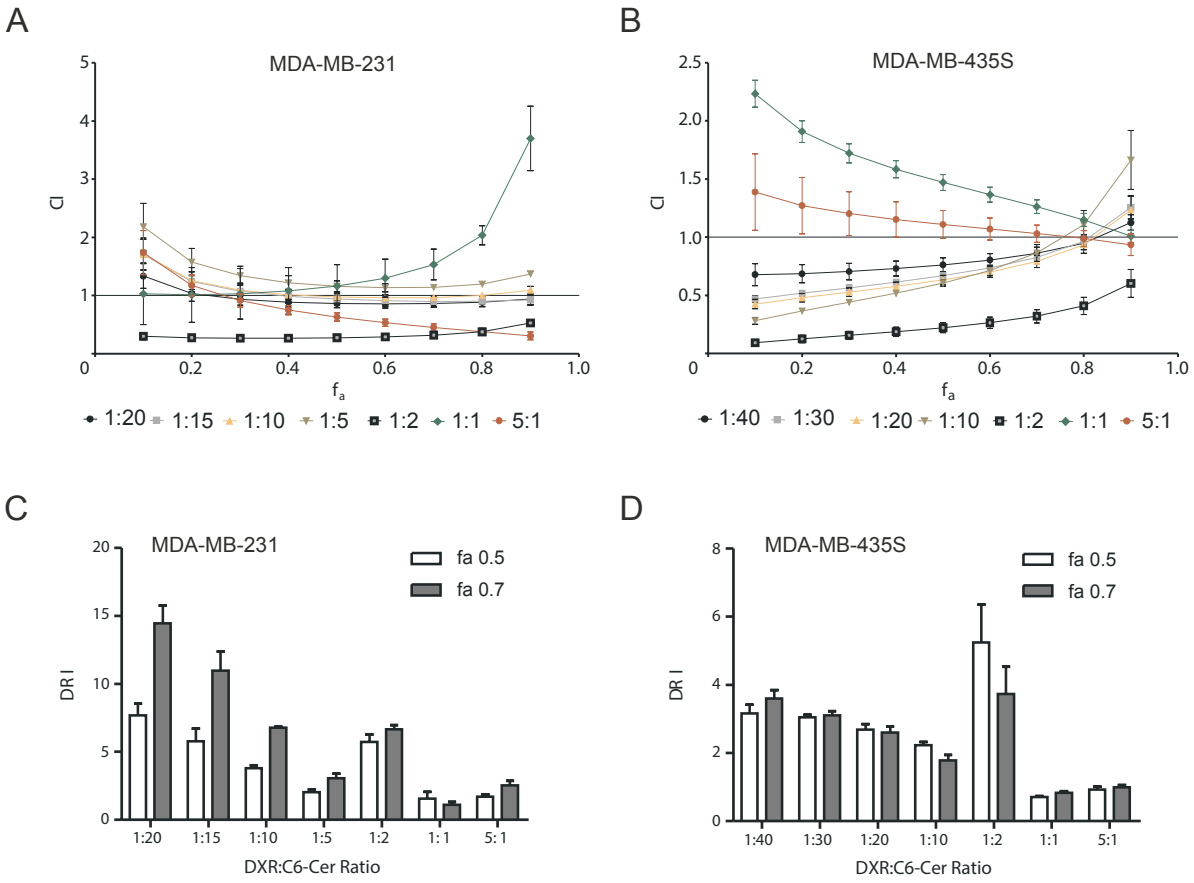

Figure 2.2* - In vitro *screening for synergy of different doxorubicin (DXR):C6-ceramide (C6-Cer) ratios.

Following incubation with different doxorubicin (DXR):C6-ceramide (C6-Cer) molar ratios, from

1:40 to 5:1, the nature of the interaction between the two drugs was assessed against MDA-MB-231 breast cancer or MDA-MB-435S melanoma cell lines (A and B, respectively) as well as the Dose Reduction Index (DRI) of doxorubicin, at IC_{50} (fa 0.5) or IC_{70} (fa 0.7), for both cell lines (C and D respectively). Combination Index (CI) as a measure of the interaction between drugs was used, where CI values <1, >1 or ≈1 indicate synergy, antagonism and additivity, respectively. Data represent the mean Combination Index ± SEM. Dose reduction index (DRI) as a measure of a dose fold-reduction is obtained by the ratio of each drug alone versus the drug in a combination, both producing the similar effect "f_a". Data represent the mean DRI ± SEM.

varied according the fraction affected (f_a) (percentage of cell death), i.e. the same drug ratio may present simultaneously an antagonistic/additive or synergistic interaction depending on the levels of f_a, i.e. cell death (Figure 2.2). Surprisingly, the DXR:C6-Cer molar ratio 1:2 revealed to interact synergistically at all f_a levels, an effect that was independent of the cell line tested (Figure 2.2A and 2.2B). Such result translated into a dose-reduction index (DRI) between 4- to 6-fold for doxorubicin. Additionally, other tested drug ratios also presented relevant DRI values (Figure 2.2C and 2.2D). However, the nature of the interaction of those did not hold among all f_a range. Based on these results, the synergistic DXR:C6-Cer molar ratio 1:2 was selected for further co-encapsulation into liposomes, along with the 1:1 molar ratio (mildly additive/antagonistic), as a control for the synergy effect.

2.2.3 Effect of bilayer-incorporated ceramide on intracellular triggered delivery of pH-sensitive liposomes

The work by Moura *et al.*, using F3-targeted pH-sensitive liposomes contaning DXR, has demonstrated in a murine model of MDA-MB-435S tumors, the therapeutic advantage of endowing a nanoparticle with the capacity to enable intracellular triggered release of the encapsulated payload (Moura *et al.* 2012). Therefore, before proceeding with the loading of the established drug ratio into the pH-sensitive liposomes, the influence of the presence of ceramide in pH-sensitivity was assessed. Liposomes were thus loaded with calcein at a self-

quenching concentration as previously described (Moura *et al.* 2012).

As such, it was possible to assess the impact on the efficiency of the payload release following the probe dequenching. F3 peptide-targeted liposomes containing calcein, with or without C6-ceramide (p[F3]SL(C6) and p[F3]SL, respectively), presented a similar extent of intracellular payload release (Figure 2.3), with greater efficiency than the corresponding non-targeted counterparts (pSL(C6) and pSL). Not less significant, cell incubated with an excess of free calcein presented 4-fold higher signal than the non-targeted formulation,

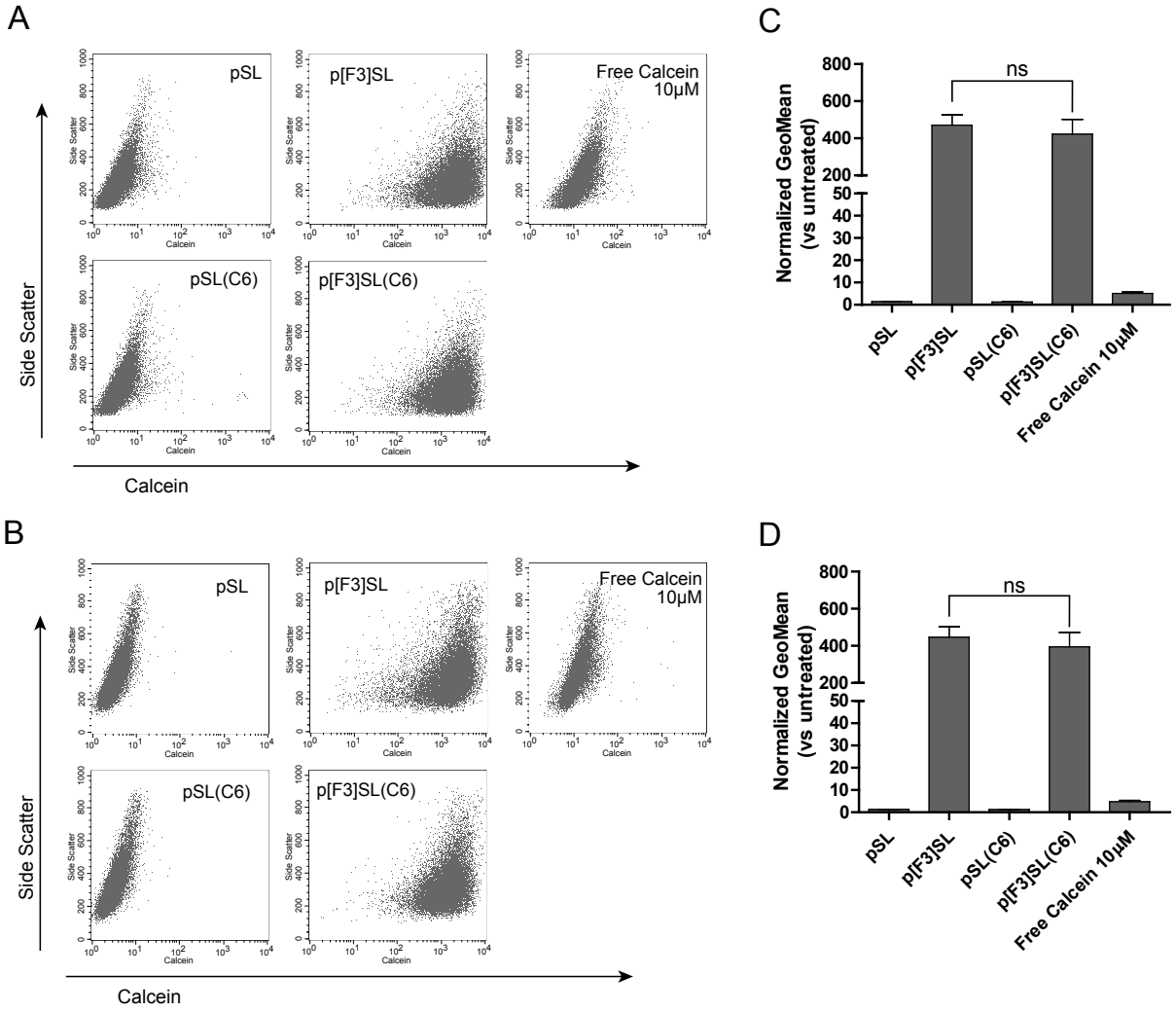

Figure 2.3 – Effect of membrane-incorporated ceramide on liposomal pH-sensitivity.
Two hundred thousand of MDA-MB-231 breast cancer and MDA-MB-435S melanoma cells were incubated with excess of free calcein (10 μM) or with pH-sensitive liposomes containing calcein either alone (non-targeted, **pSL**, or F3-targeted, **p[F3]SL**) or co-encapsulated with ceramide

(non-targeted, **pSL(C6)**, or F3-targeted, **p[F3]SL(C6)**), at 50 μM of lipid for 1 h at 37ºC and immediately analyzed through a FACScalibur flow cytometer. (A) and (B) are representative dot plots of event distribution for each tested condition. Calcein geometric mean fluorescence, normalized against the respective signal of the untreated control, is presented for MDA-MB-231 and MDA-MB-435S cell lines (C and D, respectively). Data represent the mean ± SEM (One-Way ANOVA $p<0.001$; ns $p>0.05$ Tukey's Multiple Comparison Test).

but significantly lower than the targeted ones (Figure 2.3C and 2.3D). The first indicated that calcein was clearly retained inside the liposomes, while the second points to the widespread signal of targeted formulations as result of extensive intracellular delivery.

Overall, these results demonstrated that bilayer-incorporated C6-ceramide did not affect the ability of pH-sensitive F3-targeted liposomes to promote intracellular triggered delivery of the payload located in its aqueous core.

2.2.4 Characterization of pH-sensitive F3-peptide targeted liposomes co-encapsulating doxorubicin and C6-ceramide

As shown previously, the DXR:C6-cer 1:2 molar ratio presented a synergistic interaction between the two drugs, contrasting to the 1:1 molar ratio, which was mildly additive or antagonist depending on the cell line (Figure 2.2). Therefore, pH-sensitive F3-peptide targeted and non-targeted liposomes containing the indicated DXR:C6-Cer ratio, were prepared by incorporating C6-ceramide in the liposomal bilayer at the mentioned fixed molar ratios and further characterized from a physical standpoint.

The presence of C6-ceramide in the bilayer of liposomes had minimal impact in parameters like loading efficiency, mean size and polydispersion index, when compared to the targeted (p[F3]SL) and non-targeted (pSL) counterparts without ceramide (Figures 2.4A, 2.4B and 2.4C). Interestingly, non-targeted formulations were more heterogeneous than the F3-targeted liposomes in terms of mean size (Figure 2.4C). Further evidence of improved stability arouse from drug release

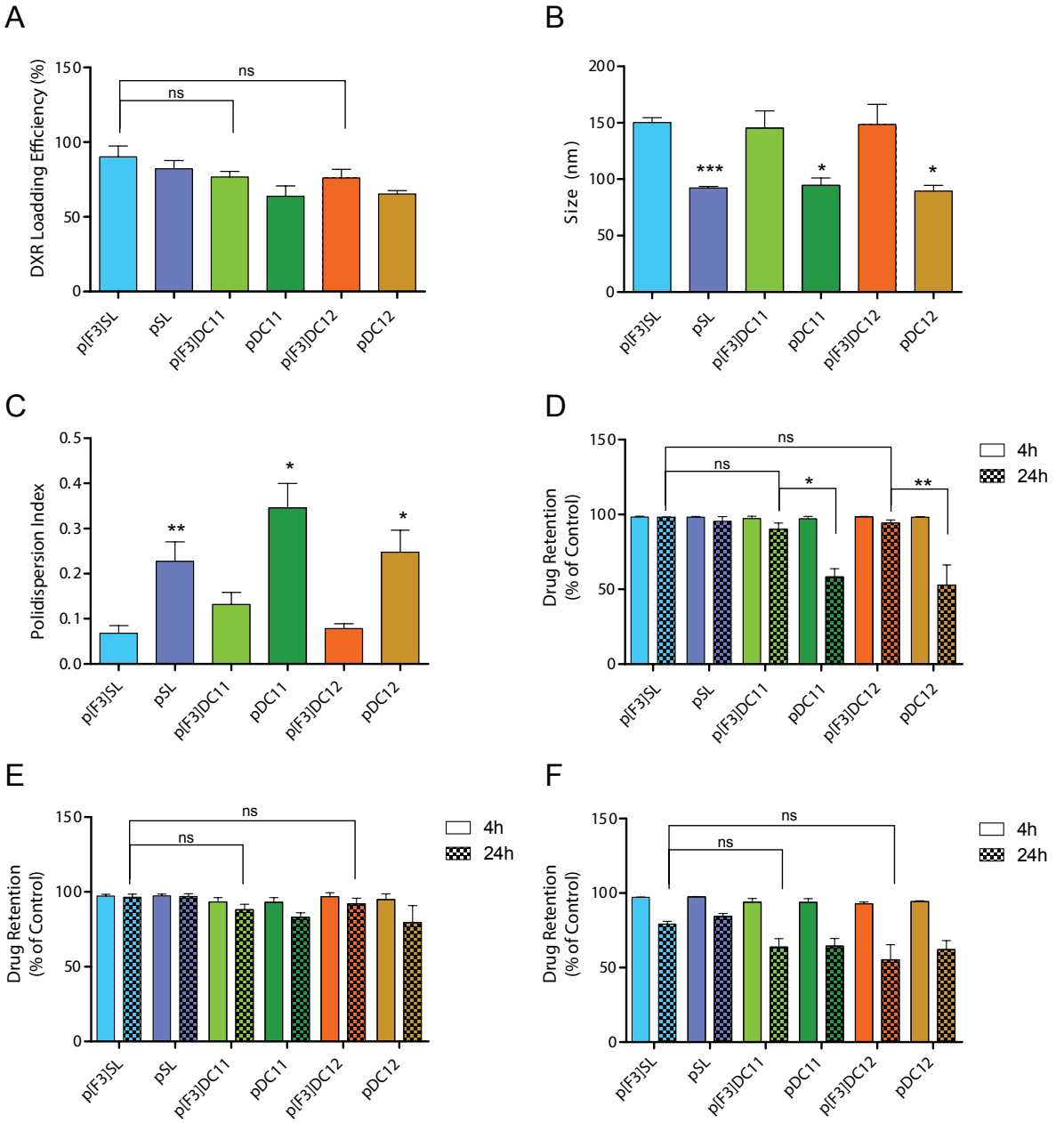

Figure 2.4 – Characterization of liposomes encapsulating doxorubicin (DXR):C6-ceramide (C6-Cer) ratios.

Different liposomal formulations incorporating doxorubicin and C6-ceramide at 1:1 or 1:2 molar ratios, either targeted (**p[F3]DC11** and **p[F3]DC12**, respectively) or non-targeted (**pDC11** and **pDC12**, respectively) have been characterized, in comparison with the corresponding controls containing only DXR, either targeted (**p[F3]SL**) or non-targeted (**pSL**), in terms of loading efficiency (A), mean size (B), and polydispersion index (C). (D), (E) and (F) represent the drug retention capacity of each liposomal formulation when incubated at 37°C in HBS pH 7.4, RPMI 1640 supplemented with 10% FBS or in 90% non-inactivated serum, respectively. Data represent mean ± SEM (One-Way ANOVA ***p<0.0001, **p<0.01, *p<0.05; ns p>0.05 by Tukey's Multiple Comparison Test).

studies performed at 37°C. None of the nanosystems tested, either F3-targeted or non-targeted, presented significant drug release in 4 h, regardless the incubation medium. At 24 h of incubation, either in cell culture medium (Figure 2.4E) or serum (Figure 2.4F), all formulations, either targeted or non-targeted, presented a similar extent of drug retention. The experiment performed in serum, evidenced a decreased on the ability to retain the encapsulated DXR, with values that varied between 55 and 84%, for both targeted and non-targeted liposomes. This was not statistically different from the counterparts without C6-ceramide (Figures 2.4F). Strikingly, the stability study performed in HBS (Figures 2.4D) clearly demonstrated that p[F3]DC11 (targeted liposomes encapsulating the DXR:C6-Cer at 1:1 molar ratio) and p[F3]DC12 (targeted liposomes encapsulating the DXR:C6-cer at 1:2 molar ratio) presented a similar extent of drug retention, relative the corresponding controls without ceramide (p[F3]SL), and were more stable than the non-targeted counterparts (pDC11 and pDC12, respectively), in accordance with the PDI results (Figure 2.4C).

2.2.5 In vitro *cytotoxic of liposomal targeted combinations of doxorubicin and C6-ceramide*

In order to evaluate the cytotoxic potential of the targeted drug combinations, the impact of each formulation on the *in vitro* viability of MDA-MB-231 and MDA-MB-435S cells was assessed. Incubation with p[F3]DC11 or p[F3]DC12 enabled an unique result for an incubation time as short as 4 h, leading to a 90% decrease on the viability of both cell lines. This level of decreased viability was not reached following incubation with the counterpart without ceramide (p[F3]SL) in any of the cell lines tested, not even for a 24 h incubation (Figure 2.5 and Table 2.1). Interestingly, the presence of C6-ceramide in non-targeted formulations elicited a decrease in cell viability higher than 90% both in MDA-MB-231 and MBA-MB-435S cells, for 24 h incubations. In any case, these non-targeted formulations

presented IC_{50} and IC_{90} values 2-fold higher than the targeted counterparts (Figure 2.5 and Table 2.1).

For short incubation time points (1 h), the previously described advantage arising from the presence of C6-ceramide was not evident. Within the selected concentrations of DXR, the value of 50% of cell death was barely surpassed. Nevertheless, the IC_{50} values determined for targeted liposomes were 2-fold lower relative to the non-targeted liposomes, an effect that was independent of the incorporation of C6-Cer (Figure 2.5 and Table 2.1).

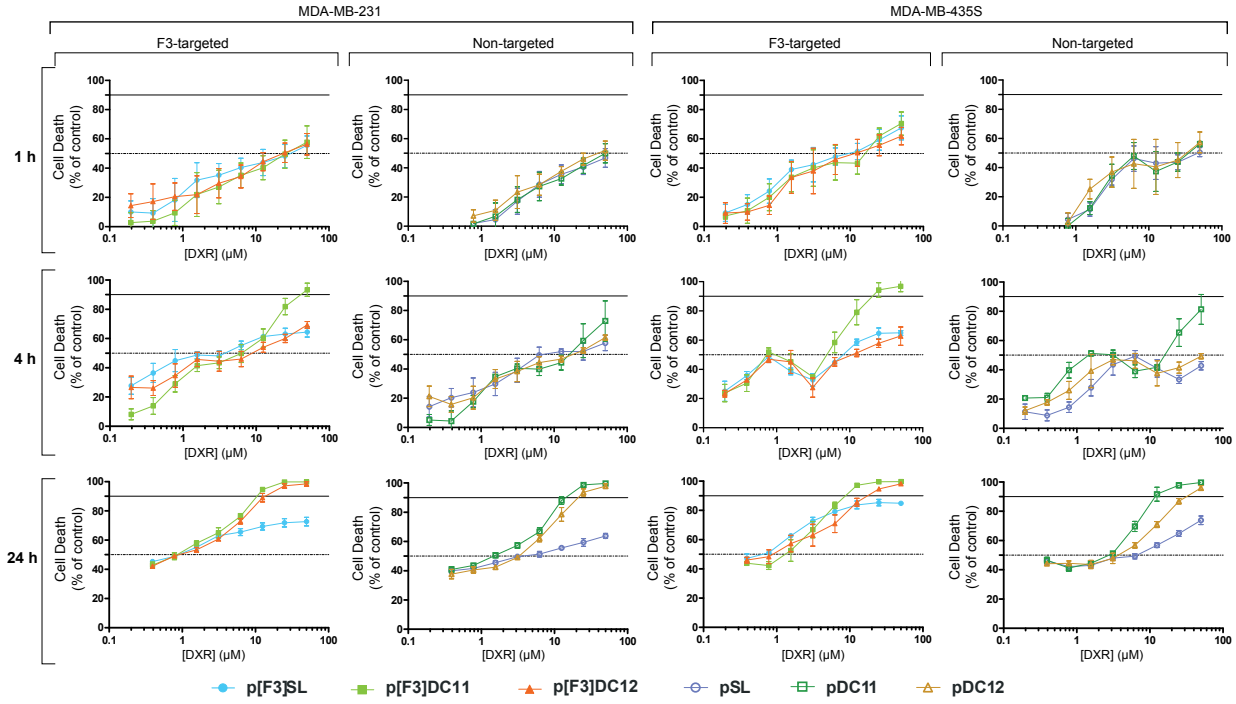

Figure 2.5 – Cytotoxicity of combinations of doxorubicin and C6-ceramide encapsulated in different liposomal formulations.

Cells were incubated for 1, 4 and 24 h with F3-targeted liposomal DXR (p[F3]SL) or DXR:C6-Cer combination at a molar ratio of 1:1 or 1:2 (p[F3]DC11 and p[F3]DC12, respectively), at DXR serially diluted concentrations, and the experiment was further prolonged for total of 96 h, after which cell death was assessed. Results were compared to the respective non-targeted counterparts (pSL, pDC11 and pDC12). Figures represent the dose-response curves for the indicated incubation time points for MDA-MB-231 triple negative breast cancer cell line, and MDA-MB-435S melanoma cell line. The data points represent the mean ± SEM for each concentration tested. Doted-line and full line represent 50 and 90% of cell death, respectively.

Table 2.1 – Cytotoxicity of different liposomal DXR:C6-Cer combinations against MDA-MB-231 and MDA-MB-435S cell lines.

Drug		Cell Line											
		MDA-MB-231						MDA-MB-435S					
		1h		4h		24h		1h		4h		24h	
		IC_{50} (μM)	IC_{90} (μM)	IC_{50} (μM)	IC_{90} (μM)	IC_{50} (μM)	IC_{90} (μM)	IC_{50} (μM)	IC_{90} (μM)	IC_{50} (μM)	IC_{90} (μM)	IC_{50} (μM)	IC_{90} (μM)
Liposomal Doxorubicin	p[F3]SL	29.53	-	3.73	-	0.89	-	9.51	-	8.14	-	0.65	-
	pSL	> 50	-	7.16	-	3.65	-	47.18	-	>50	-	6.68	-
Liposomal Combination	p[F3]DC11	25.87	-	6.35	40.79	0.85	10.51	15.98	-	4.88	20.56	1.31	8.71
	pDC11	> 50	-	16.21	-	1.47	14.22	35.27	-	15.93	-	2.77	11.85
	p[F3]DC12	23.60	-	8.85	-	0.90	13.60	11.58	-	10.92	-	0.89	17.47
	pDC12	40.12	-	18.13	-	3.28	21.19	32.94	-	>50	-	3.70	31.74

Data represent the IC_{50} and the IC_{90} of the mean dose-response curves calculated through linear interpolation of the dose values immediately below or above the 50% and 90% effect, respectively.

Overall, these results demonstrated that the co-encapsulation of the DXR:C6-Cer combination within F3-targeted liposomes increased their cytotoxic activity, even with half of the amount of doxorubicin loaded *per* liposome (corresponding to the doxorubicin:C6-ceramide molar ratio of 1:2), which ultimately may result in increased targeted cell death while minimizing collateral toxic effects of doxorubicin.

2.2.6 Effect of the developed synergistic targeted drug combinations on cell morphology

In order to gain insight into the mechanism of action of the developed nanoparticles, cell morphology was assessed using fluorescence microscopy. The collected data indicated that F3-targeted formulations altered the distribution of nuclear sizes, inducing nuclear and cell swelling to a greater extent than the non-targeted formulations (Figure 2.6 and Figure S2.5, *Supplemental Data*). The presence of C6-ceramide, in targeted or non-targeted liposomes, did neither affect the nuclear distribution nor the mean nuclear size (Figure 2.6B, 2.6C, 2.6D and 2.6E). Not less important is the fact that the liposomes encapsulating the DXR:C6-Cer 1:2 molar ratio (p[F3]DC12) presented the same pattern of performance as the

counterparts encapsulating the double amount of DXR (p[F3]SL or p[F3]DC11) (Figure 2.6E). A similar profile was obtained using the drug sensitive melanoma model, MDA-MB-435S (not shown). Overall, these data suggested that the F3-targeted formulations were more efficient in inducing nuclear and cell swelling, consistent with necrosis-induced cell death (Cummings *et al.* 2012).

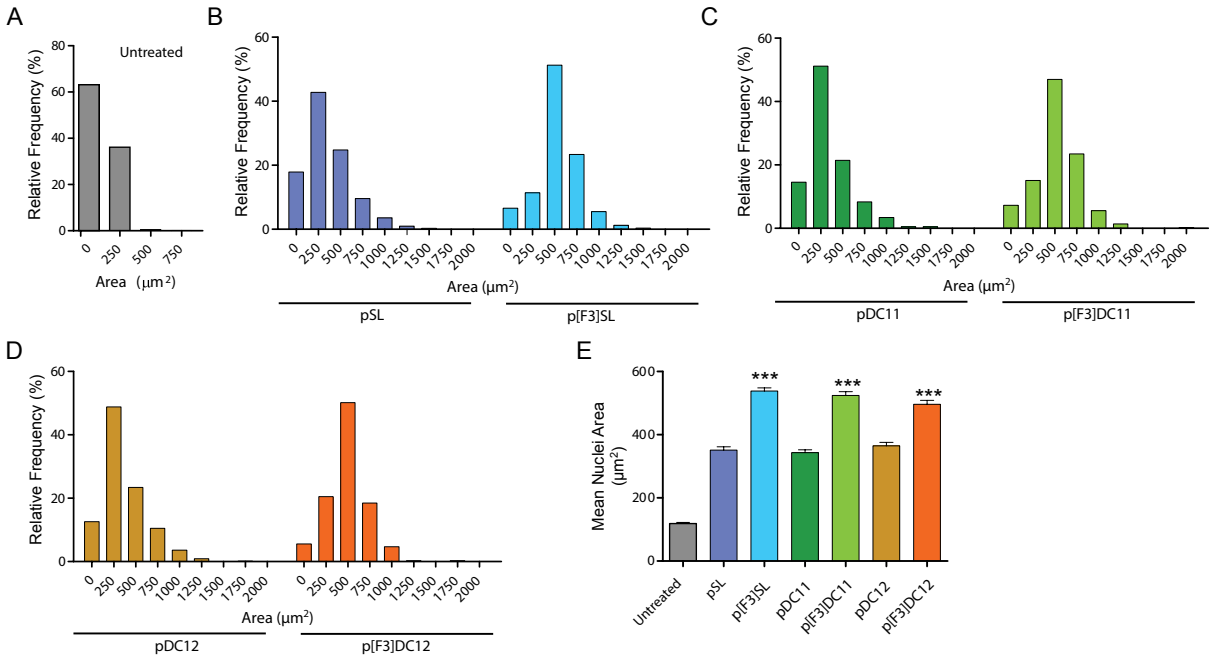

Figure 2.6 – Effect of F3–targeted combinations of doxorubicin and C6-ceramide on cell morphology.

Thirty-five thousand MDA-MB-231 cells/well were incubated for 4 h at 37ºC with F3-targeted liposomal DXR (p[F3]SL) or DXR:C6-Cer combination at a molar ratio of 1:1 or 1:2 (p[F3]DC11 and p[F3]DC12, respectively), or with the non-targeted counterparts (pSL, pDC11 or pDC12, respectively) at 2 µM DXR. The experiment was prolonged up to 92 h. Figures represent the frequency distributions of nuclear area, determined by DAPI staining analysis, for untreated cells (A), liposomal doxorubicin (B), liposomes encapsulating the DXR:C6-Cer, either at 1:1 (C) or 1:2 molar (D), respectively. (E) Represents the mean nuclear area analysis upon incubation with each of the mentioned samples (Bars represent mean area ± SEM; Kruskal-Wallis non-parametric test $p<0.0001$; ***$p<0.001$ comparing F3-targeted vs non-targeted formulations by Dunn's multicomparison test). Data were collected from a representative experiment.

2.3. Discussion

Despite all efforts, cancer drug resistance remains a distressing problem in oncology. In order to overcome this barrier, chemotherapeutics are used in combination, normally at their maximum tolerated dose (MTD), which ultimately is not beneficial to the patient as it represents an increased risk of severe toxicity. Nonetheless, it has been recognized that success demands the identification of drugs that, when combined, lead to synergistic tumor inhibition while minimizing systemic toxicity (Ramaswamy 2007; Dicko *et al.* 2010). It has been acknowledge that the nature of the interaction between those drugs varies according to the measured effect on cell viability (fraction affected, f_a), as well as with the pre-established drug molar ratio, in line with similar studies using drug combinations like irinotecan/floxuridine or cytarabin/daunorubicin (Mayer *et al.* 2006; Tardi *et al.* 2009a). Nonetheless, such scenario is far from ideal as synergistic effects would be limited to a percentage of tumor cell death above a certain threshold, which could be problematic in an *in vivo* setting. Therefore, ideally a drug combination should present a synergistic interaction at all levels of f_a. In this respect, we have identified in the present work the DXR:C6-Cer 1:2 molar ratio as synergistic, regardless the cell line or the level of f_a, enabling at least a 4-6 fold dose reduction of DXR.

However, to take full advantage of such combination, one has to develop strategies to ensure a synchronized temporal and spatial delivery of the individual drugs. Several lipid-based formulations containing ceramides have been described. Some examples include ceramides formulated either as single agent in non-targeted or transferrin-targeted nanoparticles (Stover *et al.* 2005; Koshkaryev *et al.* 2012) or in combination with paclitaxel, doxorubicin or tamoxifen (van Vlerken *et al.* 2007; Khazanov *et al.* 2008; Morad *et al.* 2013). Others have demonstrated that combination of liposomal ceramide with sorafenib increases the effectiveness of the latter (Tran *et al.* 2008). Nonetheless, despite increased

cytotoxicity of those combinations, lack of an appropriate mathematical analysis may render the selected drug ratios not necessarily synergistic. Furthermore, EPR-driven tumor accumulation of the mentioned drug combinations, though presenting higher efficacy than free drugs, could be limited by the absence of specific intracellular delivery to essential (and more accessible) cell populations within the tumor microenvironment (Hanahan *et al.* 2011; Gomes-da-Silva *et al.* 2012b). Considering the importance of targeting different components of the tumor microenvironment, as previously emphasized (Bansode 2011; Hanahan *et al.* 2011; Bocci *et al.* 2012), we have engineered the previous F3-peptide pH sensitive liposomes developed in our group, to accommodate the selected DXR:C6-Cer synergistic combination. The F3 peptide is a moiety that specifically targets nucleolin, a cell membrane protein overexpressed in cancer cells and endothelial cells of angiogenic blood vessels (Porkka *et al.* 2002; Moura *et al.* 2012).

Using calcein-loaded liposomes, we have shown that incorporation of C6-ceramide in the liposomal bilayer did not impair delivery nor promoted significant instability (Figure 2.3, non-targeted liposomes versus free calcein). Such result correlates with the one generated with the 35 mol% C6-ceramide-incorporating liposomes by Khazanov *et al.* (maximum load), well above the 18.5 mol% we used (Khazanov *et al.* 2008). The absence of impaired delivery led us to engineer a F3-targeted formulation containing the synergistic DXR:C6-Cer 1:2 molar ratio (Figure 2.2). DXR:C6-Cer 1:1 molar ratio was also loaded into liposomes to use as a control for an additive/antagonist effect (Figure 2.2).

Characterization data demonstrated that C6-ceramide had minimal impact in measured physical parameters (including drug retention) as compared to F3-targeted (p[F3]SL) or non-targeted (pSL) liposomes containing only doxorubicin (Figure 2.4). DSPC and cholesterol are known to increase drug retention in pH sensitive liposomes (Ishida *et al.* 2006). Their removal to accommodate the incorporation of C6-ceramide might have led to increased defects in membrane

bilayer promoted by the sphingolipid (Khazanov *et al.* 2008). This was likely the reason behind the differences observed on drug retention (in HBS) between doxorubicin- and combination-encapsulating liposomes. Nonetheless, the same data demonstrated that the F3 ligand stabilized the bilayer of C6-ceramide loaded liposomes, to the same extent of liposomes without C6-ceramide (Figure 2.4D). This might be explained by the additional hydration layer on the liposomal surface, arising from the charged F3 peptide. This effect seems to improve drug retention (Figure 2.4D) and minimize aggregation (Figure 2.4C). Furthermore, the differences observed in the different media, might be related to their differences in ionic and/or protein composition. Those, in turn, may promote different degrees of lipid headgroup hydration, especially of CHEMS, upon providing several counterions, which render unequal levels of membrane stabilization (Hafez *et al.* 2000; Li *et al.* 2001). This fact could explain the increased drug retention of pDC11 and pDC12 formulations in cell culture medium when compared to HBS buffer. Otherwise, in serum, all tested formulations exhibited lower drug retention than in other media, notwithstanding the fact that combination-containing liposomes have marginally lower drug retention, relative to the counterparts without ceramide (Figure 2.4F). That could be due to protein/lipid interaction known to destabilize the lipid bilayers allowing doxorubicin to escape and bind to serum proteins (Hernandez-Caselles *et al.* 1993; Agudelo *et al.* 2012).

The incorporation of pro-apoptotic ceramide in liposome bilayer, by itself, has shown to render any formulation more cytotoxic either by passive internalization of the intact liposome or by simple lipid translocation onto the cell membrane (Khazanov *et al.* 2008). The free drug combination studies clearly indicated that the 1:2 DXR:C6-cer molar ratio was synergistic, whereas the 1:1 molar ratio was mildly additive or antagonistic (Figure 2.2). Surprisingly, F3-targeted liposomes encapsulating the DXR:C6-Cer combination at 1:1 molar ratio (p[F3]DC11) enabled 90% of cell death for an incubation period as short as 4 h (Figure 2.5 and Table

2.1). This effect was unattainable even by targeted liposomes containing only doxorubicin or C6-ceramide, after 24 h of incubation (Figure S2.1, *Supplemental data*). Overall, p[F3]DC11 performed similarly to p[F3]DC12 nanoparticle against triple negative MDA-MB-231 breast cancer cells, regardless the incubation time (Figure 2.5 and Table 2.1). This unexpected result suggested that the intracellular delivery of both drugs, at the selected ratio, may change the interaction nature of the combinations, rendering them synergistic (Figure S2.2, *Supplemental data*). This result is, in some extent, different from the one reported by Tardi *et al.*, where encapsulation (in non-targeted liposomes) of antagonist 3:1 ratio of irinotecan:cisplatin rendered a lower efficacy, despite increased irinotecan loading, compared to the synergistic CPX-571 formulation (Tardi *et al.* 2009b). This thus indicated that the interaction between drugs might also be dependent on the mechanism of drug delivery, particularly on the ability to delivery intracellularly a specific drug ratio. Nonetheless, it has been demonstrated that the encapsulation of the combination at 1:2 molar ratio (p[F3]DC12) enabled increased liposomal citotoxicity using half of the drug loading utilized to prepare the standard targeted formulation (p[F3]SL). Ultimately, this could prove useful to further increase the safety associated with the use of liposomal doxorubicin.

Despite the increased cytotoxic effect, FACS analysis indicated similar mechanism of cell death for all formulations, with predominance of late apoptotic/necrotic population and higher levels of apoptotic cells over necrotic cells (Figure S2.4, *Supplemental data*). Doxorubicin has been described to induce apoptosis (caspase-dependent cell death) or necrosis (caspase-independent cell death) after mitotic catastrophe (Eom *et al.* 2005; Mansilla *et al.* 2006), in a dose-dependent manner. On the other hand, ceramides have been described to mediate apoptosis through several mechanisms including p38 MAPK, Akt-mediated induction of $p27^{kip1}$ and channel-opening in the mitochondria (Siskind 2005; Siskind *et al.* 2006; Kim *et al.* 2008; Kim *et al.* 2010; Siskind *et al.* 2010). In this context, whereas DXR depends on

cell cycle to promote cell death even at low doses, the apoptosis-induced effect by C6-ceramide is highly dependent on the dose and time of exposure (Eom *et al.* 2005; Kim *et al.* 2008). Consistently, microscopy analysis of nuclear geometry, revealed an increase in the nuclei size, indicative of nucleus swelling, and cell swelling upon incubation with F3-targeted nanoparticles containing DXR, when compared to the non-targeted counterparts, which is coherent with cell induced-necrosis (Figure 2.6) (Cummings *et al.* 2012). Therefore, at the tested concentration, observed results demonstrated mainly the contribution of doxorubicin for cell death, despite the fact that free ceramide can indeed induce apoptotic cell death, as measured by us with annexin V (Figure S2.3, *Supplemental data*) and consistent with literature (Kim *et al.* 2010).

2.4. Conclusion

In the present work, it has been demonstrated that the DXR:C6-cer combination developed a synergistic interaction at the specific 1:2 molar ratio, enabling a DXR dose reduction of, at least, 4-fold depending on the cellular model. Furthermore, we established the development of a novel triggered-release nanoparticle targeted by the F3 peptide, capable of retaining and intracellularly deliver the synergistic DXR:C6-cer combination, thus increasing the cytotoxic potential. Additionally, our study suggested that the strategy of delivery may alter the nature of drug interaction, since a F3-targeted formulation encapsulating an additive/mildly antagonistic DXR:C6-Cer, demonstrated singularly a cytotoxic effect above 90%, for an incubation period as short as 4 h. It has been further validated that the encapsulation of the synergistic DXR:C6-Cer 1:2 molar ratio enabled a cytotoxic effect above 90% after 24 h of incubation, unattainable by the F3-targeted liposomal doxorubicin encapsulating twice the amount. The characteristics of the developed nanoparticle, along with the demonstrated tropism of the F3 peptide towards breast cancer cells and the tumor microenvironment (Porkka

et al. 2002; Moura *et al.* 2012), could enable an increase in the therapeutic efficacy, overcoming drug resistance while simultaneously decreasing the severe side effects of doxorubicin. Overall, the generated data suggest that additive/ antagonistic interaction of free combinations may be potentially shifted by specific active intracellular delivery.

2.5. Materials and Methods

2.5.1 Materials

Doxorubicin hydrochloride (DXR) was from IdisPharma (UK). Calcein, 4-(2-Hydroxyethyl)piperazine-1-ethanesulfonic acid (HEPES), 2-(N-Morpholino) ethanesulfonic acid (MES), Disodium ethylenediaminetetraacetate dehydrate (EDTA), Trizma®Base, 3-(4,5-Dimethyl-2-thiazolyl)-2,5-diphenyl-2H-tetrazolium bromide (MTT), sodium chloride, 3β-hydroxy-5-cholestene-3-hemisuccinate (CHEMS) and cholesterol (CHOL) were purchased from Sigma-Aldrich (USA). The lipids 2-dioleoyl-sn-glycero-3-phosphoethanolamine (DOPE), 1,2-distearoyl-sn-glycero-3-phosphocholine (DSPC), 1,2-distearoyl-sn-glycero-3-phosphoethanolamine-N-[methoxy(polyethylene glycol)-2000] (DSPE-PEG_{2k}), 1,2-distearoyl-sn-glycero-3-phosphoethanolamine-N-[maleimide(polyethylene glycol)-2000] (DSPE-PEG_{2k}-maleimide), N-hexanoyl-D-erythro-sphingosine (C6-Ceramide) were obtained from Avanti Polar Lipids (USA). F3 (KDEPQRRSARLSAKPAPPKPEPKPKKAPAKK) and the non-specific (NS) peptides were custom synthetized by Genecust (Luxemburg).

2.5.2 Cells

MDA-MB-231 triple negative breast cancer cell line and MDA-MB-435S melanoma cell line (Rae et al. 2007) (acquired from ATCC, USA) were cultured in RPMI 1640 (Sigma-Aldrich, USA) supplemented with 10% (v/v) of heat-inactivated Fetal Bovine Serum (FBS) (Invitrogen, USA), 100 U/ml penicillin, 100 µg/ml streptomycin (Lonza, Switzerland) and maintained at 37°C in a 5% CO_2 atmosphere.

As the cells we have worked with grow adherent to the plastic of the cell culture flask, all the experiments have been performed 24 h after cell seeding, to enable cell attachment before the corresponding incubation with the tested samples.

2.5.3 In vitro *screening for synergy between DXR and C6-Ceramide*

Eight thousand MDA-MB-231 breast cancer or MDA-MB-435S melanoma cells/well were incubated with serial dilutions of doxorubicin or C6-Ceramide, alone or in combination, at fixed molar ratios, for 24 h at 37°C in an atmosphere of 5% CO_2. Following incubation, cell culture medium was exchanged for fresh one and the experiment was further prolonged up to 72 h. Cell viability was then evaluated using the MTT assay as previously described (Moreira *et al.* 2002).

2.5.4 Preparation of liposomes

pH-sensitive liposomes, with or without ceramide, were composed of DOPE:CHEMS:DSPC:CHOL:DSPE-PEG_{2k}:C6-ceramide at 4:2:1:1:0.8:2 (18 mol% of C6-ceramide) or 4:2:2:2:0.8:0 molar ratio, respectively.

Dried lipid films were hydrated at 60°C with ammonium sulfate (pH 8.5) and the resulting liposomes were extruded through 80 nm pore size polycarbonate membranes using a LiposoFast Basic mini extruder (Avestin, Canada). The buffer was exchanged in a Sephadex G-50 gel column (Sigma-Aldrich, USA) equilibrated with Trizma®Base sucrose (10%, w/v, buffered at pH 9.0). Remote encapsulation of DXR (9 or 18 mol% of total lipid, for the DXR:C6-Cer 1:2 or 1:1 molar ratio, respectively) was carried out through ammonium sulphate gradient method, upon incubation with liposomes for 1.5 h at 60°C (Haran *et al.* 1993). Non-encapsulated DXR was removed using a Sephadex G-50 gel column equilibrated with 25 mM HEPES, 140 mM NaCl buffer (HBS, pH 7.4).

To further prepare targeted liposomes, DSPE-PEG_{2k}-F3 conjugate was produced. Briefly, thiolated derivative of F3 peptide was generated by reaction at room temperature with 2-iminothiolane (Sigma-Aldrich, USA) in 25 mM HEPES, 140 mM NaCl, 1 mM EDTA buffer (pH 8.0) for 1 h in an inert N_2 atmosphere. Thiolated

derivatives were then incubated overnight at room temperature with DSPE-PEG_{2k}-maleimide micelles in 25 mM HEPES, 25 mM MES, 140 mM NaCl, 1 mM EDTA (pH 7.0). The resulting micelles of DSPE-PEG_{2k}-Peptides conjugates were post-inserted onto the liposomal membrane at 2 mol% relative to total lipid (TL), upon incubation with pre-formed liposomes, for 1 h at 50°C.

To prepare calcein-loaded liposomes, both lipid films were instead hydrated with a 40 mM isosmotic calcein solution in 25 mM HEPES, 140 mM NaCl buffer (pH 7.4), and extruded as described above. Following removal of calcein excess, through a Sephadex-G50 column equilibrated with 25 mM HEPES, 140 mM NaCl buffer (pH 7.4), liposomes were immediately submitted to the post-insertion procedure as previously described.

2.5.5 Liposome characterization

Liposome size and polidispersion index (PDI) were measured by light scattering with a N5 particle size analyzer (Beckman Coulter, USA). Final total lipid concentrations were determined upon quantification of cholesterol using Infinity® Cholesterol kit (ThermoScientific, USA). Encapsulated doxorubicin was assayed at 492 nm from a standard curve, after liposomal solubilization with 90% absolute ethanol, and the loading efficiency (%) was calculated from the equation

$$\text{Loading efficiency } (\%) = \frac{(DXR/TL)_{final}}{(DXR/TL)_{initial}} \times 100$$

To assess drug retention, an aliquot of F3-targeted and non-targeted liposomes, encapsulating either DXR or a combination of DXR and C6-Cer, was incubated in HEPES buffer saline pH 7.4 (HBS), 90% RPMI 1640 culture medium supplemented with 10% FBS (Invitrogen) or 90% of non-inactivated bovine serum, at 37°C. At different time-points (0, 4 and 24 h), DXR fluorescence dequenching was measured in a Spectramax fluorimeter (λ_{ex} = 485 nm; λ_{em} = 590 nm) (Molecular Devices, USA). Drug retention of DXR (% of control) was calculated using the following formula:

$$\text{Drug retention (\%)} = 100 - \left[\frac{TestRFU_n - MeanRFU_0}{MeanRFU_{ctr} - MeanRFU_0} \right] \times 100$$

where $TestRFU_n$ and $MeanRFU_0$ stand for the fluorescence of tested sample at different time points and time 0 h, respectively and $MeanRFU_{ctr}$ is the fluorescence corresponding to 100% of release, following incubation with 0.25% (v/v) of Triton X-100.

2.5.6 C6-ceramide effect on liposomal pH sensitivity

Two hundred thousand MDA-MB-231 breast cancer and MDA-MB-435S melanoma cells were incubated with 50 μM (total lipid) of liposomal calcein for 1 h at 37°C and immediately analyzed through a FACScalibur flow cytometer (BD Biosciences, USA). Free calcein (10 μM) was included as control. A total of 20,000 events were analyzed with Cell Quest Pro software (BD Biosciences, USA).

2.5.7 Evaluation of cytotoxicity of liposomal drug combinations

Different concentrations of F3 peptide-targeted or non-targeted liposomes, containing either single DXR (p[F3]SL or pSL, respectively) or combined with C6-ceramide at 1:1 (p[F3]DC11 and pDC11, respectively) or 1:2 molar ratio (p[F3]DC12 or pDC12, respectively) were incubated with 8000 MDA-MB-231 breast cancer or MDA-MB-435S melanoma cells/well, for 1, 4 or 24 h, at 37°C in an atmosphere of 5% of CO_2. F3 peptide-targeted and non-targeted liposomal C6-ceramide were included as controls (p[F3]SL(C6) and pSL(C6), respectively). Afterwards, cell culture medium was exchanged for fresh one and the experiment was prolonged for a total of 96 h. Cell viability was then evaluated using the MTT assay as previously described (Moreira *et al.* 2002).

In order to assess the mechanism of cell death induced by the intracellular delivery of DXR:C6-Cer combination, cell death was evaluated by flow cytometry as previously described, upon incubation of 35,000 adherent cells/well with each formulation at 2 μM DXR for 4 h at 37°C (Santos *et al.* 2008). Assessment of cell morphology following DAPI (Applichem, Germany) staining was also performed.

Images were captured using a 5X objective mounted in an Axiovert 200M microscope equipped with an AxioCamHR (Carl Zeiss, Germany). Image analysis was carried out using FIJI software (National Institutes of Health, USA).

2.5.8 Median effect analysis of doxorubicin and C6-Ceramide combinations

The nature of the interaction between doxorubicin and C6-Ceramide (synergism, additivity or antagonism) was evaluated using the median-effect model developed by Chou and Talalay (Chou *et al.* 1984; Chou 2006; Chou 2011). The model relies on the median-effect equation (1) to describe any dose-response relationship

$$\frac{f_a}{f_u} = \left(\frac{D}{D_{50}} \right)^m \quad (1)$$

where f_a and f_u represent the fraction affected and unaffected, respectively (i.e. the response), D the dose responsible for a given f_a, D_{50} the median-effect dose and m the sigmoidicity of a dose-response curve. The acquired data from dose-response studies, using single drugs or their combination, was fitted to the *median-effect plot* equation (2)

$$\log\left[\frac{1}{1-f_a} \right] = m\log\left(D\right) - m\log\left(D_{50}\right) \quad (2)$$

enabling one to estimate m, the slope of the plot, and D_{50}, the dose responsible for 50% of the effect.

These parameters establish a dose-response model for each drug or combination tested, enabling the determination of the Combination Index (CI) using the equation (3)

$$CI = \frac{D_1 + D_2}{\left(Dx\right)_1 + \left(Dx\right)_2} \quad (3)$$

where $(Dx)_1$ and $(Dx)_2$ are the doses of each single drug responsible for a certain effect f_a, and D_1 and D_2 are the doses of each drug in a given mixture enabling the same effect f_a (Chou 2006). As a measure of the nature of interaction, a CI value

< 1, ≈ 1 or >1 is indicative of synergism, additivity or antagonism, respectively (Chou 2006; Chou 2011). Further calculations enable one to estimate the Dose Reduction Index (DRI) by the equation (4)

$$DRI_n = \frac{(Dx)_n}{D_n} (4)$$

for the drug *n*, understood as the drug fold decrease in a combination as compared to the same drug given alone, for a determined effect level (Chou 2006; Chou 2011).

2.6. Supplemental data

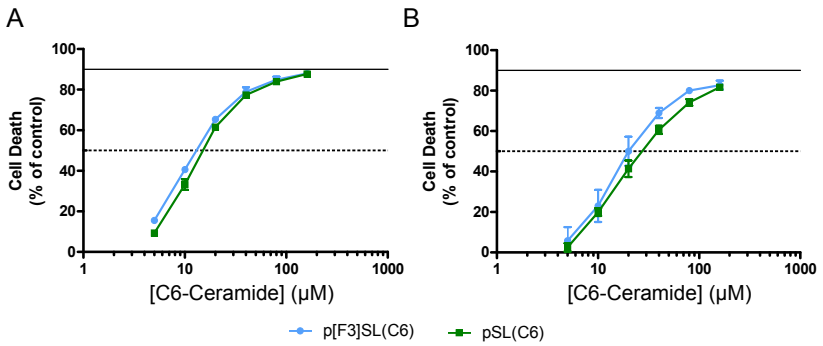

Cytotoxicity of liposomal C6-ceramide against MDA-MB-231 and MDA-MB-435S cell lines

Drug	IC_{50} (μM)	
	MDA-MB-231	MDA-MB-435S
p[F3]SL(C6)	13.01	19.97
pSL(C6)	15.07	27.28

Figure S2.1 - Cytotoxicity of liposomal C6-ceramide.

Cells were incubated for 24 h with F3-targeted (p[F3]SL(C6)) or non-targeted (pSL(C6)) liposomal C6-Ceramide, at C6-ceramide serially diluted concentrations, and the experiment was further prolonged for a total of 96 h, after which cell death was assessed. (A) and (B) represent the dose-response curves for MDA-MB-231 triple negative breast cancer cell line and MDA-MB-435S melanoma cell line, respectively. Inserted table presents the IC_{50} values calculated from mean dose-response curves by linear interpolation of the dose values immediately below or above the 50% effect. Data points represent the mean ± SEM. Doted-line and full line represent 50 and 90% cell death, respectively.

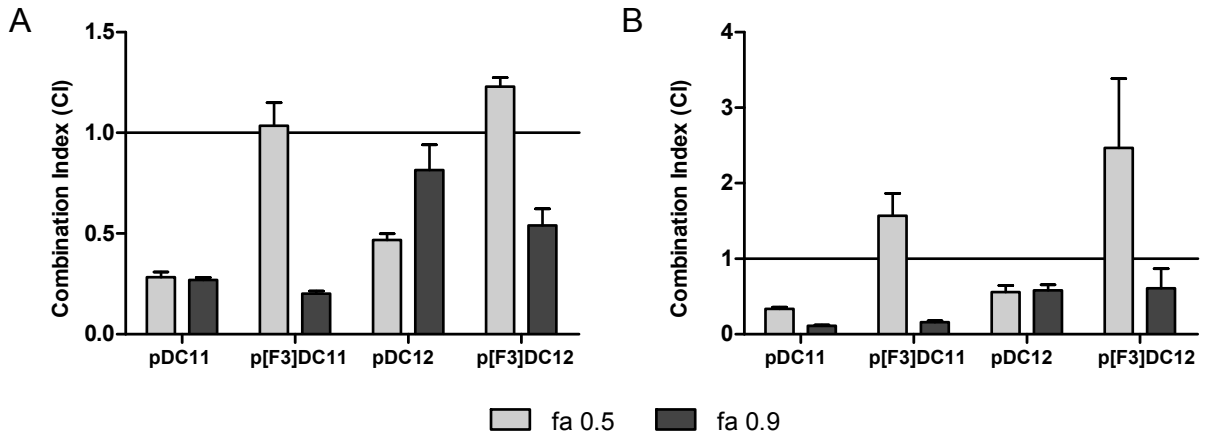

Figure S2.2* - In vitro *estimation of synergy of liposomal combinations of doxorubicin (DXR) and C6-ceramide (C6-Cer).

Following 24 h incubation with F3-targeted liposomes encapsulating either the DXR:C6-Cer molar ratio 1:1 or 1:2 (p[F3]DC11 or p[F3]DC12, respectively) or non-targeted liposomes encapsulating the same ratios (pDC11 or pDC12), the nature of the interaction between the two drugs upon encapsulation was assessed by median-effect analysis. (A) and (B) represent the Combination Index (CI) at IC_{50} (fa 0.5) or IC_{90} (fa 0.9) for the MDA-MB-231 breast cancer or MDA-MB-435S melanoma cell lines, respectively. Combination Index (CI) as a measure of the interaction between drugs was used, where CI values <1, >1 or ≈1 indicate synergy, antagonism and additivity, respectively. Data represent the mean ± SEM.

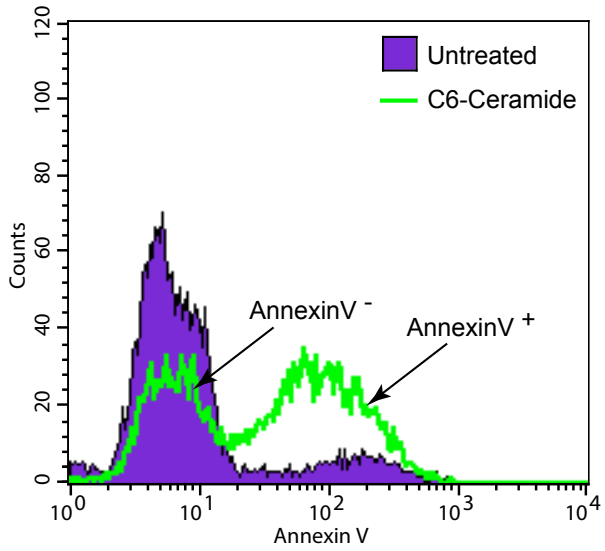

Figure S2.3 – Assessment of C6-Ceramide apoptosis induction.

Two hundred and fifty thousand MDA-MB-435S melanoma cells were incubated with 40 μM C6-Ceramide for 24 h at 37ºC. Subsequently, cells were stained with Annexin V-PE. Figure represents a typical distribution of Annexin V-labeled cells upon C6-ceramide incubation, compared to untreated control. Annexin V^- - viable cells; Annexin V^+ - apoptotic cells.

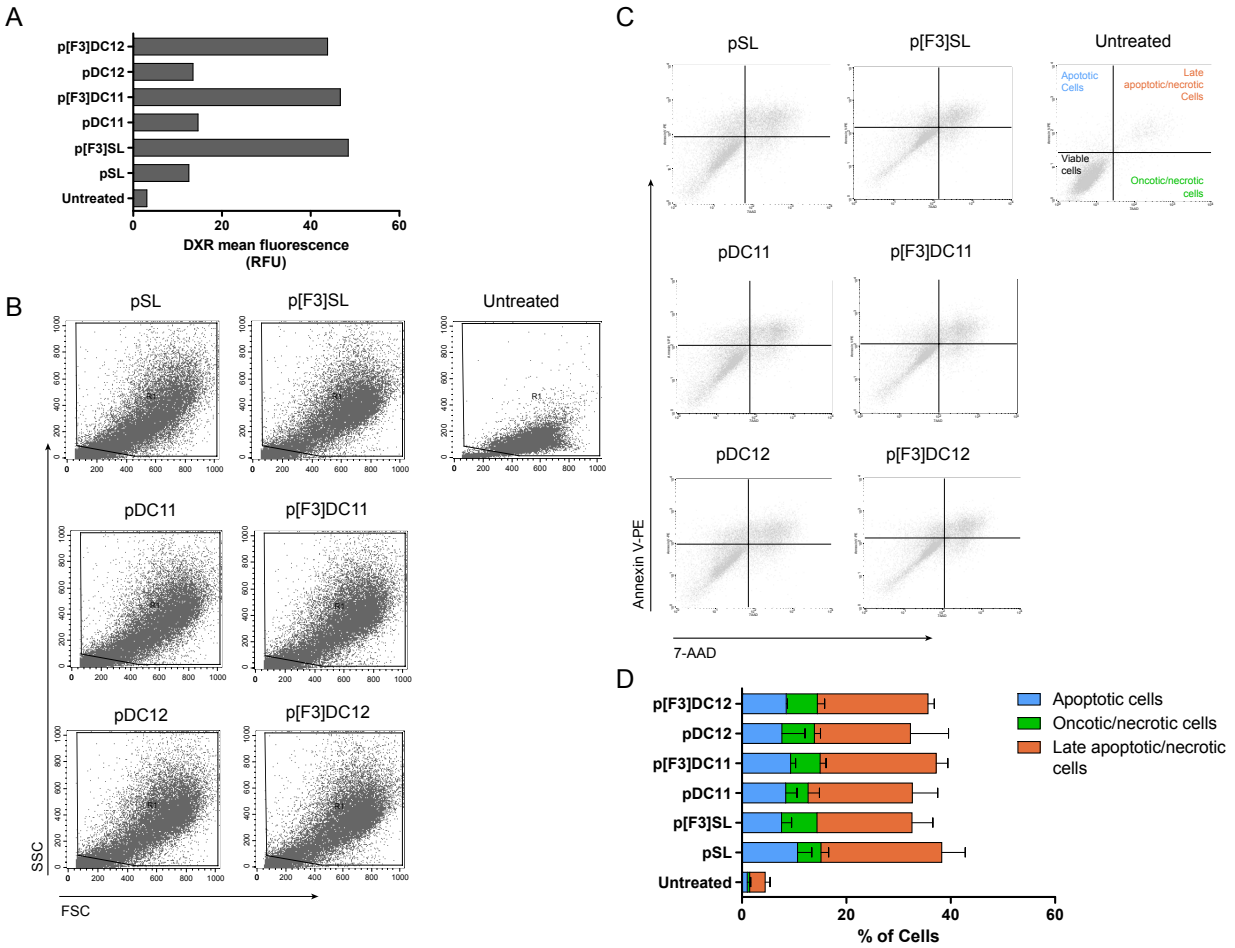

Figure S2.4 - Evaluation of F3-targeted combinations of doxorubicin and C6-ceramide on cell death mechanism.

Thirty-five thousand MDA-MB-231 cells/well were incubated for 4 h at 37ºC with F3-targeted liposomal DXR (p[F3]SL) or DXR:C6-Cer combination at a molar ratio of 1:1 or 1:2 (p[F3]DC11 and p[F3]DC12, respectively), or with the non-targeted counterparts (pSL, pDC11 or pDC12, respectively) at 2 µM DXR. The experiment was prolonged up to 92 h. Cells were subsequently stained with annexin V-PE and 7-AAD and analyzed by FACS. (A) is a representative doxorubicin (DXR) mean fluorescence upon liposomal delivery. (B) and (C) are representative forward scatter (FSC)-side scatter (SSC) and 7-AAD/Annexin V-PE event distribution dot plots, respectively. Quadrants in the former were established accounting the doxorubicin fluorescence from unstained controls. (D) Represents the percentage of apoptotic, oncotic/necrotic and late apoptotic/necrotic cells upon incubation with the tested samples (Data represent the mean ± SEM).

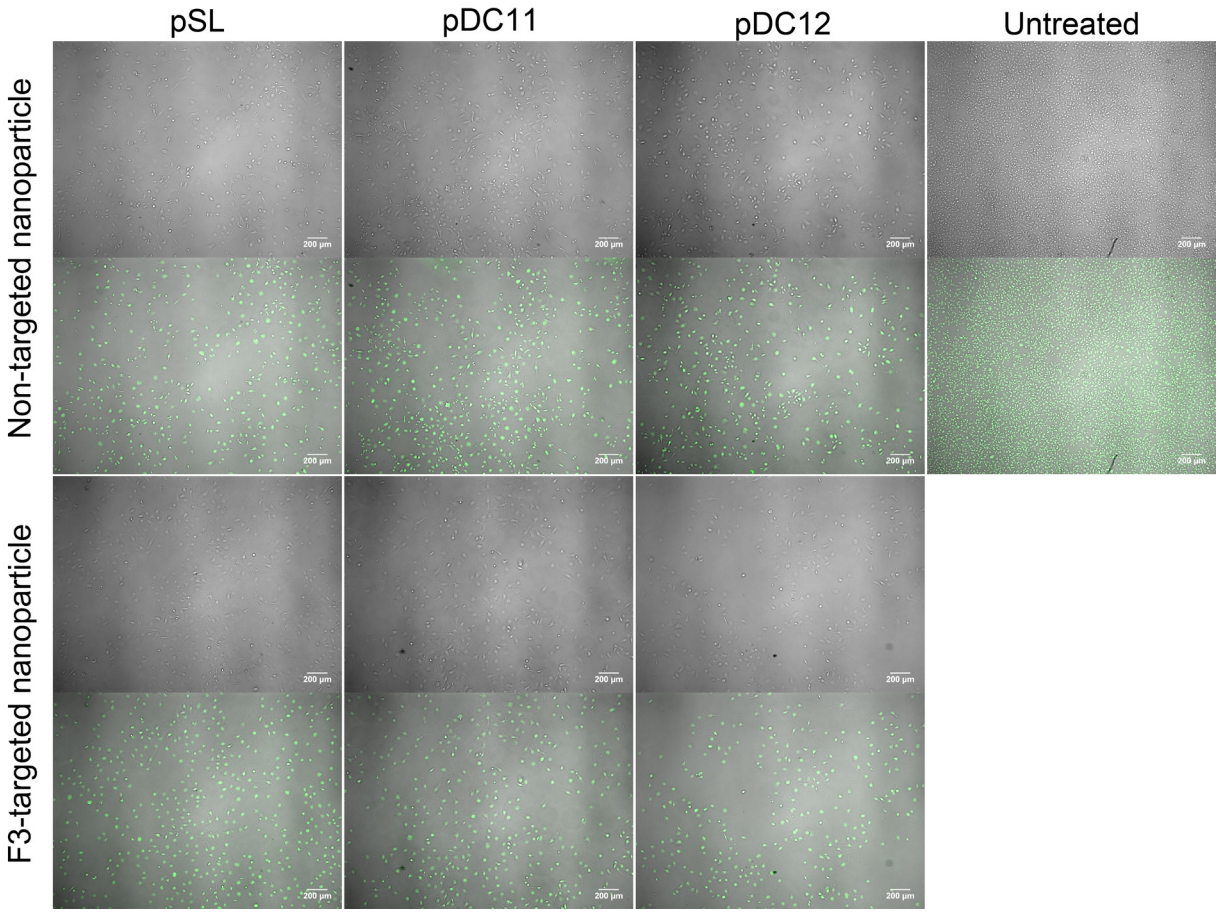

Figure S2.5 - Effect of F3–targeted combinations of doxorubicin and C6-ceramide on cell morphology.

Representative fluorescence microscopy images of cells (wide field) with DAPI nuclear staining (green).

Chapter 3

Nucleolin overexpression in breast cancer cell sub-populations with different stem-like phenotype enables targeted intracellular delivery of synergistic drug combination

Abstract

Breast cancer stem cells (CSC) are a cell sub-population with stem-like characteristics, presenting several fundamental deregulated signaling pathways, responsible for tumor growth and relapse, metastization, and active evasion to standard chemotherapy. A denser landscape emerged by the acknowledgment that CSC may originate from non-stem cancer cells (non-SCC), turning these into two relevant cell therapeutic targets, provided the necessary accessibility to the CSC niche. In this work we have assessed whether nucleolin was a common surface receptor among those sub-populations and if it could enable dual cellular targeting of a liposomal synergistic drug combination, as a strategy to increase therapeutic efficacy.

It was demonstrated that liposomes functionalized with the F3 peptide, targeting cell surface nucleolin (NCL), associated with both breast non-SCC and putative CSC, but in higher extent with the latter (2.6- and 3.2-fold for triple negative MDA-MB-231 and luminal-like MCF-7 cells, respectively), in an energy-dependent process. Increased mRNA levels of NANOG and OCT4 transcription factors, paralleled by nucleolin, were found in putative breast CSC as compared to non-SCC, from triple negative breast cancer cells. Additionally, using mouse embryonic stem cells (mESC) as stemness *bona fide* model, it was shown that both nucleolin mRNA levels and cellular association of F3 peptide-targeted liposomes were dependent on stemness status. In addition, it was demonstrated that triple negative breast NCL^+ cells were more tumorigenic than NCL^- cells, paralleling putative breast CSC behavior. Moreover, F3 peptide-targeted triggered-release liposomes, previously developed by us (*Chapter 2*), promoted the efficient and simultaneous delivery of doxorubicin:C6-Ceramide combinations into triple negative breast CSCs, enabling 100% cell death.

Altogether, our results suggested a clear link between nucleolin expression (including cell membrane nucleolin) and the stem cell-like phenotype, namely

in triple negative breast cancer, enabling the simultaneous intracellular delivery of drug combinations-containing liposomes functionalized with the F3 peptide into both CSC and non-SCC. This technology has the potential to simultaneously debulk multiple cellular compartments of the tumor microenvironment, while decreasing tumor recurrence and systemic toxicity, ultimately providing long-term disease free survival.

3.1. Introduction

Breast cancer remains the leading cause of death among women, responsible for 29% of newly diagnosed cases (Desantis *et al.* 2013). It is a highly complex disease owing to intrinsic molecular and cellular heterogeneity associated with the tumor microenvironment (Hanahan *et al.* 2011; Eccles *et al.* 2013). The discovery of cancer stem cells (CSC) in solid tumors, as in breast (Al-Hajj *et al.* 2003), has greatly contributed to the establishment of the cancer stem cell model as a driver of tumor heterogeneity (Visvader *et al.* 2012). According to this model, tumor initiating cells (TIC) are a selected subset of CSC, with increased capacity to generate tumors *in vivo* (Scheel *et al.* 2012). Established *in vivo* by the limiting dilution assay, a given cell population, selected by any given marker(s), is considered to have a CSC phenotype when they are more tumorigenic (thus TIC-enriched) as compared to other cell sub-populations (Clarke *et al.* 2006; Scheel *et al.* 2012). Several markers, including CD44, CD24 and aldehyde dehydrogenase (ALDH), have successfully been used to identify highly tumorigenic putative CSC sub-populations in breast tumors (Al-Hajj *et al.* 2003; Ginestier *et al.* 2007).

The sub-populations of breast cancer cells with stem-like characteristics, with increased tumorigenic capacity and the ability to recapitulate the tumor environment, have been associated with metastization, tumor relapse, poor disease prognosis and active evasion to standard chemotherapy (Al-Hajj *et al.* 2003; Ginestier *et al.* 2007; Morimoto *et al.* 2009; Marcato *et al.* 2011; Visvader 2011; Visvader *et al.* 2012). Overall, CSC represent a relevant therapeutic target aiming at successfully tackle of tumor development and drug resistance. Currently, different drugs targeting developmental-associated pathways, such as Notch or Wnt signaling, known to control CSC self-renewal and maintenance are in clinical development (Takebe *et al.* 2011). This includes, for example, inhibitors of γ-secretase (a Notch checkpoint activator), such as MK0752 or RO492909, for the treatment of advanced (NCT00106145) or triple negative

breast cancer (NCT01238133), respectively (Liu *et al.* 2010a; Takebe *et al.* 2011). In addition, canonical pathways, including PI3k/Akt signaling, are essential for CSC proliferation and survival (Zhou *et al.* 2007; Dubrovska *et al.* 2009). A double PI3k/mTOR inhibitor, VS-5584, is under clinical development against advanced non-hematologic malignancies and lymphoma (NCT01991938) (Hart *et al.* 2012). However, single drug regimes, targeting specifically cells with CSC phenotype, could be undermined by their plasticity and adaptability, enabling tumors to evade treatments and CSC enrichment (Visvader *et al.* 2008; Badve *et al.* 2012). In spite of combination chemotherapy is a widely adopted strategy to overcome drug resistance (Ramaswamy 2007), its efficacy, upon systemic administration, can be limited owing to differences in pharmacokinetics, thus impairing tumor accumulation of the needed drug ratio, essential to hinder growth and proliferation of different cells within a solid tumor (Dicko *et al.* 2010).

Provided the necessary accessibility to the CSC niche (Borovski *et al.* 2011), nanotechnology-based strategies enabling the simultaneous temporal and spatial delivery of drug combinations, targeting different signaling pathways activated in different tumor cells sub-populations, endows great potential to specifically overcome drug resistance. However, success is highly dependent on the identification of surface receptors (Wang *et al.* 2012), preferentially overexpressed in both CSC and non-SCC (non-stem cancer cells) (Visvader *et al.* 2012). This is an aspect of primordial importance from a therapeutic standpoint, as it has been demonstrated that CSC can originate from non-SCC in an Epithelial-to-Mesenchymal Transition (EMT) dependent process, fuelling tumor growth (Chaffer *et al.* 2013; Marjanovic *et al.* 2013).

Nucleolin, besides being overexpressed in cancer cells (Porkka *et al.* 2002), is a marker of angiogenic blood vessels, mediating the anti-angiogenic and anti-tumoral activity of endostatin (Christian *et al.* 2003; Shi *et al.* 2007). Such features rendered nucleolin as an important target in cancer therapy, reinforced by the

further development of several targeting moieties towards this protein (Porkka *et al.* 2002; Krust *et al.* 2011; Moura *et al.* 2012). Accordingly, we have recently developed a F3 peptide-targeted liposomal strategy, targeting cell surface nucleolin (Moura *et al.* 2012), for the simultaneous delivery of a synergistic combination of the pro-apoptotic C6-ceramide (C6-Cer), an inhibitor of PI3K/Akt signaling (Hannun *et al.* 2011), and doxorubicin (DXR) (*Chapter 2*), a cornerstone topoisomerase II inhibitor for breast cancer treatment (Minotti *et al.* 2004), aiming at promoting cancer cell death.

Building on current state-of-the-art, we recognize that identification of surface receptors enabling specific targeting of both CSC and non-SCC will be crucial to provide long-term disease free survival. Exploiting the described nucleolin role in the stemness maintenance of embryonic stem cells (Yang *et al.* 2011), as well as its increasing relevance in cancer development (Storck *et al.* 2007), the present work aims at assessing the potential of cell surface nucleolin as a target receptor in breast CSC (and non-SCC) for active intracellular delivery of the F3 peptide-targeted liposomal synergistic DXR/C6-Cer combination, aiming at ablating both breast CSC and non-SCC, strong contributors for tumor heterogeneity and drug resistance.

3.2. Results

3.2.1 Association of F3 peptide-targeted liposomes with putative breast cancer stem cells

Identification of putative breast CSC in MCF-7 and triple negative MDA-MB-231 breast cancer cell lines was carried out using ALDEFLUOR® reagent and CD44 as previously described (Croker *et al.* 2009). ALDEFLUOR® staining demonstrated that MCF-7 cells presented a lower percentage of $ALDH^{hi}$ cells than MDA-MB-231 cells (Figure 3.1A). These results are in line with reported data (Croker *et al.* 2009; Marcato *et al.* 2011), providing support for an accurate identification of cells

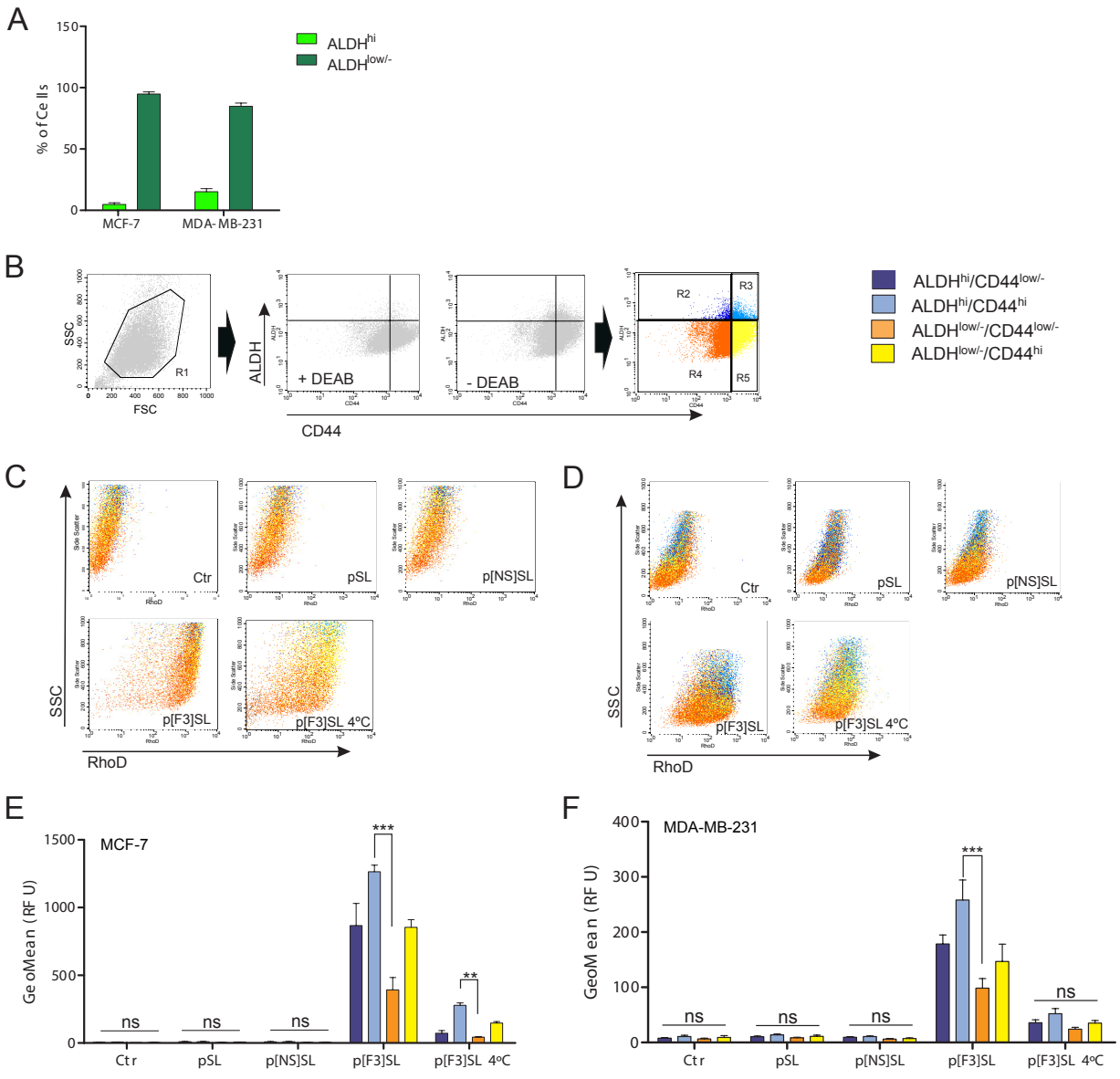

Figure 3.1 – Cellular association of F3 peptide-targeted liposomes with putative cancer stem cells.

Half million MCF-7 and MDA-MB-231 cells were incubated with 0.4 mM of Rhod-labelled F3 peptide-targeted (**p[F3]SL**), non-specific peptide targeted (**p[NS]SL**) or non-targeted (**pSL**) liposomes for 1 h at 4 or 37ºC and subsequently stained with anti-CD44-PECy5 antibody and with ALDEFLUOR® reagent, and immediately analyzed by flow cytometry. (A) Represents the relative number of cells with high ALDH activity ($ALDH^{hi}$) and low or absent ALDH activity ($ALDH^{low/-}$) present in each cell line tested. (B) Representative region criteria for the identification of CSC-enriched (R3) and non-SCC (R4) sub-populations based on the selected markers. (C, D) Represent the rhodamine side scatter dot-plots reflecting the signal distribution in each identified sub-population for the MCF-7 and MDA-MB-231 cell lines, respectively, following incubation with several tested liposomal formulations. (E, F) represent the rhodamine geometric

mean fluorescence of each sub-population for MCF-7 and MDA-MB-231 cell line, respectively (**light-blue:** putative cancer stem cells; **orange:** non-stem cancer cells). Data represent mean ± SEM (2-Way ANOVA $p<0.0001$ for formulations tested and cell sub-populations assessed; ^{ns} $p>0.05$ and $^{***}p<0.001$ Bonferroni's post test).

with high ALDH activity. In addition, almost all cells from both breast cancer cell lines expressed CD44, with values spanning a wide range, thus enabling one to identify cells with high and low/negative expression of the marker (Figure 3.1B), as previously reported (Croker *et al.* 2009; Chaffer *et al.* 2013).

Accordingly, in order to understand if one could actually deliver a payload into identified putative breast CSC, we defined a gating strategy (Figure 3.1B) enabling the evaluation of cellular association of F3 peptide-targeted liposomes with the different sub-populations expressing various levels of ALDH and CD44 (Figures 3.1C and 3.1D). The results clearly indicated that the F3 peptide-targeted liposomes (p[F3]SL) presented 3.2 (MCF-7, Figure 3.1E) and 2.6-fold (MDA-MB-231, Figure 3.1F) higher cellular association with $ALDH^{hi}/CD44^{hi}$ population (CSC) when compared to the $ALDH^{-/low}/CD44^{low/-}$ population (non-SCC), an effect that was dependent on the presence of the F3 peptide. Additionally, F3 peptide-targeted liposomes (p[F3]SL) also associated with $ALDH^{hi}/CD44^{-/low}$ and $ALDH^{-/low}/CD44^{hi}$ populations, which might represent intermediate stages in the hierarchical organization of the cancer cell lines (Figures 3.1E and 3.1F). Furthermore, at $4^{o}C$, a temperature not permissive to endocytosis, the F3 peptide-targeted liposomes presented lower cellular association with the different sub-populations in both cell line models, thus indicating that an energy-dependent internalization was taking place in all of them (Figures 3.1E and 3.1F).

3.2.2 Assessment of drug delivery to mammosphere-derived cancer stem cells

In order to validate the previous results, firstly, it was relevant to assess the *in vitro* phenotypical characteristics of the selected $ALDH^{hi}/CD44^{hi}$ and $ALDH^{low/-/}$

$CD44^{low/-}$ populations. Central to the characterization of cancer stem cells is the *in vitro* formation of mammospheres and evaluation of self-renewal (Shaw *et al.* 2012). Therefore, both cell sub-populations were sorted using the aforementioned staining strategy. Afterwards, cells were seeded in low attachment plates to

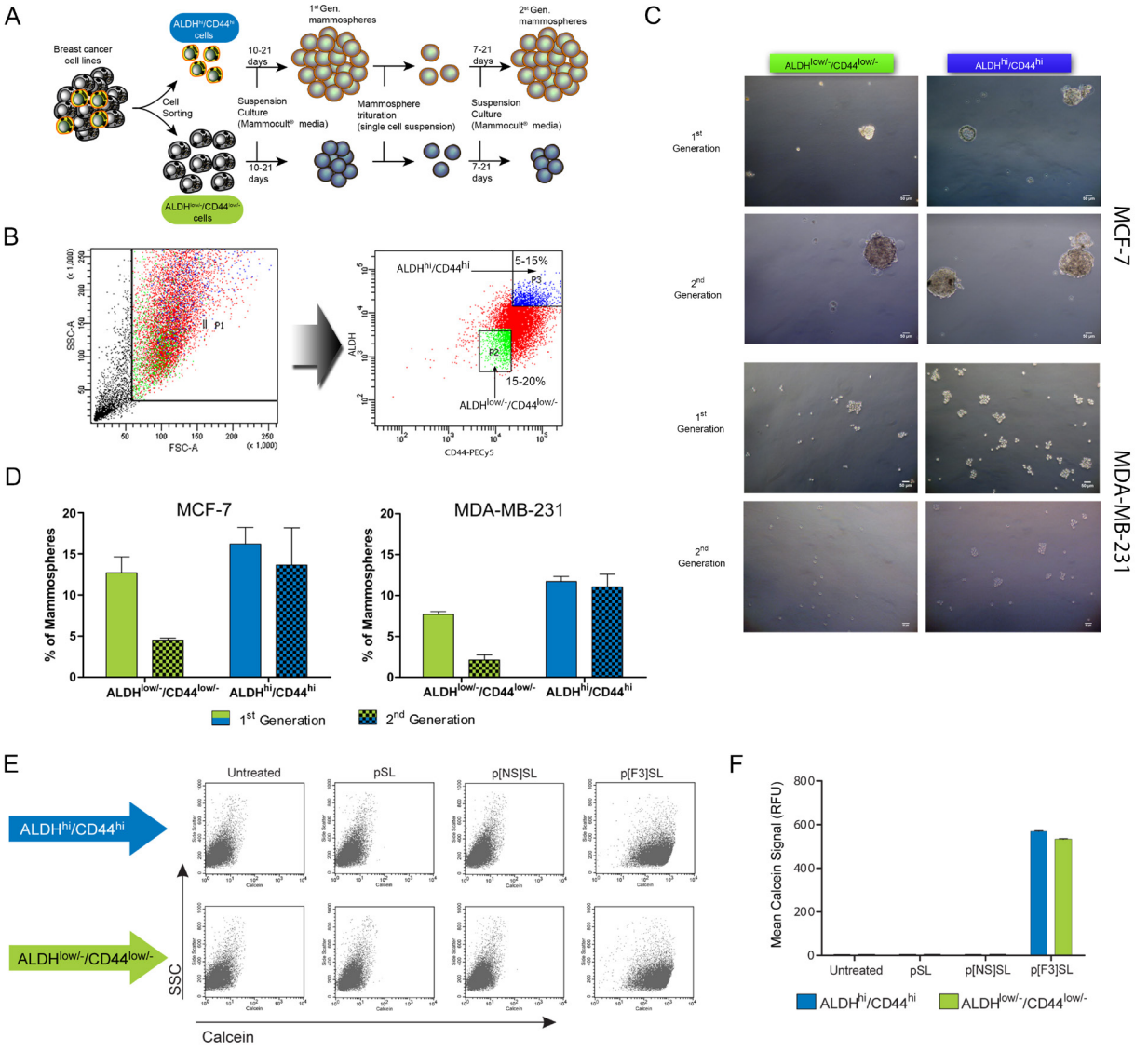

Figure 3.2 – Assessment of payload delivery by F3 peptide-targeted liposomes to mammosphere-derived putative cancer stem cells.

(A) Two-million MCF-7 and MDA-MB-231 cells were stained with CD44-PECy5 and ALDEFLUOR® reagent, and immediately sorted for isolation of $ALDH^{hi}/CD44^{hi}$ (putative cancer stem cells) and $ALDHl^{ow/-}/CD44^{low/-}$ (non-stem cancer cells). Sorted cells were cultured using fully supplemented Mammocult® Medium. (B) Representative sorting criteria for all cell lines tested, where P1 is the

gate to exclude debris and death cells from cell sorting. Gating-criteria for $ALDH^{hi}/CD44^{hi}$ and $ALDH^{low/-}/CD44^{low/-}$ cell populations enabled the collection of 5-15% (P2) and 15-20% (P3) of total events depending on the assessed sub-population. (C) and (D) Representative images of 1st and 2nd generation (self-renewal) mammospheres and mammosphere formation efficiency data of $ALDH^{hi}/CD44^{hi}$ and $ALDH^{low/-}/CD44^{low/-}$ sub-populations, from MCF-7 and MDA-MB-231 cell lines (bar = 50 μm). (E) Representative dot-plots of calcein signal and (F) corresponding mean signal from 2nd generation mammosphere-derived single cells obtained from MDA-MB-231 cells, upon incubation with non-targeted (**pSL**), non-specific peptide- (**p[NS]SL**) and F3 peptide-targeted (**p[F3]SL**) liposomes at 37ºC for 1 h (representative data from independent experiment).

evaluate 1st and 2nd generation mammosphere development (Figure 3.2A).

Results demonstrated that both isolated sub-populations from each of the cell lines tested (Figure 3.2B) were able to form mammospheres (Figure 3.2C). Additionally, cells derived from 1st generation mammospheres were able to form secondary mammospheres, and maintained shape resemblance between generations (Figure 3.2C). However, the $ALDH^{hi}/CD44^{hi}$ sub-population had increased mammosphere formation potential when compared to $ALDH^{low/-}/CD44^{low/-}$ cells, more evident for the MDA-MB-231 cell line than for the MCF-7 (Figure 3.2D). Strikingly though, while $ALDH^{hi}/CD44^{hi}$ population maintained 2nd generation mammosphere formation efficiency, for both of MCF-7 and MDA-MB-231, $ALDH^{low/-}/CD44^{low/-}$ lost, in part, their capacity to generate spheres (Figure 3.2D). Overall, these results indicated that both populations have different stem and self-renewal potentials, thus suggesting that each sub-population could belong to different hierarchical clusters. Moreover, F3 peptide-targeted liposomes enabled efficient delivery of encapsulated calcein to single cell derived from 2nd generation mammospheres of both sub-populations, with similar efficiency (Figures 3.2E and 3.2F). These reinforce the ability of liposomes functionalized with F3 peptide to target both breast CSC and non-SCC. These results also suggest similar levels of expression of cell surface nucleolin in mammosphere-derived cells from both $ALDH^{hi}/CD44^{hi}$ and $ALDH^{low/-}/CD44^{low/-}$ sub-populations.

3.2.3 Nucleolin and pluripotency markers mRNA levels in breast CSC and mESC

In the previous sections, it has been demonstrated that F3 peptide-targeted liposomes associated in a higher extent with putative breast CSC than with non-SCC (Figure 3.1), notwithstanding the efficient payload delivery promoted for both cellular populations (Figure 3.2). Overall, these results suggested that nucleolin expression in breast CSC could be paralleled by the expression of pluripotency genes, also known to be upregulated in cancer (Ling *et al.* 2012). To test this hypothesis, we evaluated the pluripotency transcription factors NANOG and OCT4 and, concomitantly, the nucleolin mRNA levels in sorted sub-populations from breast cancer cell lines. In addition, we assessed the same mRNA targets upon culturing mESC in different conditions, used herein as phenotypic controls owing to the high conservation of nucleolin among species (Ginisty *et al.* 1999) (Figure 3.3A). Indeed, when mESC were cultured in conditions favoring pluripotency loss, there was a decrease of NANOG and OCT4 mRNA levels that were paralleled by nucleolin (Figure 3.3B and S3.2, *Supplemental data*), in agreement with data from Yang and colleagues (Yang *et al.* 2011).

According to its role in cancer, one could think that nucleolin would be homogenously expressed in cancer cells. Strikingly, MDA-MB-231 putative breast CSC ($ALDH^{hi}/CD44^{hi}$) presented 1.5-fold higher nucleolin mRNA level relative to non-SCC ($ALDH^{low/-}/CD44^{low/-}$) (Figure 3.3C). Moreover, the increased levels of nucleolin were paralleled by the overexpression of NANOG and OCT4 in breast CSC (Figure 3.3C). In spite of following the same trend, the results obtained with MCF-7 cell line were highly variable (Figure 3.3D). These results support the enhanced cellular association of F3 peptide-targeted liposomes with putative breast CSC, as well as the increased mammosphere formation efficiency of those as compared to non-SCC (Figures 3.1E, 3.1F and 3.2D).

Overall, the identified putative CSC populations are enriched for stem-like cells, as compared to non-SCC, indicating that nucleolin is in fact associated with the former phenotype.

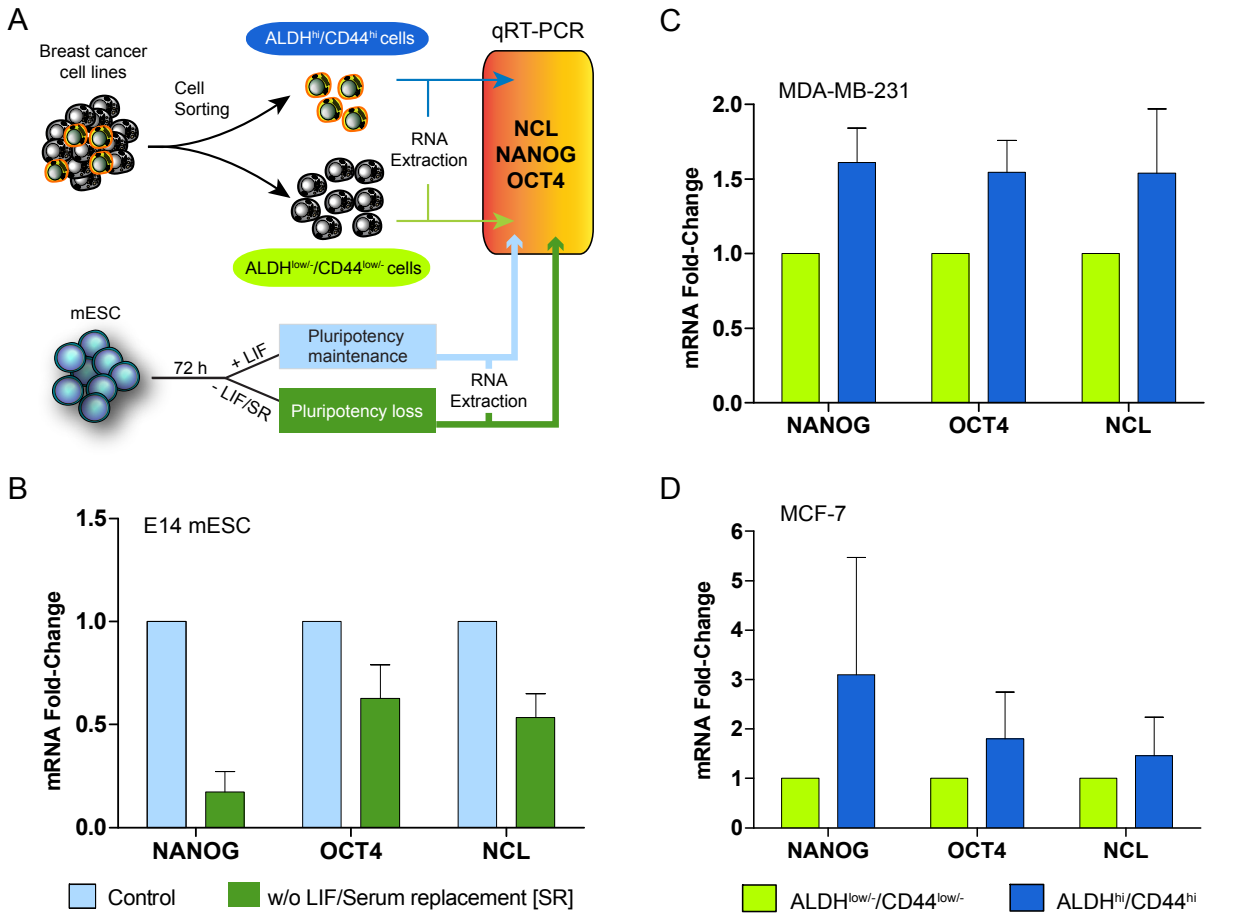

Figure 3.3 – Comparative analysis of pluripotency genes and nucleolin mRNA levels in putative breast cancer stem cells (CSC) and mouse embryonic stem cells (mESC).
(A) MCF-7 and MDA-MB-231 breast cancer cells were stained with CD44-PECy5 and ALDEFLUOR® reagent, and immediately sorted for isolation of ALDH^{hi}/CD44^{hi} (putative CSC) and ALDH$^{low/-}$/CD44$^{low/-}$ (non-SCC) similarly as in Mammosphere assay. E14 mESC were cultured for 72 h either in medium without LIF and Serum replacement [SR] (inducing loss of pluripotency) or in fully supplemented medium containing LIF (Control). (B) Effect on NANOG, OCT4 and nucleolin (NCL) mRNA levels from mESC cultured in conditions inducing pluripotency loss. (C, D) Represent the relative mRNA fold-change of NANOG, OCT4 and NCL of ALDH^{hi}/CD44^{hi} relative to ALDH$^{low/-}$/CD44$^{low/-}$ cells for both MDA-MB-231 and MCF-7 breast cancer cells lines, respectively. Data represent the mean ± SEM.

3.2.4 Cellular association of F3 peptide-targeted nanoparticles with embryonic stem cells

Besides of its expression in different cellular compartments, it has been recently demonstrated that nucleolin is involved in embryonic stem cell self-renewal by modulating p53-dependent pathway (Christian *et al.* 2003; Yang *et al.* 2011). Those facts, supported by the results from previous sections, raised the question on whether the cellular association of F3 peptide-targeted liposomes, reliant on cell surface nucleolin, would be dependent on the stemness status. As such, we evaluated the cellular association of F3 peptide-targeted liposomes after culturing mESC in conditions either impairing or favoring pluripotency (Figure 3.4A).

F3 peptide-targeted liposomes (p[F3]SL) associated with mESC in a high extent, when compared to the non-targeted or non-specific targeted counterparts, and in a ligand-specific manner (Figures 3.4B-D). Furthermore, the association of F3 peptide-targeted liposomes decreased upon incubation at 4ºC, a temperature non-permissive to endocytosis, suggesting that an active internalization through receptor-mediated endocytosis was taking place (Figures 3.4B and 3.4C). Strikingly, culturing E14-GFP mESC cells without LIF and serum replacement (thus inducing pluripotency loss, a condition supported by the decreased levels of the Oct4-GFP fusion protein, Figure 3.4E) resulted in a significant reduction in cellular association, to levels close to the ones observed for non-targeted liposomes (Figure 3.4C). It is important to emphasize that even when the experiment was performed with cell colonies, F3 peptide-targeted liposomes associated with E14-GFP mESC cells, nonetheless in a lower extent (6.6-fold) (Figures 3.4B or 3.4D) than the one observed with cells in suspension (Figure 3.4C). Such results could be explained by the lower accessibility of the targeted liposomes to E14 cells in colony, as well as by the increased surface area available for targeting when the experiment is performed with the cells in suspension. This was reinforced by the 3.2-fold increase in cellular association obtained for cells grown in absence of LIF

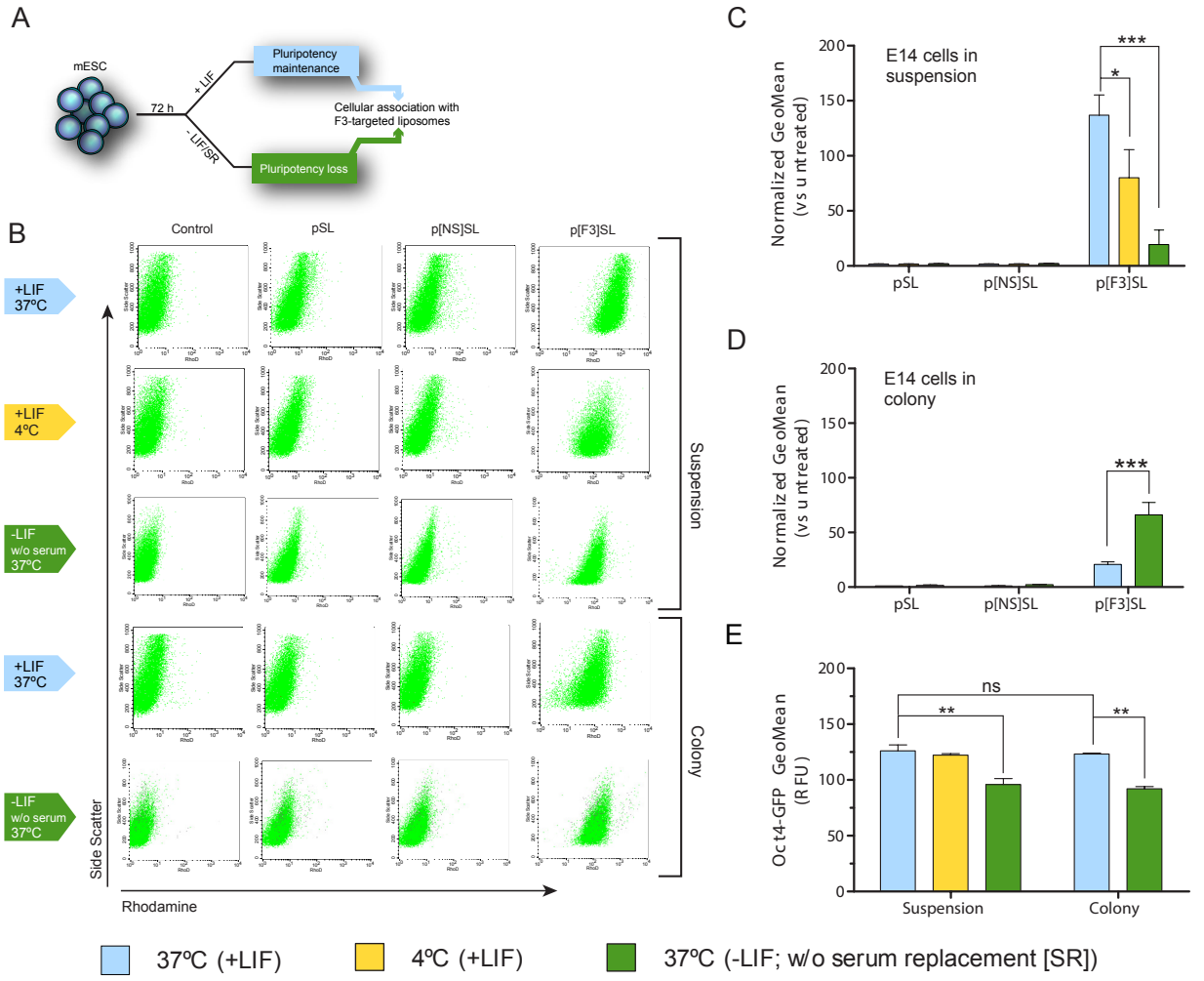

Figure 3.4 – Cellular association of F3 peptide-targeted liposomes with mouse embryonic stem cells.

(A) E14-GFP mouse embryonic stem cells (mESC) or the corresponding colonies, were incubated with 0.4 mM total lipid of F3 peptide-targeted (**p[F3]SL**), non-specific peptide targeted (**p[NS]SL**) or non-targeted (**pSL**) liposomes incorporating 1 mol% of Rhodamine-PE, for 1 h at 4 or 37ºC and analyzed by flow cytometry, after 72 h in culture either in the presence of LIF (pluripotency maintenance) or in the absence of LIF and serum replacement [SR]. (B) Represents the rhodamine-side scatter dot-plots reflecting the signal distribution. (C) and (D) represent the geometric mean of rhodamine fluorescence for each nanosystem normalized against the corresponding signal of the untreated E14 mESC cells, in suspension and in colony, respectively (2-Way ANOVA $p \leq 0.016$ for both culture conditions and liposome formulation variables; ***$p<0.001$ and *$p<0.05$ Bonferroni's post-test). (E) Represents the OCT4-GFP levels of E14-GFP mESC cells according to culture conditions used (1-Way Anova $p<0.0024$; **$p<0.01$ and $^{ns}p>0.05$ Tukey's post-test). Non-viable cells were excluded from the analysis using 7-AAD. E14-wt mESC were used as controls to correct autofluorescence. Data represent the mean ± SEM.

and serum replacement, as compared to standard growth conditions, since the resulting colonies were smaller thus facilitating the nanosystem access (Figure 3.4D).

Overall, these results strongly suggest that cell membrane nucleolin levels decrease according to cell pluripotency status, which is accompanied by reduction of OCT4 protein and therefore highly consistent with mRNA levels determination (Figure 3.3B), thus revealing that cellular association of F3 peptide-targeted liposomes is stemness status-dependent.

3.2.5 Evaluation of the tumorigenic potential of cell surface nucleolin positive cells and putative breast CSC

We have previously demonstrated that $ALDH^{hi}/CD44^{hi}$ cells (putative breast CSC) had increased *in vitro* self-renewal capacity (Figure 3.2), as well as a higher extent of association of F3 peptide-functionalized liposomes, targeting nucleolin, relative to $ALDH^{low/-}/CD44^{low/-}$ cells (non-SCC) (Figure 3.1). In addition, we have demonstrated in mESC that nucleolin expression was dependent on stemness status (Figures 3.3 and 3.4), ruling cell surface nucleolin-dependent cellular association of F3 peptide-targeted liposomes (Figure 3.4). Overall, these results led one to question whether cell surface nucleolin overexpression could enable the identification of highly tumorigenic cells.

Tumor development latency analysis revealed faster tumor initiation capacity of $ALDH^{hi}/CD44^{hi}$ cells as compared with $ALDH^{low/-}/CD44^{low/-}$ (1.32 and 1.37-fold for 2000 and 20000 inoculated cells, respectively) (Figure 3.5), a feature consistent with data from the literature (Ginestier *et al.* 2007; Croker *et al.* 2009). Notwithstanding, NCL^+ and NCL^- cell populations shared a similar latency in tumor development (Figure 3.5). Nevertheless, NCL^+ and $ALDH^{hi}/CD44^{hi}$ cell populations demonstrated an increased capacity to generate orthotopic tumors as compared with NCL^- and $ALDH^{low/-}/CD44^{low/-}$ populations, respectively, especially at lower cell density (Table

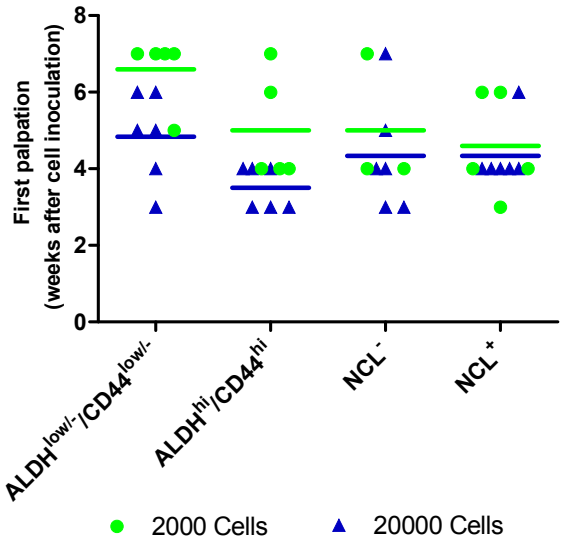

Figure 3.5 – Tumor development latency of sorted cell populations upon inoculation in NOD scid gamma mice.

Following staining of MDA-MB-231 cells with ALDEFLUOR®/CD44-PECy5 or with anti-nucleolin-Alexa488 antibody (NCL), sorted populations, as presented in the x-axis, were orthotopically inoculated in the mammary fat pad of NOD scid gamma (NSG) mice. Dots and triangles represent the lapsed time for first palpation after inoculation, for a cell density of 2000 or 20000 cells, respectively. Bars represent the mean latency time for first palpation (2-way ANOVA: p = 0.0081 and p = 0.0318, for cell density and sorted population variables, respectively)

Table 3.1 – Tumorigenic potential of different cell sub-populations sorted from the triple negative breast cancer cell line MDA-MB-231.

MDA-MB-231	**Time (weeks after cell inoculation)**								
	4 weeks			*6 weeks*			*7 weeks*		
Sorted sub-population	**Number of Tumors**		**TIC frequency^{-1}**	**Number of Tumors**		**TIC frequency^{-1}**	**Number of Tumors**		**TIC frequency^{-1}**
	2000 cells	*20000 cells*		*2000 cells*	*20000 cells*		*2000 cells*	*20000 cells*	
ALDH$^{low/-}$/CD44$^{low/-}$	0/6	2/6	55400	1/6	6/6	6141	5/6	6/6	1116
ALDH^{hi}/CD44^{hi}	3/6	6/6	2848	4/6	6/6	1820	5/6	6/6	1116
NCL^{-}	2/6	4/6	13391	2/6	5/6	8957	3/6	6/6	2848
NCL^{+}	3/6	5/6	7310	5/6	6/6	1116	5/6	6/6	1116

Data represent the number of tumors generated per sorted population injected (as presented in the table) in NOD scid gamma mice. Tumor initiating cell (TIC) frequency was calculated by the limiting dilution analysis (Hu *et al.* 2009) using the L-calc™ software.

3.1). This translated into a higher frequency of tumor initiating cells (TIC) within ALDH^{hi}/CD44^{hi} (putative breast CSC) and NCL^{+} sub-populations compared to the non-stem cancer cells (ALDH$^{low/-}$/CD44$^{low/-}$) and NCL^{-} sub-populations (3.4 and 8-fold respectively, at 6 weeks) (Table 3.1). Of notice was the fact that, overtime (until 7 weeks post cell inoculation), all sorted populations were able to seed the majority of new tumors (Table 3.1).

Overall, these results suggest that overexpression of cell surface nucleolin *per se* could be useful for the identification of highly tumorigenic cells. The tumorigenic potential of putative CSC, non-SCC and nucleolin-driven isolated

cells emphasizes the need to target simultaneously several populations within the tumor microenvironment, aiming at successful therapeutic intervention.

In this respect, and based on the results previously presented, liposomes functionalized with the F3 peptide and targeting nucleolin are a drug carrier with great therapeutic potential.

3.2.6 Cellular cytotoxicity mediated by F3 peptide-targeted combination of doxorubicin and C6-ceramide

In order to overcome drug resistance, often associated with CSC, it has been recognized that the successful application of small molecules in cancer therapy requires the identification of agents that, when combined, lead to synergistic tumor inhibition without significant systemic toxicity (Mayer *et al.* 2007; Ramaswamy 2007; Visvader *et al.* 2008; Croker *et al.* 2011; Lee *et al.* 2011). Such strategy offers the potential to target simultaneously multiple pathways, commonly deregulated in cancer, and inherently, in CSC (Dubrovska *et al.* 2009; Baselga 2011; Ciriello *et al.* 2013). Nanotechnology-based systems allow one to explore those synergistic interactions, by enabling simultaneous spatial and temporal delivery of combinations at tumor site, thus providing a mean to translate *in vitro* information to the *in vivo* setting (Dicko *et al.* 2010). Engineering nanoparticles' surface with an internalizing targeting moiety enables one to specifically direct the delivery of such combination towards tumor cells, like endothelial or cancer cells (Moura *et al.* 2012; Fonseca *et al.* 2014). We have previously developed F3 peptide-targeted triggered release liposomes co-encapsulating combinations of doxorubicin and the pro-apoptotic sphingolipid C6-ceramide, enabling synergistic cellular cytotoxicity against triple negative breast cancer cell line (*Chapter 2*). Therefore, herein we explored the cytotoxic impact of this novel targeted synergistic combination against putative breast CSC.

At the highest concentration tested, C6-ceramide induced a 2.5- and 2.1-fold

decrease in the number of viable ALDH^{hi} cells (ALDH^{hi}/7AAD^{-}) from MCF-7 and MDA-MB-231 breast cancer cells, respectively, an effect apparently independent of C6-ceramide dose (Figures 3.6A and 3.6B). CSC have been shown to be highly resilient to DXR action, compared to non-SCC (Croker *et al.* 2011). By impairing ALDH^{hi} cell viability, the aforementioned result supported the use of C6-Ceramide

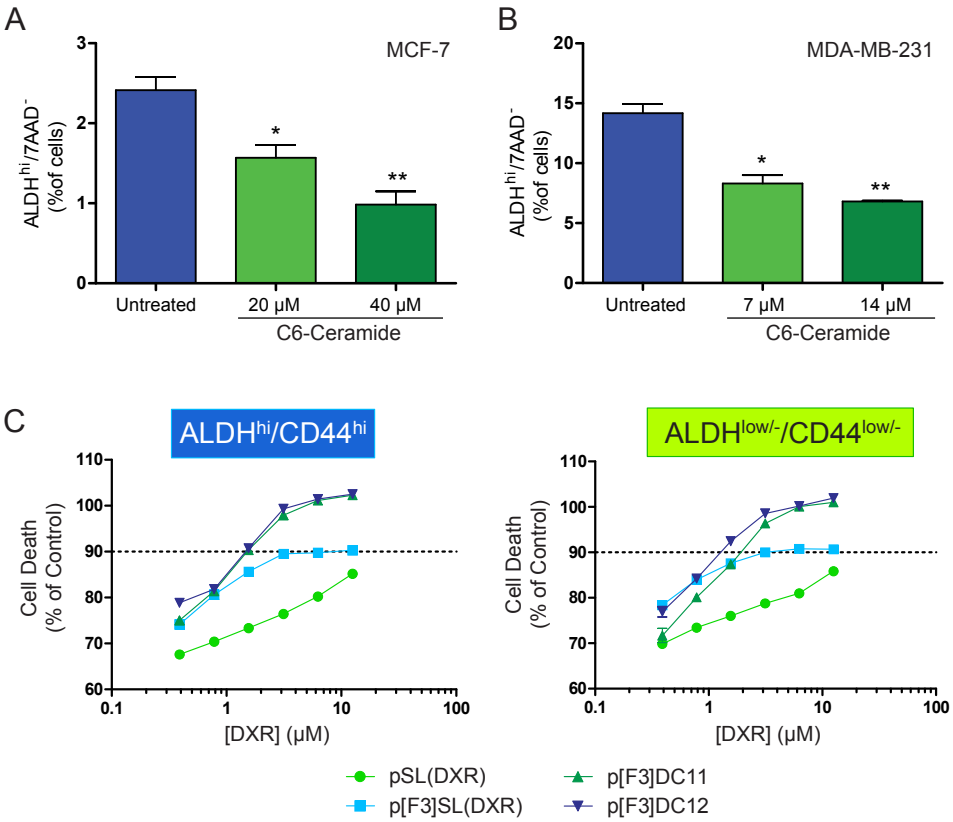

Citotoxicity (IC_{90}) of liposomal formulations of DXR or DXR/C6-Cer against mammospheres derived from ALDH^{hi}/CD44^{hi} and ALDH$^{low/-}$/CD44$^{low/-}$ sub-populations sorted from MDA-MB-231 triple breast cancer cells.

Formulation	ALDH^{hi}/CD44^{hi}		ALDH$^{low/-}$/CD44$^{low/-}$	
	IC_{90}	SEM	IC_{90}	SEM
pSL(DXR)	N/D		N/D	
p[F3]SL(DXR)	8.08	2.82	2.98	0.25
p[F3]DC11	1.52	0.03	1.91	0.05
p[F3]DC12	1.48	0.07	1.27	0.05

Figure 3.6 – Cellular cytotoxicity of doxorubicin (DXR):C6-ceramide (C6-Cer) combinations delivered by F3 peptide-targeted liposomes.

(A) and (B) Represent the effect of free C6-ceramide on viable ALDH^{hi} cell sub-population from MCF-7 and MDA-MB-231 breast cancer cells, respectively (data represent mean ± SEM; *p<0.05 and **p<0.01 Tukey's test, compared to untreated). (C) Representative dose-response curves of MDA-MB-231 (ALDH^{hi}/CD44^{hi} and ALDH$^{low/-}$/CD44$^{low/-}$) cells derived from 2nd generation

mammospheres, incubated with F3 peptide-targeted liposomes either encapsulating DXR (**p[F3]SL**) or a combination of DXR and C6-Cer at 1:1 (**p[F3]DC11**) or 1:2 molar ratio (**p[F3]DC12**) or non-targeted liposomal DXR (**pSL**) (Inserted Table - IC_{90} values calculated from representative dose-response experiment by linear interpolation of dose values immediately above or below 90% effect)

and DXR combinations. Accordingly, we evaluated the cytotoxicity of the DXR/C6-Cer synergistic combination encapsulated in F3 peptide-targeted triggered release liposomes against mammospheres, known to better predict *in vivo* drug responses (Kim *et al.* 2013).

The cytotoxicity results obtained with 2nd generation mammospheres derived from MDA-MB-231 breast cancer cell line, indicated that ALDH^{hi}/CD44^{hi} cells were more resistant to F3 peptide-targeted doxorubicin (p[F3]SL(DXR)) than ALDH$^{low/-}$/CD44$^{low/-}$ cells. Notwithstanding, targeting these different cell sub-populations through the nucleolin receptor with the liposomal DXR, functionalized with the F3 peptide, enabled an IC_{90} lower than non-targeted formulation (pSL(DXR)) (Figure 3.6C and insert table). However, the co-encapsulation of DXR and C6-Cer at 1:1 (p[F3]DC11) and 1:2 (p[F3]DC12) molar ratios in the F3 peptide-targeted nanoparticle enabled 100% cell death, while decreasing DXR IC_{90} (4-fold in case of ALDH^{hi}/CD44^{hi} cells) (Figure 3.6C and insert table), a condition not achievable with the single drug (DXR)-containing F3 peptide targeted nanoparticle. In addition, it was apparent that F3 peptide-targeted delivery of DXR:C6-Cer combination decreased the IC_{90} of DXR to similar values in both sensitive (ALDH$^{low/-}$/CD44$^{low/-}$) and more resistant (ALDH^{hi}/CD44^{hi}) cell sub-populations (Figure 3.6 – Insert Table), thus seemingly overcoming putative CSC-associated DXR resistance.

3.3. Discussion

Cancer remains as a complex and elusive disease. The introduction of the CSC model significantly contributed to that complexity by postulating the existence of cellular populations with stem-like features responsible for tumor

development and heterogeneity, drug resistance and disease relapse (Visvader *et al.* 2012). Notwithstanding, a denser landscape emerged by the knowledge that CSC may originate from non-SCC, interconverting through an EMT-mediated process (Chaffer *et al.* 2013). This has turned these cell sub-populations into two relevant therapeutic targets (Visvader *et al.* 2012). Therefore, to specifically tackle the disease at its roots, one has to find suitable molecular targets that enable simultaneous targeting of both CSC and non-SCC, provided the necessary accessibility to the CSC niche (Borovski *et al.* 2011; Visvader *et al.* 2012).

Nucleolin, thought as homogenously overexpressed by cancer and angiogenic endothelial cells, has been exploited as a molecular target for drug delivery with nanotechnology-based strategies (Moura *et al.* 2012). It was demonstrated herein that a F3 peptide-targeted lipid-based nanoparticle is actively internalized by both breast non-SCC ($ALDH^{low/-}/CD44^{low/-}$) and, in a higher extent, putative CSC ($ALDH^{hi}/CD44^{hi}$) (Figure 3.1), enabling the delivery of the liposomal payload (Figure 3.2F) into these sub-populations of cells with different stem-like phenotype (Figure 3.2D). This simultaneous targeting of multiple cancer cell populations introduces a critical feature sought to be essential for next generation of cancer therapy (Visvader *et al.* 2012). Those results suggested that nucleolin could be expressed at different densities among those sub-populations. In addition, it is known that nucleolin (Moura *et al.* 2012) and pluripotency markers (Ling *et al.* 2012) are expressed in both tumors and breast cancer cells. Nonetheless, the simultaneous upregulation in putative breast CSC has never been described.

We have shown an upregulation of mRNA levels of the pluripotency markers NANOG and OCT4, which was paralleled by nucleolin, in triple negative putative breast CSC as compared to non-SCC (Figure 3.3C), supporting the cellular association both with cells (Figure 3.1F) and 2^{nd} generation mammosphere-derived single MDA-MB-231 cells (Figure 3.2F) as well as differences in stem-like phenotype (Figure 3.2D). To our best knowledge, this association was only

described in mESC (Yang *et al.* 2011). A similar trend in upregulation of both pluripotency markers and nucleolin was observed for MCF-7 breast cancer cell line, though highly variable (Figure 3.3D). It has been suggested that ALDH and CD44 may identify CSC with different degrees of differentiation according to the histological types of breast cancer (for example, luminal, MCF-7 *versus* the less differentiated triple negative type, MDA-MB-231) (Ricardo *et al.* 2011), which could account for these results (Figure 3.3C vs Figure 3.3D).

We confirmed the aforementioned results using mESC as stemness gold-standard system, as nucleolin is an highly conserved protein among mammal species (Ginisty *et al.* 1999). Culturing mESC in conditions favoring pluripotency loss (absence of LIF and serum replacement), led to a downregulation of NANOG, OCT4 and nucleolin mRNA levels (Figure 3.3B), and, consistently, a strong decrease in cellular association of F3 peptide-targeted liposomes (Figure 3.4B and 3.4C) and OCT4-GFP fusion protein (Figure 3.4E). Nucleolin has been described to regulate self-renewal in mESC in p53 pathway dependent manner (Yang *et al.* 2011). Yang *et al.* demonstrated that differentiation overtime, led to a decrease in nucleolin and OCT4 expression (Yang *et al.* 2011), in agreement with our results (Figure 3.3B, 3.4 and S3.2, *Supplemental data*). Overall, the aforementioned results led to question whether cell surface nucleolin expression *per se*, would enable the identification of tumorigenic cells. Strikingly NCL^{+} triple negative breast cancer cells presented increased tumorigenic capacity, paralleling $ALDH^{hi}/CD44^{hi}$ cells from the same histological origin (Table 3.1), already described as highly tumorigenic (Ginestier *et al.* 2007; Croker *et al.* 2009). Besides nucleolin role in angiogenesis and targeted drug delivery (Christian *et al.* 2003; Moura *et al.* 2012), it has been shown that AS1411 aptamer (a.k.a. AGRO100), targeting cell surface nucleolin (Reyes-Reyes *et al.* 2010), impairs cellular growth of cancer cells of different histological origins, including breast cancer (Girvan *et al.* 2006), consequently establishing nucleolin as a disease driver. Our results reinforce the previous observation, suggesting

that a small population of surface nucleolin-overexpressing triple negative breast cancer cells may contribute, at least in part, to tumor development. Interestingly though, over time all tested cell sub-populations gave rise to, approximately, an equal number of tumors, especially at higher cell density, resulting in similar TIC frequency estimation (Table 3.1). Consistently, it has been suggested that TIC frequency may increase with observation time length (Quintana *et al.* 2008; Ishizawa *et al.* 2010). Chaffer and colleagues demonstrated that notwithstanding basal-like $CD44^{lo}$ breast cancer cells generated tumors rather inefficiently, those tumors had high levels of $CD44^{hi}$ cells (Chaffer *et al.* 2013). Once re-injected in NOD/SCID mice, these $CD44^{hi}$ cells readily formed new tumors as compared to inefficient $CD44^{lo}$ cells (Chaffer *et al.* 2013). This established the EMT-mediated dynamic cell plasticity as fundamental for the spontaneous conversion of basal-like non-SCC ($CD44^{lo}$) to CSC ($CD44^{hi}$), a tumorigenicity-enhancing feature (Chaffer *et al.* 2013; Marjanovic *et al.* 2013). This is also consistent with less differentiated, thus more aggressive, nature of basal-like breast cancers (Schmitt *et al.* 2012). Thus, at least in the case of basal-like breast cancer cells, as MDA-MB-231, cell plasticity, under a stimulus, as hypoxia (Conley *et al.* 2012), might enable the conversion from low into highly tumorigenic cells (Chaffer *et al.* 2013), an event that could support, in part, our observations (Figure 3.5 and Table 3.1). Overall, our data reinforce the need to strategically target multiple cell sub-populations, including both non-SCC and CSC, within the tumor microenvironment.

Efficient eradication of both CSC and non-SCC may reside in the identification of synergistic drug combinations that simultaneously tackle several deregulated signaling pathways (Ramaswamy 2007). Nonetheless, translation of the *in vitro* efficacy information to *in vivo* remains a bottleneck due to pharmacokinetic differences of the combined drugs (Dicko *et al.* 2010). Ligand-mediated targeted nanotechnology has the advantage of enabling the simultaneous intracellular delivery of drug combinations, on a receptor-dependent manner, besides

synchronizing the pharmacokinetics of the encapsulated drugs and subsequent tumor accumulation (Dicko *et al.* 2010; Moura *et al.* 2012; Fonseca *et al.* 2014). We have previously developed F3-targeted liposomes encapsulating defined ratios of C6-Cer and DXR, which enabled synergistic cell cytotoxicity against the triple negative breast cancer cells (*Chapter 2*).

The above cellular association and delivery results (Figure 3.1F and 3.2F, respectively), led us to evaluate this innovative strategy against CSC-derived mammospheres, better predictors of *in vivo* drug responses (Kim *et al.* 2013). It has been reasoned that CSC eradication may be dependent of targeting developmental-related pathways, such as Notch or Wnt (Takebe *et al.* 2011). However, tackling classical signaling pathways such as PI3k/Akt pathway is also noteworthy (Dubrovska *et al.* 2009). Indeed, free C6-ceramide, targeting PI3k/Akt pathway (Hannun *et al.* 2011), was able to induce death of $ALDH^{hi}$ cells (Figure 3.6A, 3.6B and S3.3, *Supplemental data*), known to be resistant to DXR (Croker *et al.* 2011), thus confirming it as a valuable agent against CSC. Herein, the F3 peptide-targeted combination strategy enabled 100% cell death against mammospheres of both putative CSC and non-SCC, even unattainable by targeted liposomal DXR (Figure 3.6C), thus apparently overcoming DXR resistance (Croker *et al.* 2011).

Using nanotechnologies based on EPR (Enhanced Permeability and Retention)-driven tumor accumulation, others have already demonstrated that co-encapsulated C6-ceramide in combination doxorubicin increased the overall survival as compared to single drug (Khazanov *et al.* 2008). However, this type of approach is devoided of the ability to target cell populations within the tumor microenvironment responsible for tumor resistance and relapse (Hanahan *et al.* 2011). Engineering nanoparticles' surface with internalizing ligands, targeting, for example, the HER2 or transferrin receptors, has shown increased specificity and efficacy against tumors of breast or other solid malignancies relative to the non-targeted (without ligand) counterparts (Reynolds *et al.* 2012; Wang *et al.* 2012).

However, many of those ligands target receptors not necessarily providing specific targeting to the tumor microenvironment, and particularly, to CSC. Addressing this issue, nanoparticle-mediated targeting exploring the overexpression of CSC putative markers, like CD44 or CD133, have been proposed for small drugs and siRNA delivery into CSC, mainly as single agents (Ganesh *et al.* 2013; Swaminathan *et al.* 2013; Pesarrodona *et al.* 2014). Despite overexpressed in cancer cells and tumor angiogenic cells, CD44 has also been described to regulate normal vascular endothelial barrier integrity (Griffioen *et al.* 1997; Flynn *et al.* 2013). Thus, a CD44-based targeting strategy would not be necessarily devoided of side effects. In contrast, a nucleolin-targeted approach would be less prone to collateral toxicity owing to specific surface nucleolin overexpression by endothelial cells of tumor angiogenic blood vessels, as compared to its absence in normal tissues, such as liver or lung (Christian *et al.* 2003; Shi *et al.* 2007). Therefore, the described F3 peptide-mediated targeting towards cell surface nucleolin, of both putative CSC and non-SCC combines with the specific targeting of endothelial cells of tumor angiogenic blood vessels (Christian *et al.* 2003; Moura *et al.* 2012). Moreover, the F3 peptide-mediated intracellular delivery of a synergistic cytotoxic combination of DXR:C6-Ceramide into those cells may represent a suitable multitarget approach, tackling simultaneously multiple pillars sustaining breast cancer.

3.4. Conclusion

In the present work, we demonstrated the ability of F3-targeted liposomes to target simultaneously both putative breast CSC and non-SCC expressing nucleolin at different densities (particularly triple negative breast cancer cells). Using *bone fide* murine embryonic stem cells, it was demonstrated that both nucleolin mRNA levels and F3 peptide-targeted liposomes cellular association were dependent on the stemness status. In addition, we suggested that overexpression of cell surface nucleolin *per se* could be useful for the identification of highly tumorigenic cells.

Overall, our results suggested a clear link between nucleolin expression (including cell membrane nucleolin) and the stem cell-like phenotype in breast cancer, namely in the triple negative molecular subtype. It enabled the intracellular, F3 peptide-mediated, delivery of drug combinations into both CSC and non-SCC, rendering 100% cell death. Combined with the established nucleolin-mediated targeting of tumor angiogenic blood vessels, the described strategy has the potential to simultaneously debulk multiple cellular compartments in the tumor microenvironment, while decreasing tumor recurrence and systemic toxicity, ultimately enabling long-term disease free survival.

3.5. Materials and methods

3.5.1 Materials

MCF-7, MDA-MB-231 and MDA-MB-435S cell lines were from ATCC (Virginia, USA). Doxorubicin hydrochloride (DXR) was from IdisPharma (UK). Calcein, 4-(2-Hydroxyethyl)piperazine-1-ethanesulfonic acid (HEPES), 2-(N-Morpholino) ethanesulfonic acid (MES), Disodium ethylenediaminetetraacetate dehydrate (EDTA), Trizma®Base, 3-(4,5-Dimethyl-2-thiazolyl)-2,5-diphenyl-2H-tetrazolium bromide (MTT), sodium chloride (NaCl), 3β-hydroxy-5-cholestene-3-hemisuccinate (CHEMS) and cholesterol (CHOL) were purchased from Sigma-Aldrich (USA). The lipids 2-dioleoyl-sn-glycero-3-phosphoethanolamine (DOPE), 1,2-distearoyl-sn-glycero-3-phosphocholine (DSPC), 1,2-distearoyl-sn-glycero-3-phosphoethanolamine-N-[methoxy(polyethylene glycol)-2000] (DSPE-PEG_{2k}), 1,2-distearoyl-sn-glycero-3-phosphoethanolamine-N-[maleimide(polyethylene glycol)-2000] (DSPE-PEG_{2k}-maleimide), L-**α**-Phosphatidylethanolamine-N-(lissamine rhodamine B sulfonyl) (RhoB-PE), N-hexanoyl-D-erythro-sphingosine (C6-Ceramide) were acquired from Avanti Polar Lipids (USA). F3 (KDEPQRRSARLSAKPAPPKPEPKPKKAPAKK) and the non-specific (NS) peptides were custom synthetized by Genecust (Luxemburg). All other chemicals were of

analytical grade purity.

3.5.2 Cell culture

Wild-type E14 mESC (E14-wt), derived by Dr. Martin Hooper from the mouse strain 129/Ola, or OCT4-GFP fusion protein-expressing E14 mESC (E14-GFP) (Hooper *et al.* 1987; Wakayama *et al.* 1999; Ohtsuka *et al.* 2006; Feldman *et al.* 2012) were maintained in feed-layer free conditions in KnockOut-Dubelcco's Modified Eagle's Medium (GIBCO Life Technologies, USA) supplemented with 15% KnockOut Serum Replacement (GIBCO Life Technologies), 100 U/mL of penicillin and 100 µg/mL of streptomycin (GIBCO Life Technologies, USA), 1% Minimum Essential Medium non-essential aminoacids (Sigma-Aldrich, USA), 1% L-glutamine (2 mM) (GIBCO Life Technologies, USA), 0.1 mM β-Mercaptoethanol (Sigma-Aldrich, USA) in the presence of 10 U/mL of leukemia-inducible factor (LIF) (Millipore, USA) at 37ºC in an atmosphere of 5% CO_2.

MCF-7 (luminal) and MDA-MB-231 (triple negative) breast cancer cells lines, and MDA-MB-435S melanoma cell line, were cultured in RPMI 1640 (Sigma-Aldrich, USA) supplemented with 10% (v/v) of heat-inactivated Fetal Bovine Serum (FBS) (Invitrogen, USA), 100 U/mL penicillin, 100 µg/mL streptomycin (Lonza, Switzerland) and maintained at 37°C in a 5% CO2 atmosphere.

3.5.3 Preparation of Liposomes

pH-sensitive liposomes without ceramide were composed of DOPE:CHEMS:DSPC:CHOL:DSPE-PEG_{2k} (4:2:2:2:0.8 molar ratio) and pH-sensitive liposomes incorporating ceramide were composed of DOPE:CHEMS:DSPC:CHOL:DSPE-PEG_{2k}:C6-ceramide (4:2:1:1:0.8:2 molar ratio).

Liposomes were prepared by the ethanol injection procedure (Gomes-da-Silva *et al.* 2013b). Ethanolic lipid mixtures were added to ammonium sulfate buffer (pH 8.5) at 60°C and the resulting liposomes were extruded through 80 nm pore size polycarbonate membranes using a LiposoFast Basic mini extruder (Avestin, Canada). The buffer was exchanged in a Sephadex G-50 gel column (Sigma-Aldrich,

USA) equilibrated with Trizma®Base sucrose (10%) buffer (pH 9.0). Encapsulation of DXR was carried out through ammonium gradient method, upon incubation with liposomes for 1.5 h at 60°C. Non-encapsulated DXR was removed using a Sephadex G-50 gel column equilibrated with 25 mM HEPES, 140 mM NaCl buffer (pH 7.4).

Targeted liposomes were prepared by post-insertion of DSPE-PEG_{2k}-F3 conjugate in a micellar form (Moreira *et al.* 2002). Briefly, thiolated derivative of F3 peptide was generated by reaction at room temperature with 2-iminothiolane (Sigma-Aldrich) in 25 mM HEPES, 140 mM NaCl, 1 mM EDTA buffer (pH 8.0) for 1 h in an inert N_2 atmosphere. Thiolated derivatives were then incubated overnight at room temperature with DSPE-PEG_{2k}-maleimide micelles in 25 mM HEPES, 25 mM MES, 140 mM NaCl, 1 mM EDTA (pH 7.0). Micelles were then added to pre-formed liposomes, at 2 mol% relative to total lipid (TL), and DSPE-PEG_{2k}-Peptide conjugates post-inserted onto the liposomal membrane upon incubation for 1 h at 50°C.

For preparation of calcein-loaded liposomes, ammonium sulfate buffer was replaced by a 40 mM calcein solution, and the resulting liposomes were extruded as described above. Calcein excess was removed through a Sephadex-G50 column equilibrated with 25 mM HEPES, 140 mM NaCl buffer (pH 7.4), and the liposomes immediately submitted to the post-insertion procedure as previously described.

Additionally, to prepare rhodamine B-tagged liposomes, RhoB-PE lipid was added to the above lipid mixture (1 mol% of total lipid), and the ethanol solution was added to 25 mM HEPES, 140 mM NaCl buffer (pH 7.4). The resulting liposomes were extruded and preceded to post-insertion, as described above.

3.5.4 Cellular association of F3 peptide-targeted nanoparticles with putative breast cancer stem cells

Half-million MCF-7 or MDA-MB-231 breast cancer cells, known to contain functional cancer stem cells (Charafe-Jauffret *et al.* 2009; Croker *et al.* 2011;

Marcato *et al.* 2011; Han *et al.* 2012), were incubated with F3 peptide- or non-targeted rhodamine-labelled liposomes, or liposomes targeted by a non-specific peptide, at 0.4 mM of total lipid, for 1 h at 37^0C or 4^0C. After washing, cells were stained aiming at identifying cancer stem cells, as previously described (Croker *et al.* 2011). Briefly, cells were first incubated with anti-CD44-PECy5 antibody [rat IM7 clone] (Abcam, UK) or $IgG2_b$ isotype control (Biolegend, USA) for 30 min at 4^0C, in PBS buffer with 1% bovine serum albumin (BSA) and 0.1% sodium azide (PBS-BSA). Cells were then washed with PBS-BSA and incubated with ALDEFLUOR® reagent (StemCell Technologies, Canada) for identification of aldehyde dehydrogenase (ALDH) activity, according to the manufacturer instructions. The cell-associated rhodamine signal was immediately analyzed by flow cytometry in a FACScalibur system (BD Biosciences, USA) and a total of 30,000 events were collected. Appropriate controls were used to assure correct compensation of fluorescence signals in each channel.

3.5.5 Establishment of mammospheres from sorted sub-populations

Mammosphere formation assay was used as a measure of stemness capability of sub-populations isolated from cell lines. Briefly, 2 x 10^6 MDA-MB-231 or MCF-7 cells were stained with CD44-PECy5 and ALDEFLUOR® reagent as described above in PBS buffer with 1% BSA. Afterwards, sorting of $ALDH^{hi}/CD44^{hi}$ and $ALDH^{low/-}/CD44^{low/-}$ cells was performed with a FACSaria III cell sorter (BD Biosciences, USA), collecting 5-15% and 15-20% of each selected sub-population, respectively, depending on the cell line tested (Croker *et al.* 2009). Sorted cells were then seeded for mammosphere formation, as previously described (Han *et al.* 2012; Shaw *et al.* 2012). Briefly, 5000 single $ALDH^{hi}/CD44^{hi}$ or $ALDH^{low/-}/CD44^{low/-}$ cells were seeded in 2 mL Mammocult® Medium supplemented with 4 µg/mL of heparin and 0.5 µg/mL of hydrocortisone (StemCell Technologies, Canada) *per* well, in low-adhesion 6-well plates (Greiner, Austria). For 1st generation sphere formation, cells were maintained for 10-21 days, depending on the cell line. To

assess self-renewal, 1st generation spheres were collected by centrifugation at 115 g for 5 min, and then dissociated with 0.5% Trypsin (Sigma-Aldrich, USA). Five thousand mammosphere-derived single cells of each population were then seeded as described above for 7 to 21 days. Mammosphere formation efficiency was assessed upon image acquisition (9 random images *per* well) using either an Axiovert 200M microscope (5x objective) or an Axiovert 40C coupled to Canon Powershot G10 camera (10x objective), both controlled by Axiovision software (version 4.8.2) (Zeiss, Germany). Image analysis and mammosphere counting was performed using Fiji software (US National Institutes of Health). Mammosphere formation efficiency (%) was calculated by the formula [(Number of spheres/ Number of total events)] x 100, where *Total events* are a sum of the number of mammospheres and single cells.

3.5.6 Intracellular delivery to 2nd generation mammospheres-derived single cells

Second generation mammospheres of each population from the triple negative MDA-MB-231 breast cancer cell line were dissociated as described above to obtain single-cell suspensions. Fifty thousand cells were incubated with 50 μM of calcein-loaded liposomes for 1 h at 37°C. After washing, cells were analyzed by flow cytometry and events were assessed using Cell Quest Pro software (BD Biosciences, USA).

3.5.7 Evaluation of mRNA levels of nucleolin and pluripotency transcription factors NANOG and OCT4

Nucleolin, NANOG and OCT4 mRNA levels in both mESC and breast CSC and non-SCC were evaluated. Briefly, E14 mESC were cultured for 72 h, as colonies, in medium either fully supplemented, maintaining pluripotency status (as described in *Cell Culture section*), in the absence of LIF or in the absence of both LIF and serum replacement, conditions under which pluripotency is lost. Additionally, 16 x 10^6 MDA-MB-231 or 24 x 10^6 MCF-7 cells were stained with

CD44-PECy5 and ALDEFLUOR® as described above, and both $ALDH^{hi}/CD44^{hi}$ (CSC) and $ALDH^{low/-}/CD44^{low/-}$ (non-SCC) sub-populations were sorted as described in the mammosphere assay. Upon cell collection, total RNA isolation was performed using the TRIzol® reagent (Invitrogen, Life Technologies, USA). A step of DNA cleanup was introduced using DNA-free™ kit (Ambion, Life Techologies, USA) as *per* manufacturer instructions. Afterwards RNA concentration and quality were determined using NanoDrop 2000 (Thermo Scientific, USA). Samples presenting a 260nm/280nm ratio under 1.8 were discarded. Samples of total RNA were stored at -80°C until use (Varum *et al.* 2011). cDNA was obtained using the iScript™ cDNA Synthesis kit (BioRad) according to the protocol established from the manufacturer, using a S1000™ Thermal Cycler (BioRad, USA) programmed as follows: 5 min at 25°C; 30 min at 42°C; 5 min at 85°C and hold at 4°C for 1 h. Using species-specific pairs of primers, nucleolin, NANOG and OCT4 gene expression was quantified by qRT-PCR using β-ACTIN as housekeeping gene for data normalization. The primers (see Table S3.1, *Supplemental Data*) were obtained from a primer bank data base (http://pga.mgh.harvard.edu/primerbank/) and acquired from Integrated DNA Technologies (IDT). SsoFast™ EvaGreen® Supermix (Bio-Rad, USA) was used to perform analysis of samples that were run in CFX96 Touch™ Real-Time PCR Detection System (BioRad, USA). mRNA fold change was calculated using the $2^{-\Delta\Delta Ct}$ method (Gomes-da-Silva *et al.* 2013b).

3.5.8 Cellular association of F3 peptide-targeted nanoparticles with embryonic stem cells

For the cellular association studies, E14-wt or E14-GFP mESC cells were cultured for 72 h, as colonies, in medium either fully supplemented, maintaining pluripotency status (as described in *Cell Culture* section), or in the absence of LIF and serum replacement (conditions under which pluripotency status is lost). Cells were then incubated with 0.4 mM of rhodamine-labelled F3 peptide-targeted or non-targeted liposomes, or liposomes targeted by a non-specific peptide for 1

h, at 4ºC or 37ºC, either as cell suspension or as colonies. Upon washing, cellular association was analyzed by flow cytometry. Non-viable cells were excluded from the analysis using 7-aminoactinomycin D (7-AAD) (Sigma-Aldrich, USA).

3.5.9 Assessment of tumorigenic potential of sorted breast cancer cell sub-populations

The tumor initiating capacity of sorted sub-populations from triple negative breast cancer cell line (either ALDH/CD44 or cell surface NCL-based selection), was evaluated. Briefly, 8 x 10^6 MDA-MB-231 breast cancer cells were stained with ALDEFLUOR® and CD44-PECy5, and both $ALDH^{hi}/CD44^{hi}$ (CSC) and $ALDH^{low/-}/CD44^{low/-}$ (non-SCC) sub-populations were sorted as described in the mammosphere assay. Additionally, 90 x 10^6 cells were stained with anti-NCL-Alexa488 [mouse 364-5 clone] (Abcam, UK) or IgG_1k isotype control (Affymetrix, USA) for 30 min at 4ºC in PBS buffer with 1% BSA. Non-viable cells were excluded using 7-AAD to ensure that only viable, cell surface nucleolin positive (NCL^+) and negative (NCL^-) cells, were sorted. All cell sub-populations were further resuspended in 1:1 PBS:Extracellular Matrix (ECM) (Sigma-Aldrich, USA) mixture and 2000 or 20000 cells were orthotopically inoculated in both contralateral mammary fat pads of immunocompromised female mice (NOD.Cg-*Prkdc*^{scid}*Il2rg*^{tm1Wjl}/SzJ strain, a.k.a. NOD scid gamma (NSG)), Charles River, France), as previously described (Charafe-Jauffret *et al.* 2009). Mice were monitored for tumor formation by palpation once-a-week post-inoculation by two independent researchers. Tumor-initiating cell (TIC) frequency was determined by limiting dilution analysis (Hu *et al.* 2009) using the L-Calc™ software package (v1.1) (StemCell Technologies, Canada). The animal experiments were conducted according to accepted standards of animal care (2010/63/EU directive and Portuguese Act 113/2013).

3.5.10 Cytotoxicity of F3 peptide-targeted doxorubicin (DXR):C6-ceramide (C6-Cer) liposomal synergistic combinations against putative breast cancer stem cells

The cytotoxic potential of F3 peptide targeted delivery of the synergistic DXR:C6-Cer drug combinations was further evaluated. First, to validate C6-Ceramide as valuable drug against putative CSC, impact on cell viability was assessed. Briefly, 0.25 x 10^6 MDA-MB-231, MCF-7 or MDA-MB-435S cells were incubated with indicated concentrations of C6-ceramide for 24 h at 37°C. Cells were then double-stained with ALDEFLUOR reagent, as described by the manufacturer, and 7-AAD (Sigma-Aldrich, USA), as an indicator of cell viability (Santos *et al.* 2008). Cells were immediately analyzed by flow cytometry and the collected events evaluated with Cell Quest Pro software.

The cytotoxic potential of F3 peptide-targeted doxorubicin (DXR):C6-ceramide (C6-Cer) liposomal synergistic combinations (*Chapter 1*) against putative breast cancer stem cells was then assessed. In brief, 2nd generation spheres from MDA-MB-231 cell line adhered to 96-well plates for 4 h, in RPMI 1640 supplemented with 10% FBS. Afterwards, cells were incubated with serial dilutions of DXR-encapsulating liposomes, for 24 h at 37°C/5% CO_2, after which cell culture medium was exchanged for fresh one and the experiment extended up to 96 h. Cell viability was assessed by the resazurin reduction assay, by monitoring absorbance at 570 nm and 600 nm (background) in a Spectramax Gemini EM (Molecular Devices, USA). Cell death was calculated by the formula [100 – (($Test_{570-600}$ – $CtrNeg_{570-600}$)/ ($Ctr_{570-600}$ – $CtrNeg_{570-600}$)) x 100)], where $Test_{570-600}$ is the corrected absorbance for treated cells, $Ctr_{570-600}$ is the corrected absorbance for untreated controls and $CtrNeg_{570-600}$ is the corrected absorbance for the negative control.

3.6. Supplemental data

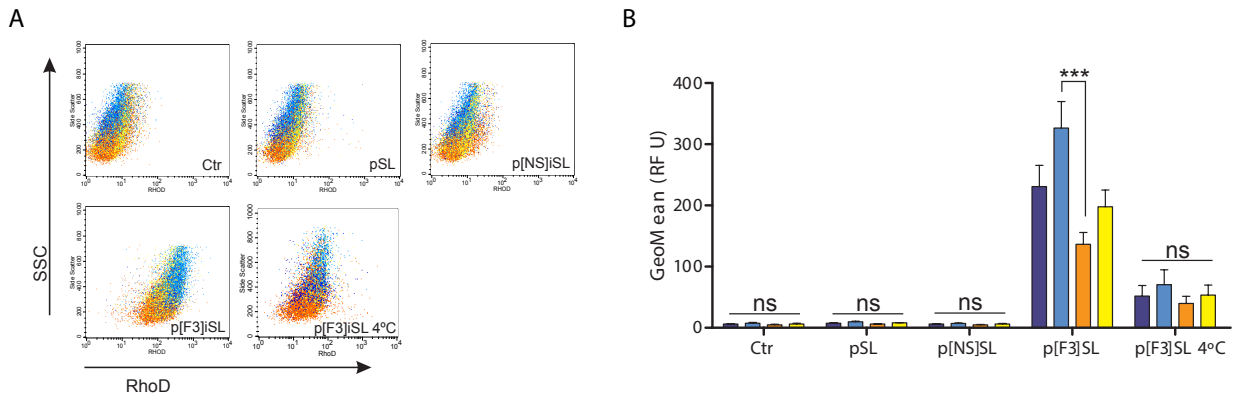

Figure S3.1 - Cellular association of F3 peptide-targeted liposomes with putative cancer stem cells.

Half million MDA-MB-435S melanoma cells were incubated with 0.4 mM of Rhod-labelled F3 peptide-targeted (**p[F3]SL**), non-specific peptide targeted (**p[NS]SL**) or non-targeted (**pSL**) liposomes for 1 h at 4 or 37ºC and subsequently stained with anti-CD44-PECy5 antibody and with ALDEFLUOR® reagent, and immediately analyzed through flow cytometry system. (A) Represents the rhodamine-side scatter dot-plots reflecting the signal distribution of each identified sub-population. (B) Represents the rhodamine geometric mean fluorescence of each sub-population (**light-blue:** putative cancer stem cells; **orange:** non-cancer stem cells). Data represent mean ± SEM (2-Way ANOVA $p<0.0001$ for formulations tested and cell sub-populations assessed; $^{ns}p>0.05$ and $^{**}p<0.01$, Bonferroni's post test).

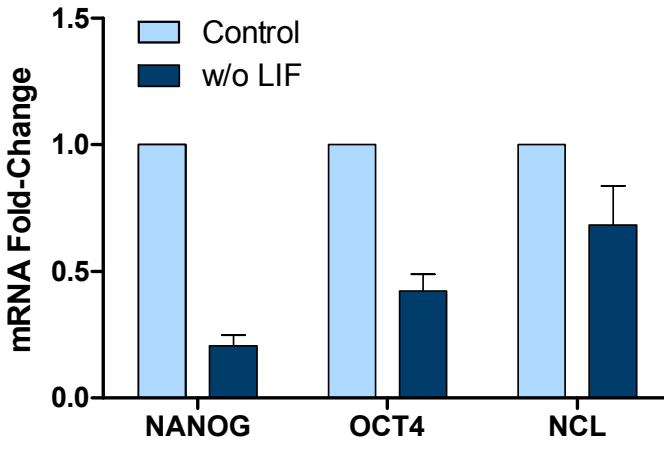

Figure S3.2 - Comparative analysis of pluripotency genes and nucleolin mRNA levels in mouse embryonic stem cells (mESC).

E14 mESC were cultured in fully supplemented medium in the presence of LIF (Control) or in absence of LIF (w/o LIF) for 72 h. Figure represents the fold-change in mRNA levels of pluripotency markers NANOG, OCT4 and nucleolin (NCL) relative to control (data represents mean ± SEM).

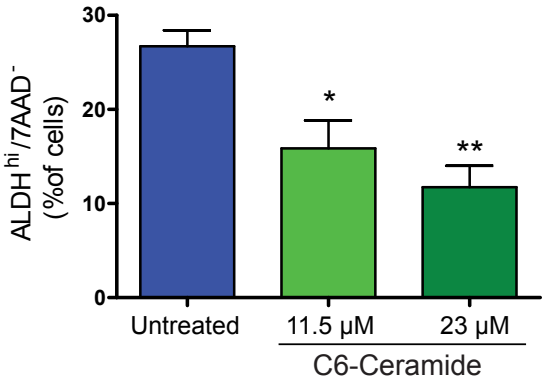

Figure S3.3 – Cytotoxicity of C6-ceramide against ALDH^{hi} sub-population from MDA-MB-435S melanoma cells.

(Data represent mean ± SEM; *p<0.05 and **p<0.01 Tukey's test, compared to untreated).

Table S3.1 – List of primer nucleotide sequences for qRT-PCR.

	Gene	Primer Bank ID		Nucleotide Sequence 5'-3'
Mouse	NUCLEOLIN	31543315a1	FW	AAAGGCAAAAAGGCTACCACA
			RV	GGAATGACTTTGGCTGGTGTAA
	OCT4	356995852c3	FW	CGGAAGAGAAAGCGAACTAGC
			RV	ATTGGCGATGTGAGTGATCTG
	NANOG	31338864a1	FW	TCTTCCTGGTCCCCACAGTTT
			RV	GCAAGAATAGTTCTCGGGATGAA
	β-ACTIN	6671509a1	FW	GGCTGTATTCCCCTCCATCG
			RV	CCAGTTGGTAACAATGCCATGT
Human	NUCLEOLIN	55956787c2	FW	GCACCTGGAAAACGAAAGAAGG
			RV	GAAAGCCGTAGTCGGTTCTGT
	OCT4	4505967a1	FW	CTTGAATCCCGAATGGAAAGGG
			RV	GTGTATATCCCAGGGTGATCCTC
	NANOG	153945815c3	FW	CCCCAGCCTTTACTCTTCCTA
			RV	CCAGGTTGAATTGTTCCAGGTC
	β-ACTIN	4501885a1	FW	CATGTACGTTGCTATCCAGGC
			RV	CTCCTTAATGTCACGCACGAT

Chapter 4

Concluding remarks and future work

Cancer disease represents an enormous burden worldwide in terms of both social and economic impact, imposing innumerous and particular challenges from the patients, health professionals and health systems point-of-view. Among them, resistance to standard chemotherapeutic drugs remains a cumbersome threat undermining therapeutic intervention in cancer, particularly in breast cancer. The multiple signaling pathways deregulated in breast cancer, as well as cell dynamics, enforce the need to develop drug synergistic combinatorial approaches for a successful therapeutic intervention. However, pharmacokinetic profiles are a major bottleneck in this strategy preventing two given drugs to reach the tumor site simultaneously at given synergistic ratio. Nanotechnology-based delivery systems, through modification of drug pharmacokinetics, enable one to achieve this goal upon temporal and spatial synchronized delivery of a drug combination at the tumor site. They can be functionalized at their surface with internalizing ligands to target receptors of specific cellular compartments, increasing specificity and efficacy.

Herein, it has been described a targeted triggered-release liposome enabling the specific and simultaneous intracellular delivery of drug combinations into triple negative breast cancer cells. Upon screening, a synergistic ratio of DXR (entrapped in the inner aqueous core) and the pro-apoptotic C6-Cer (incorporated in the liposomal bilayer) was encapsulated into F3 peptide-targeted pH-sensitive liposomes, targeting cell surface nucleolin, with limited impact on the physicochemical properties of the latter. The specific intracellular delivery of such combination enabled cytotoxic effect above 90%, unattainable by the F3 peptide-targeted liposomal DXR. Singularly, a F3 peptide-targeted formulation encapsulating an additive/mildly antagonistic DXR:C6-Cer ratio demonstrated a cytotoxic effect above 90%, for an incubation period as short as 4 h, suggesting that additive/antagonistic interaction of free combinations may be potentially shifted by specific active intracellular delivery. Thus, intracellular delivery of drug

combinations aiming at multiple pathway targeting has the potential to be highly effective against resistant cells.

Recently introduced to explain in part the heterogeneity and hierarchical tumor organization, putative CSC have been related to drug resistance, metastization and disease recurrence, thus representing relevant therapeutic targets. In addition, the demonstration that CSC can originate from non-SCC unveiled the need to simultaneous target both sub-populations.

Herein, it has been shown that liposomes functionalized with the F3 peptide target both putative breast CSC and non-SCC, in an active- and ligand-specific manner. It has been demonstrated that putative breast CSC, particularly from triple negative molecular subtype, express higher levels of OCT4 and NANOG transcription factors, paralleled by nucleolin, than non-SCC. Using *bone fide* murine embryonic stem cells, it was demonstrated that both nucleolin mRNA levels and F3 peptide-targeted liposomes cellular association were dependent on the stemness status. In addition, it was suggested that overexpression of cell surface nucleolin *per se* enabled the identification of highly tumorigenic cells, similarly to pre-established markers (ALDH and CD44). Altogether, those results suggested a link between nucleolin expression (including cell membrane nucleolin) and the stem cell-like phenotype in breast cancer, namely in the triple negative molecular subtype, enabling the intracellular delivery of a liposomal synergistic DXR:C6-Cer drug combination, targeted by the F3 peptide, into both CSC and non-SCC, rendering 100% cell death.

Overall, the tumorigenic potential of the different triple negative cell sub-populations emphasizes the need to target those simultaneously within the tumor microenvironment, aiming at successful therapeutic intervention. As described herein, F3 peptide mediates the intracellular delivery of drug combinations targeting multiple signaling pathways to different cancer cells with tumorigenic potential. Alongside with the demonstrated specific tropism of the F3 peptide

towards tumor angiogenic vessel network, the described strategy can potentially tackle the pillars sustaining breast cancer disease. An increase in the therapeutic efficacy would be expected, while decreasing tumor recurrence and systemic toxicity, ultimately enabling long-term disease free survival.

Notwithstanding, the current *in vitro* proof-of-concept demands an *in vivo* demonstration. Though stable *in vitro*, the pharmacokinetic profile of the developed F3 peptide-targeted strategy needs to be established in order to understand if the defined ratio of a DXR:C6-Cer combination can actually reach the tumor and be specifically delivered to tumor cells. Consequently, an *in vivo* efficacy study would be essential to predict and establish the therapeutic value of this innovative strategy. Overall impact at the level of the targeted signaling pathways, such as PI3K/Akt pathway and topoisomerase inhibition, should be assessed concomitantly with the effect on cell cycle progression. Additionally, the specific impact on CSC and non-SCC in terms of frequency and distribution should be addressed, alongside with the evaluation of expected impairment of tumor recurrence. Finally, as F3 peptide also targets tumor angiogenic vasculature, it would be important to evaluate the impact of the targeted delivery of the developed combination on tumor vasculature, correlating this data with above results.

Altogether, from the results presented herein, it is envisaged that the specific multi-target approach combined with synergistic drug co-delivery represents an innovative strategy. It addresses the demanding challenges faced by current cancer therapeutic modalities, and posed by intrinsic cancer heterogeneity, with potential application on tumors of histological origin other than breast cancer. It might represent one of the next generation strategies in the battle against cancer, where translation of tumor biology knowledge to the bed side will enable the continuous offering of safer and more efficacious, tailor-made state-of-the-art products, addressing unmet medical needs, for the patients benefit.

References

List of bibliographic references
(ordered alphabetically)

Adewumi, O., Aflatoonian, B., Ahrlund-Richter, L., Amit, M., Andrews, P. W.*, et al.* **(2007)**. *Characterization of human embryonic stem cell lines by the International Stem Cell Initiative.* Nat Biotechnol 25(7): 803-816.

Agudelo, D., Bourassa, P., Bruneau, J., Berube, G., Asselin, E.*, et al.* **(2012)**. *Probing the binding sites of antibiotic drugs doxorubicin and N-(trifluoroacetyl) doxorubicin with human and bovine serum albumins.* PLoS One 7(8): e43814.

Ahmed, M. A., Aleskandarany, M. A., Rakha, E. A., Moustafa, R. Z., Benhasouna, A.*, et al.* **(2012)**. *A CD44(-)/CD24(+) phenotype is a poor prognostic marker in early invasive breast cancer.* Breast Cancer Res Treat 133(3): 979-995.

Al-Hajj, M., Wicha, M. S., Benito-Hernandez, A., Morrison, S. J. and Clarke, M. F. **(2003)**. *Prospective identification of tumorigenic breast cancer cells.* Proc Natl Acad Sci U S A 100(7): 3983-3988.

Allen, T. M., Austin, G. A., Chonn, A., Lin, L. and Lee, K. C. **(1991a)**. *Uptake of liposomes by cultured mouse bone marrow macrophages: influence of liposome composition and size.* Biochim Biophys Acta 1061(1): 56-64.

Allen, T. M. and Hansen, C. **(1991b)**. *Pharmacokinetics of stealth versus conventional liposomes: effect of dose.* Biochim Biophys Acta 1068(2): 133-141.

Arboleda, G., Cardenas, Y., Rodriguez, Y., Morales, L. C., Matheus, L.*, et al.* **(2010)**. *Differential regulation of AKT, MAPK and GSK3beta during C(2)-ceramide-induced neuronal death.* Neurotoxicology 31(6): 687-693.

Badve, S. and Nakshatri, H. **(2012)**. *Breast-cancer stem cells-beyond semantics.* Lancet Oncol 13(1): e43-48.

Bansode, R. R. **(2011)**. *CouplingIn vitroandIn vivoParadigm Reveals a Dose Dependent Inhibition of Angiogenesis Followed by Initiation of Autophagy by C6-Ceramide.* International Journal of Biological Sciences: 629-644.

Barenholz, Y. **(2012)**. *Doxil(R)--the first FDA-approved nano-drug: lessons learned.* J Control Release 160(2): 117-134.

Barker, N., Ridgway, R. A., van Es, J. H., van de Wetering, M., Begthel, H.*, et al.* **(2009)**. *Crypt stem cells as the cells-of-origin of intestinal cancer.* Nature 457(7229): 608-611.

Baselga, J. **(2011)**. *Targeting the phosphoinositide-3 (PI3) kinase pathway in breast cancer.* Oncologist 16 Suppl 1: 12-19.

Batist, G., Ramakrishnan, G., Rao, C. S., Chandrasekharan, A., Gutheil, J.*, et al.* **(2001)**. *Reduced cardiotoxicity and preserved antitumor efficacy of liposome-encapsulated doxorubicin and cyclophosphamide compared with conventional doxorubicin and cyclophosphamide in a randomized, multicenter trial of metastatic breast cancer.* J Clin Oncol 19(5): 1444-1454.

Berenson, J. R., Yellin, O., Chen, C. S., Patel, R., Bessudo, A.*, et al.* **(2011)**. *A modified regimen of pegylated liposomal doxorubicin, bortezomib and dexamethasone (DVD) is effective and well tolerated for previously untreated multiple myeloma patients.* Br J Haematol 155(5): 580-587.

Bocci, G., Fioravanti, A., Orlandi, P., Di Desidero, T., Natale, G.*, et al.* **(2012)**. *Metronomic ceramide analogs inhibit angiogenesis in pancreatic cancer through up-regulation of caveolin-1 and thrombospondin-1 and down-regulation of cyclin D1.* Neoplasia 14(9): 833-845.

Bolos, V., Mira, E., Martinez-Poveda, B., Luxan, G., Canamero, M.*, et al.* **(2013)**. *Notch activation stimulates migration of breast cancer cells and promotes tumor growth.* Breast Cancer Res 15(4): R54.

Bonnet, D. and Dick, J. E. **(1997)**. *Human acute myeloid leukemia is organized as a hierarchy that originates from a primitive hematopoietic cell.* Nat Med 3(7): 730-737.

Borovski, T., De Sousa, E. M. F., Vermeulen, L. and Medema, J. P. **(2011)**. *Cancer stem cell niche: the place to be.* Cancer Res 71(3): 634-639.

Boyer, L. A., Lee, T. I., Cole, M. F., Johnstone, S. E., Levine, S. S.*, et al.* **(2005)**. *Core transcriptional regulatory circuitry in human embryonic stem cells.* Cell 122(6): 947-956.

Cai, W. Y., Wei, T. Z., Luo, Q. C., Wu, Q. W., Liu, Q. F.*, et al.* **(2013)**. *The Wnt-beta-catenin pathway represses let-7 microRNA expression through transactivation of Lin28 to augment breast cancer stem cell expansion.* J Cell Sci 126(Pt 13): 2877-2889.

Canals, D., Perry, D. M., Jenkins, R. W. and Hannun, Y. A. **(2011)**. *Drug targeting of sphingolipid metabolism: sphingomyelinases and ceramidases.* Br J Pharmacol 163(4): 694-712.

Carmeliet, P. and Jain, R. K. **(2011a)**. *Principles and mechanisms of vessel normalization for cancer and other angiogenic diseases.* Nat Rev Drug Discov 10(6): 417-427.

Carmeliet, P. and Jain, R. K. **(2011b)**. *Molecular mechanisms and clinical applications of angiogenesis.* Nature 473(7347): 298-307.

Carpinteiro, A., Dumitru, C., Schenck, M. and Gulbins, E. **(2008)**. *Ceramide-induced cell death in malignant cells.* Cancer Lett 264(1): 1-10.

Chaffer, C. L., Brueckmann, I., Scheel, C., Kaestli, A. J., Wiggins, P. A.*, et al.* **(2011)**. *Normal and neoplastic nonstem cells can spontaneously convert to a stem-like state.* Proc Natl Acad Sci U S A 108(19): 7950-7955.

Chaffer, C. L., Marjanovic, N. D., Lee, T., Bell, G., Kleer, C. G.*, et al.* **(2013)**. *Poised Chromatin at the ZEB1 Promoter Enables Breast Cancer Cell Plasticity and Enhances Tumorigenicity.* Cell 154(1): 61-74.

Chang, S. S., Reuter, V. E., Heston, W. D., Bander, N. H., Grauer, L. S.*, et al.* **(1999)**. *Five different anti-prostate-specific membrane antigen (PSMA) antibodies confirm PSMA expression in tumor-associated neovasculature.* Cancer Res 59(13): 3192-3198.

Charafe-Jauffret, E., Ginestier, C., Iovino, F., Wicinski, J., Cervera, N.*, et al.* **(2009)**. *Breast cancer cell lines contain functional cancer stem cells with metastatic capacity and a distinct molecular signature.* Cancer Res 69(4): 1302-1313.

Chen, C., Zhang, C., Xu, J. M. and Han, Y. **(2013a)**. *LGR5 is a biomarker for stratification of HER-2 positive breast cancer patients and personalized treatment.* Med Hypotheses 81(3): 439-442.

Chen, P. Y., Ozawa, T., Drummond, D. C., Kalra, A., Fitzgerald, J. B.*, et al.* **(2013b)**. *Comparing routes of delivery for nanoliposomal irinotecan shows superior anti-tumor activity of local administration in treating intracranial glioblastoma xenografts.* Neuro Oncol 15(2): 189-197.

Chonn, A., Semple, S. C. and Cullis, P. R. **(1992)**. *Association of blood proteins with large unilamellar liposomes in vivo. Relation to circulation lifetimes.* J Biol Chem 267(26): 18759-18765.

Chou, T. C. **(2006)**. *Theoretical basis, experimental design, and computerized simulation of synergism and antagonism in drug combination studies.* Pharmacol Rev 58(3): 621-681.

Chou, T. C. **(2011)**. *The mass-action law based algorithm for cost-effective approach for cancer drug discovery and development.* Am J Cancer Res 1(7): 925-954.

Chou, T. C. and Talalay, P. **(1984)**. *Quantitative analysis of dose-effect relationships: the combined effects of multiple drugs or enzyme inhibitors.* Adv Enzyme Regul 22: 27-55.

Christian, S., Pilch, J., Akerman, M. E., Porkka, K., Laakkonen, P.*, et al.* **(2003)**. *Nucleolin expressed at the cell surface is a marker of endothelial cells in angiogenic blood vessels.* J Cell Biol 163(4): 871-878.

Cinghu, S., Yellaboina, S., Freudenberg, J. M., Ghosh, S., Zheng, X.*, et al.* **(2014)**. *Integrative framework for identification of key cell identity genes uncovers determinants of ES cell identity and homeostasis.* Proc Natl Acad Sci U S A.

Ciriello, G., Miller, M. L., Aksoy, B. A., Senbabaoglu, Y., Schultz, N.*, et al.* **(2013)**. *Emerging landscape of oncogenic signatures across human cancers.* Nat Genet 45(10): 1127-1133.

Clarke, M. F., Dick, J. E., Dirks, P. B., Eaves, C. J., Jamieson, C. H.*, et al.* **(2006)**. *Cancer stem cells--perspectives on current status and future directions: AACR Workshop on cancer stem cells.* Cancer Res 66(19): 9339-9344.

Conley, S. J., Gheordunescu, E., Kakarala, P., Newman, B., Korkaya, H.*, et al.* **(2012)**. *Antiangiogenic agents increase breast cancer stem cells via the generation of tumor hypoxia.* Proc Natl Acad Sci U S A.

Corominas-Faja, B., Cufi, S., Oliveras-Ferraros, C., Cuyas, E., Lopez-Bonet, E.*, et al.* **(2013)**. *Nuclear reprogramming of luminal-like breast cancer cells generates Sox2-overexpressing cancer stem-like cellular states harboring transcriptional activation of the mTOR pathway.* Cell Cycle 12(18): 3109-3124.

Cortes, J. E., Goldberg, S. L., Feldman, E. J., Rizzeri, D. A., Hogge, D. E.*, et al.* **(2014)**. *Phase II, multicenter, randomized trial of CPX-351 (cytarabine:daunorubicin) liposome injection versus intensive salvage therapy in adults with first relapse AML.* Cancer.

Courtney, K. D., Corcoran, R. B. and Engelman, J. A. **(2010)**. *The PI3K pathway as drug target in human cancer.* J Clin Oncol 28(6): 1075-1083.

Croker, A. K. and Allan, A. L. **(2011)**. *Inhibition of aldehyde dehydrogenase (ALDH) activity reduces chemotherapy and radiation resistance of stem-like ALDH(hi)CD44 (+) human breast cancer cells.* Breast Cancer Res Treat.

Croker, A. K., Goodale, D., Chu, J., Postenka, C., Hedley, B. D*., et al.* **(2009)**. *High aldehyde dehydrogenase and expression of cancer stem cell markers selects for breast cancer cells with enhanced malignant and metastatic ability.* J Cell Mol Med 13(8B): 2236-2252.

Cummings, B. S., Wills, L. P. and Schnellmann, R. G. **(2012)**. *Measurement of cell death in Mammalian cells.* Curr Protoc Pharmacol Chapter 12: Unit12 18.

Davis, M. E. **(2009)**. *The first targeted delivery of siRNA in humans via a self-assembling, cyclodextrin polymer-based nanoparticle: from concept to clinic.* Mol Pharm 6(3): 659-668.

Davis, M. E., Zuckerman, J. E., Choi, C. H., Seligson, D., Tolcher, A*., et al.* **(2010)**. *Evidence of RNAi in humans from systemically administered siRNA via targeted nanoparticles.* Nature 464(7291): 1067-1070.

de Beca, F. F., Caetano, P., Gerhard, R., Alvarenga, C. A., Gomes, M*., et al.* **(2013)**. *Cancer stem cells markers CD44, CD24 and ALDH1 in breast cancer special histological types.* J Clin Pathol 66(3): 187-191.

De Miguel, M. P., Fuentes-Julian, S. and Alcaina, Y. **(2010)**. *Pluripotent stem cells: origin, maintenance and induction.* Stem Cell Rev 6(4): 633-649.

Desantis, C., Ma, J., Bryan, L. and Jemal, A. **(2013)**. *Breast cancer statistics, 2013*. CA Cancer J Clin.

Dicko, A., Mayer, L. D. and Tardi, P. G. **(2010)**. *Use of nanoscale delivery systems to maintain synergistic drug ratios in vivo.* Expert Opin Drug Deliv 7(12): 1329-1341.

Drummond, D. C., Noble, C. O., Guo, Z., Hong, K., Park, J. W*., et al.* **(2006)**. *Development of a highly active nanoliposomal irinotecan using a novel intraliposomal stabilization strategy.* Cancer Res 66(6): 3271-3277.

Dubrovska, A., Kim, S., Salamone, R. J., Walker, J. R., Maira, S. M*., et al.* **(2009)**. *The role of PTEN/Akt/PI3K signaling in the maintenance and viability of prostate cancer stem-like cell populations.* Proc Natl Acad Sci U S A 106(1): 268-273.

Duda, D. G., Cohen, K. S., Kozin, S. V., Perentes, J. Y., Fukumura, D*., et al.* **(2006)**. *Evidence for incorporation of bone marrow-derived endothelial cells into perfused blood vessels in tumors.* Blood 107(7): 2774-2776.

Duncan, R. and Gaspar, R. **(2011)**. *Nanomedicine(s) under the microscope.* Mol Pharm 8(6): 2101-2141.

Duncan, R. and Vicent, M. J. **(2013)**. *Polymer therapeutics-prospects for 21st century: the end of the beginning.* Adv Drug Deliv Rev 65(1): 60-70.

Eccles, S. A., Aboagye, E. O., Ali, S., Anderson, A. S., Armes, J*., et al.* **(2013)**. *Critical research gaps and translational priorities for the successful prevention and treatment of breast cancer.* Breast Cancer Res 15(5): R92.

Eom, Y. W., Kim, M. A., Park, S. S., Goo, M. J., Kwon, H. J*., et al.* **(2005)**. *Two distinct modes of cell death induced by doxorubicin: apoptosis and cell death through mitotic catastrophe accompanied by senescence-like phenotype.* Oncogene 24(30): 4765-4777.

Etheridge, M. L., Campbell, S. A., Erdman, A. G., Haynes, C. L., Wolf, S. M.*, et al.* **(2012)**. *The big picture on nanomedicine: the state of investigational and approved nanomedicine products.* Nanomedicine 9(1): 1-14.

Evans, M. J. and Kaufman, M. H. **(1981)**. *Establishment in culture of pluripotential cells from mouse embryos.* Nature 292(5819): 154-156.

Farin, K., Schokoroy, S., Haklai, R., Cohen-Or, I., Elad-Sfadia, G.*, et al.* **(2011)**. *Oncogenic synergism between ErbB1, nucleolin, and mutant Ras.* Cancer Res 71(6): 2140-2151.

Feldman, D. E., Chen, C., Punj, V., Tsukamoto, H. and Machida, K. **(2012)**. *Pluripotency factor-mediated expression of the leptin receptor (OB-R) links obesity to oncogenesis through tumor-initiating stem cells.* Proc Natl Acad Sci U S A 109(3): 829-834.

Feldman, E. J., Lancet, J. E., Kolitz, J. E., Ritchie, E. K., Roboz, G. J.*, et al.* **(2011)**. *First-in-man study of CPX-351: a liposomal carrier containing cytarabine and daunorubicin in a fixed 5:1 molar ratio for the treatment of relapsed and refractory acute myeloid leukemia.* J Clin Oncol 29(8): 979-985.

Ferrara, N. and Kerbel, R. S. **(2005)**. *Angiogenesis as a therapeutic target.* Nature 438(7070): 967-974.

Flynn, K. M., Michaud, M., Canosa, S. and Madri, J. A. **(2013)**. *CD44 regulates vascular endothelial barrier integrity via a PECAM-1 dependent mechanism.* Angiogenesis 16(3): 689-705.

Fogal, V., Sugahara, K. N., Ruoslahti, E. and Christian, S. **(2009)**. *Cell surface nucleolin antagonist causes endothelial cell apoptosis and normalization of tumor vasculature.* Angiogenesis 12(1): 91-100.

Fonseca, N. A., Gregorio, A. C., Valerio-Fernandes, A., Simoes, S. and Moreira, J. N. **(2014)**. *Bridging cancer biology and the patients' needs with nanotechnology-based approaches.* Cancer Treat Rev 40(5): 626-635.

Gaber, M. H., Hong, K., Huang, S. K. and Papahadjopoulos, D. **(1995)**. *Thermosensitive sterically stabilized liposomes: formulation and in vitro studies on mechanism of doxorubicin release by bovine serum and human plasma.* Pharm Res 12(10): 1407-1416.

Gaber, M. H., Wu, N. Z., Hong, K., Huang, S. K., Dewhirst, M. W.*, et al.* **(1996)**. *Thermosensitive liposomes: extravasation and release of contents in tumor microvascular networks.* Int J Radiat Oncol Biol Phys 36(5): 1177-1187.

Gabizon, A., Catane, R., Uziely, B., Kaufman, B., Safra, T.*, et al.* **(1994)**. *Prolonged circulation time and enhanced accumulation in malignant exudates of doxorubicin encapsulated in polyethylene-glycol coated liposomes.* Cancer Res 54(4): 987-992.

Gabizon, A., Chisin, R., Amselem, S., Druckmann, S., Cohen, R.*, et al.* **(1991)**. *Pharmacokinetic and imaging studies in patients receiving a formulation of liposome-associated adriamycin.* Br J Cancer 64(6): 1125-1132.

Gabizon, A., Dagan, A., Goren, D., Barenholz, Y. and Fuks, Z. **(1982)**. *Liposomes as in vivo carriers of adriamycin: reduced cardiac uptake and preserved antitumor activity in mice.* Cancer Res 42(11): 4734-4739.

Gabizon, A., Shiota, R. and Papahadjopoulos, D. **(1989)**. *Pharmacokinetics and tissue distribution of doxorubicin encapsulated in stable liposomes with long circulation times.* J Natl Cancer Inst 81(19): 1484-1488.

Ganesh, S., Iyer, A. K., Morrissey, D. V. and Amiji, M. M. **(2013)**. *Hyaluronic acid based self-assembling nanosystems for CD44 target mediated siRNA delivery to solid tumors.* Biomaterials 34(13): 3489-3502.

Geng, S. Q., Alexandrou, A. T. and Li, J. J. **(2014)**. *Breast cancer stem cells: Multiple capacities in tumor metastasis.* Cancer Lett.

Gill, P. S., Espina, B. M., Muggia, F., Cabriales, S., Tulpule, A., *et al.* **(1995)**. *Phase I/II clinical and pharmacokinetic evaluation of liposomal daunorubicin.* J Clin Oncol 13(4): 996-1003.

Ginestier, C., Hur, M. H., Charafe-Jauffret, E., Monville, F., Dutcher, J., *et al.* **(2007)**. *ALDH1 is a marker of normal and malignant human mammary stem cells and a predictor of poor clinical outcome.* Cell Stem Cell 1(5): 555-567.

Ginestier, C., Liu, S., Diebel, M. E., Korkaya, H., Luo, M., *et al.* **(2010)**. *CXCR1 blockade selectively targets human breast cancer stem cells in vitro and in xenografts.* J Clin Invest 120(2): 485-497.

Ginisty, H., Sicard, H., Roger, B. and Bouvet, P. **(1999)**. *Structure and functions of nucleolin.* J Cell Sci 112 (Pt 6): 761-772.

Girvan, A. C., Teng, Y., Casson, L. K., Thomas, S. D., Juliger, S., *et al.* **(2006)**. *AGRO100 inhibits activation of nuclear factor-kappaB (NF-kappaB) by forming a complex with NF-kappaB essential modulator (NEMO) and nucleolin.* Mol Cancer Ther 5(7): 1790-1799.

Giussani, P., Tringali, C., Riboni, L., Viani, P. and Venerando, B. **(2014)**. *Sphingolipids: key regulators of apoptosis and pivotal players in cancer drug resistance.* Int J Mol Sci 15(3): 4356-4392.

Gomes-da-Silva, L. C., Fernandez, Y., Abasolo, I., Schwartz, S., Jr., Ramalho, J. S., *et al.* **(2013a)**. *Efficient intracellular delivery of siRNA with a safe multitargeted lipid-based nanoplatform.* Nanomedicine (Lond) 8(9): 1397-1413.

Gomes-da-Silva, L. C., Fonseca, N. A., Moura, V., Pedroso de Lima, M. C., Simoes, S., *et al.* **(2012a)**. *Lipid-based nanoparticles for siRNA delivery in cancer therapy: paradigms and challenges.* Acc Chem Res 45(7): 1163-1171.

Gomes-da-Silva, L. C., Ramalho, J. S., Pedroso de Lima, M. C., Simoes, S. and Moreira, J. N. **(2013b)**. *Impact of anti-PLK1 siRNA-containing F3-targeted liposomes on the viability of both cancer and endothelial cells.* Eur J Pharm Biopharm 85(3 Pt A): 356-364.

Gomes-da-Silva, L. C., Santos, A. O., Bimbo, L. M., Moura, V., Ramalho, J. S., *et al.* **(2012b)**. *Towards a siRNA-containing nanoparticle targeted to breast cancer cells and the tumor microenvironment.* Int J Pharm 434(1-2): 9-19.

Gomes-da-Silva, L. C., Simoes, S. and Moreira, J. N. **(2013c)**. *Challenging the future of siRNA therapeutics against cancer: the crucial role of nanotechnology.* Cell Mol Life Sci.

Gottesman, M. M. **(2002)**. *Mechanisms of cancer drug resistance.* Annu Rev Med 53: 615-627.

Gouaze-Andersson, V., Yu, J. Y., Kreitenberg, A. J., Bielawska, A., Giuliano, A. E.*, et al.* **(2007)**. *Ceramide and glucosylceramide upregulate expression of the multidrug resistance gene MDR1 in cancer cells.* Biochim Biophys Acta 1771(12): 1407-1417.

Gouaze, V., Liu, Y. Y., Prickett, C. S., Yu, J. Y., Giuliano, A. E.*, et al.* **(2005)**. *Glucosylceramide synthase blockade down-regulates P-glycoprotein and resensitizes multidrug-resistant breast cancer cells to anticancer drugs.* Cancer Res 65(9): 3861-3867.

Gradishar, W. J. **(2005)**. *Albumin-bound nanoparticle paclitaxel.* Clin Adv Hematol Oncol 3(5): 348-349.

Gradishar, W. J. **(2006)**. *Albumin-bound paclitaxel: a next-generation taxane.* Expert Opin Pharmacother 7(8): 1041-1053.

Gradishar, W. J., Tjulandin, S., Davidson, N., Shaw, H., Desai, N.*, et al.* **(2005)**. *Phase III trial of nanoparticle albumin-bound paclitaxel compared with polyethylated castor oil-based paclitaxel in women with breast cancer.* J Clin Oncol 23(31): 7794-7803.

Griffioen, A. W., Coenen, M. J., Damen, C. A., Hellwig, S. M., van Weering, D. H.*, et al.* **(1997)**. *CD44 is involved in tumor angiogenesis; an activation antigen on human endothelial cells.* Blood 90(3): 1150-1159.

Gupta, V., Bhinge, K. N., Hosain, S. B., Xiong, K., Gu, X.*, et al.* **(2012)**. *Ceramide glycosylation by glucosylceramide synthase selectively maintains the properties of breast cancer stem cells.* J Biol Chem 287(44): 37195-37205.

Hafez, I. M. and Cullis, P. R. **(2000)**. *Cholesteryl hemisuccinate exhibits pH sensitive polymorphic phase behavior.* Biochim Biophys Acta 1463(1): 107-114.

Hamaguchi, T., Matsumura, Y., Nakanishi, Y., Muro, K., Yamada, Y.*, et al.* **(2004)**. *Antitumor effect of MCC-465, pegylated liposomal doxorubicin tagged with newly developed monoclonal antibody GAH, in colorectal cancer xenografts.* Cancer Sci 95(7): 608-613.

Han, Y. K., Lee, J. H., Park, G. Y., Chun, S. H., Han, J. Y.*, et al.* **(2012)**. *A possible usage of a CDK4 inhibitor for breast cancer stem cell-targeted therapy.* Biochem Biophys Res Commun.

Hanahan, D. and Weinberg, R. A. **(2000)**. *The hallmarks of cancer.* Cell 100(1): 57-70.

Hanahan, D. and Weinberg, R. A. **(2011)**. *Hallmarks of cancer: the next generation.* Cell 144(5): 646-674.

Hannun, Y. A. and Obeid, L. M. **(2008)**. *Principles of bioactive lipid signalling: lessons from sphingolipids.* Nat Rev Mol Cell Biol 9(2): 139-150.

Hannun, Y. A. and Obeid, L. M. **(2011)**. *Many ceramides.* J Biol Chem 286(32): 27855-27862.

Haran, G., Cohen, R., Bar, L. K. and Barenholz, Y. **(1993)**. *Transmembrane ammonium sulfate gradients in liposomes produce efficient and stable entrapment of amphipathic weak bases.* Biochim Biophys Acta 1151(2): 201-215.

Harris, L., Batist, G., Belt, R., Rovira, D., Navari, R.*, et al.* **(2002)**. *Liposome-encapsulated doxorubicin compared with conventional doxorubicin in a randomized multicenter trial as first-line therapy of metastatic breast carcinoma.* Cancer 94(1): 25-36.

Hart, S., Novotny-Diermayr, V., Goh, K. C., Williams, M., Tan, Y. C.*, et al.* **(2012)**. *VS-5584, a Novel and Highly Selective PI3K/mTOR Kinase Inhibitor for the Treatment of Cancer.* Molecular Cancer Therapeutics 12(2): 151-161.

Hernandez-Caselles, T., Villalain, J. and Gomez-Fernandez, J. C. **(1993)**. *Influence of liposome charge and composition on their interaction with human blood serum proteins.* Mol Cell Biochem 120(2): 119-126.

Hong, C. W., Libutti, S. K. and Wood, B. J. **(2013)**. *Liposomal doxorubicin plus radiofrequency ablation for complete necrosis of a hepatocellular carcinoma.* Curr Oncol 20(3): e274-277.

Hooper, M., Hardy, K., Handyside, A., Hunter, S. and Monk, M. **(1987)**. *HPRT-deficient (Lesch-Nyhan) mouse embryos derived from germline colonization by cultured cells.* Nature 326(6110): 292-295.

Hovanessian, A. G., Soundaramourty, C., Khoury, D. E., Nondier, I., Svab, J.*, et al.* **(2010)**. *Surface expressed nucleolin is constantly induced in tumor cells to mediate calcium-dependent ligand internalization.* PLoS One 5(12): e15787.

Hrkach, J., Von Hoff, D., Mukkaram Ali, M., Andrianova, E., Auer, J.*, et al.* **(2012)**. *Preclinical development and clinical translation of a PSMA-targeted docetaxel nanoparticle with a differentiated pharmacological profile.* Sci Transl Med 4(128): 128ra139.

Hu, Y. and Smyth, G. K. **(2009)**. *ELDA: extreme limiting dilution analysis for comparing depleted and enriched populations in stem cell and other assays.* J Immunol Methods 347(1-2): 70-78.

Idowu, M. O., Kmieciak, M., Dumur, C., Burton, R. S., Grimes, M. M.*, et al.* **(2012)**. *CD44(+)/CD24(-/low) cancer stem/progenitor cells are more abundant in triple-negative invasive breast carcinoma phenotype and are associated with poor outcome.* Hum Pathol 43(3): 364-373.

Immordino, M. L., Dosio, F. and Cattel, L. **(2006)**. *Stealth liposomes: review of the basic science, rationale, and clinical applications, existing and potential.* Int J Nanomedicine 1(3): 297-315.

Ishida, T., Okada, Y., Kobayashi, T. and Kiwada, H. **(2006)**. *Development of pH-sensitive liposomes that efficiently retain encapsulated doxorubicin (DXR) in blood.* Int J Pharm 309(1-2): 94-100.

Ishizawa, K., Rasheed, Z. A., Karisch, R., Wang, Q., Kowalski, J.*, et al.* **(2010)**. *Tumor-initiating cells are rare in many human tumors.* Cell Stem Cell 7(3): 279-282.

Ithimakin, S., Day, K. C., Malik, F., Zen, Q., Dawsey, S. J.*, et al.* **(2013)**. *HER2 drives luminal breast cancer stem cells in the absence of HER2 amplification: implications for efficacy of adjuvant trastuzumab.* Cancer Res 73(5): 1635-1646.

Jaggupilli, A. and Elkord, E. **(2012)**. *Significance of CD44 and CD24 as cancer stem cell markers: an enduring ambiguity.* Clin Dev Immunol 2012: 708036.

Jemal, A., Bray, F., Center, M. M., Ferlay, J., Ward, E.*, et al.* **(2011)**. *Global cancer statistics.* CA Cancer J Clin 61(2): 69-90.

Jemal, A., Siegel, R., Ward, E., Murray, T., Xu, J.*, et al.* **(2006)**. *Cancer statistics, 2006.* CA Cancer J Clin 56(2): 106-130.

Ji, C., Yang, B., Yang, Y. L., He, S. H., Miao, D. S., *et al.* **(2010)**. *Exogenous cell-permeable C6 ceramide sensitizes multiple cancer cell lines to Doxorubicin-induced apoptosis by promoting AMPK activation and mTORC1 inhibition.* Oncogene 29(50): 6557-6568.

Johansson, H., Svensson, F., Runnberg, R., Simonsson, T. and Simonsson, S. **(2010)**. *Phosphorylated nucleolin interacts with translationally controlled tumor protein during mitosis and with Oct4 during interphase in ES cells.* PLoS One 5(10): e13678.

Jordan, M. A., Thrower, D. and Wilson, L. **(1991)**. *Mechanism of inhibition of cell proliferation by Vinca alkaloids.* Cancer Res 51(8): 2212-2222.

Kamaly, N., Xiao, Z., Valencia, P. M., Radovic-Moreno, A. F. and Farokhzad, O. C. **(2012)**. *Targeted polymeric therapeutic nanoparticles: design, development and clinical translation.* Chem Soc Rev 41(7): 2971-3010.

Karamboulas, C. and Ailles, L. **(2013)**. *Developmental signaling pathways in cancer stem cells of solid tumors.* Biochim Biophys Acta 1830(2): 2481-2495.

Karanth, H. and Murthy, R. S. **(2007)**. *pH-sensitive liposomes--principle and application in cancer therapy.* J Pharm Pharmacol 59(4): 469-483.

Kaspers, G. J., Zimmermann, M., Reinhardt, D., Gibson, B. E., Tamminga, R. Y., *et al.* **(2013)**. *Improved outcome in pediatric relapsed acute myeloid leukemia: results of a randomized trial on liposomal daunorubicin by the International BFM Study Group.* J Clin Oncol 31(5): 599-607.

Khazanov, E., Priev, A., Shillemans, J. P. and Barenholz, Y. **(2008)**. *Physicochemical and biological characterization of ceramide-containing liposomes: paving the way to ceramide therapeutic application.* Langmuir 24(13): 6965-6980.

Kim, H. J., Oh, J. E., Kim, S. W., Chun, Y. J. and Kim, M. Y. **(2008)**. *Ceramide induces p38 MAPK-dependent apoptosis and Bax translocation via inhibition of Akt in HL-60 cells.* Cancer Lett 260(1-2): 88-95.

Kim, S. and Alexander, C. M. **(2013)**. *Tumorsphere assay provides more accurate prediction of in vivo responses to chemotherapeutics.* Biotechnol Lett.

Kim, S. W., Kim, H. J., Chun, Y. J. and Kim, M. Y. **(2010)**. *Ceramide produces apoptosis through induction of p27(kip1) by protein phosphatase 2A-dependent Akt dephosphorylation in PC-3 prostate cancer cells.* J Toxicol Environ Health A 73(21-22): 1465-1476.

Korkaya, H., Liu, S. and Wicha, M. S. **(2011)**. *Breast cancer stem cells, cytokine networks, and the tumor microenvironment.* J Clin Invest 121(10): 3804-3809.

Korkaya, H., Paulson, A., Charafe-Jauffret, E., Ginestier, C., Brown, M., *et al.* **(2009)**. *Regulation of mammary stem/progenitor cells by PTEN/Akt/beta-catenin signaling.* PLoS Biol 7(6): e1000121.

Koshkaryev, A., Piroyan, A. and Torchilin, V. P. **(2012)**. *Increased apoptosis in cancer cells in vitro and in vivo by ceramides in transferrin-modified liposomes.* Cancer Biol Ther 13(1): 50-60.

Kreso, A. and Dick, J. E. **(2014)**. *Evolution of the cancer stem cell model.* Cell Stem Cell 14(3): 275-291.

Krust, B., El Khoury, D., Nondier, I., Soundaramourty, C. and Hovanessian, A. G. **(2011)**. *Targeting surface nucleolin with multivalent HB-19 and related Nucant pseudopeptides results in distinct inhibitory mechanisms depending on the malignant tumor cell type.* BMC Cancer 11: 333.

Kurtz, J. E., Kaminsky, M. C., Floquet, A., Veillard, A. S., Kimmig, R.*, et al.* **(2011)**. *Ovarian cancer in elderly patients: carboplatin and pegylated liposomal doxorubicin versus carboplatin and paclitaxel in late relapse: a Gynecologic Cancer Intergroup (GCIG) CALYPSO sub-study.* Ann Oncol 22(11): 2417-2423.

Lamb, R., Ablett, M. P., Spence, K., Landberg, G., Sims, A. H.*, et al.* **(2013)**. *Wnt pathway activity in breast cancer sub-types and stem-like cells.* PLoS One 8(7): e67811.

Lancet, J. E., Cortes, J. E., Hogge, D. E., Tallman, M. S., Kovacsovics, T. J.*, et al.* **(2014)**. *Phase 2 trial of CPX-351, a fixed 5:1 molar ratio of cytarabine/daunorubicin, vs cytarabine/daunorubicin in older adults with untreated AML.* Blood 123(21): 3239-3246.

Lasic, D. D., Martin, F. J., Gabizon, A., Huang, S. K. and Papahadjopoulos, D. **(1991)**. *Sterically stabilized liposomes: a hypothesis on the molecular origin of the extended circulation times.* Biochim Biophys Acta 1070(1): 187-192.

Le Bourhis, X., Romon, R. and Hondermarck, H. **(2010)**. *Role of endothelial progenitor cells in breast cancer angiogenesis: from fundamental research to clinical ramifications.* Breast Cancer Res Treat 120(1): 17-24.

Lee, H. E., Kim, J. H., Kim, Y. J., Choi, S. Y., Kim, S. W.*, et al.* **(2011)**. *An increase in cancer stem cell population after primary systemic therapy is a poor prognostic factor in breast cancer.* Br J Cancer 104(11): 1730-1738.

Leis, O., Eguiara, A., Lopez-Arribillaga, E., Alberdi, M. J., Hernandez-Garcia, S.*, et al.* **(2012)**. *Sox2 expression in breast tumours and activation in breast cancer stem cells.* Oncogene 31(11): 1354-1365.

Leonard, R. C., Williams, S., Tulpule, A., Levine, A. M. and Oliveros, S. **(2009)**. *Improving the therapeutic index of anthracycline chemotherapy: focus on liposomal doxorubicin (Myocet).* Breast 18(4): 218-224.

Li, L., Ten Hagen, T. L., Hossann, M., Suss, R., van Rhoon, G. C.*, et al.* **(2013)**. *Mild hyperthermia triggered doxorubicin release from optimized stealth thermosensitive liposomes improves intratumoral drug delivery and efficacy.* J Control Release 168(2): 142-150.

Li, X. and Schick, M. **(2001)**. *Theory of tunable pH-sensitive vesicles of anionic and cationic lipids or anionic and neutral lipids.* Biophys J 80(4): 1703-1711.

Lim, W. S., Tardi, P. G., Dos Santos, N., Xie, X., Fan, M.*, et al.* **(2010)**. *Leukemia-selective uptake and cytotoxicity of CPX-351, a synergistic fixed-ratio cytarabine:daunorubicin formulation, in bone marrow xenografts.* Leuk Res 34(9): 1214-1223.

Lin, L., Hutzen, B., Lee, H. F., Peng, Z., Wang, W.*, et al.* **(2013)**. *Evaluation of STAT3 Signaling in ALDH+ and ALDH+/CD44+/CD24- Subpopulations of Breast Cancer Cells.* PLoS One 8(12): e82821.

Ling, G. Q., Chen, D. B., Wang, B. Q. and Zhang, L. S. **(2012)**. *Expression of the pluripotency markers Oct3/4, Nanog and Sox2 in human breast cancer cell lines.* Oncol Lett 4(6): 1264-1268.

Liu, S., Ginestier, C., Ou, S. J., Clouthier, S. G., Patel, S. H.*, et al.* **(2011)**. *Breast cancer stem cells are regulated by mesenchymal stem cells through cytokine networks.* Cancer Res 71(2): 614-624.

Liu, S. and Wicha, M. S. **(2010a)**. *Targeting breast cancer stem cells.* J Clin Oncol 28(25): 4006-4012.

Liu, Y. Y., Gupta, V., Patwardhan, G. A., Bhinge, K., Zhao, Y.*, et al.* **(2010b)**. *Glucosylceramide synthase upregulates MDR1 expression in the regulation of cancer drug resistance through cSrc and beta-catenin signaling.* Mol Cancer 9: 145.

Liu, Y. Y., Yu, J. Y., Yin, D., Patwardhan, G. A., Gupta, V.*, et al.* **(2008)**. *A role for ceramide in driving cancer cell resistance to doxorubicin.* FASEB J 22(7): 2541-2551.

Loi, M., Marchio, S., Becherini, P., Di Paolo, D., Soster, M.*, et al.* **(2010)**. *Combined targeting of perivascular and endothelial tumor cells enhances anti-tumor efficacy of liposomal chemotherapy in neuroblastoma.* J Control Release 145(1): 66-73.

Lorusso, D., Di Stefano, A., Carone, V., Fagotti, A., Pisconti, S.*, et al.* **(2007)**. *Pegylated liposomal doxorubicin-related palmar-plantar erythrodysesthesia ('hand-foot' syndrome).* Ann Oncol 18(7): 1159-1164.

Maeda, H. **(2010)**. *Tumor-selective delivery of macromolecular drugs via the EPR effect: background and future prospects.* Bioconjug Chem 21(5): 797-802.

Maeda, H. and Matsumura, Y. **(2011)**. *EPR effect based drug design and clinical outlook for enhanced cancer chemotherapy.* Adv Drug Deliv Rev 63(3): 129-130.

Mansilla, S., Priebe, W. and Portugal, J. **(2006)**. *Mitotic catastrophe results in cell death by caspase-dependent and caspase-independent mechanisms.* Cell Cycle 5(1): 53-60.

Marcato, P., Dean, C. A., Pan, D., Araslanova, R., Gillis, M.*, et al.* **(2011)**. *Aldehyde dehydrogenase activity of breast cancer stem cells is primarily due to isoform ALDH1A3 and its expression is predictive of metastasis.* Stem Cells 29(1): 32-45.

Marjanovic, N. D., Weinberg, R. A. and Chaffer, C. L. **(2013)**. *Poised with purpose: Cell plasticity enhances tumorigenicity.* Cell Cycle 12(17).

Matsumura, Y., Gotoh, M., Muro, K., Yamada, Y., Shirao, K.*, et al.* **(2004)**. *Phase I and pharmacokinetic study of MCC-465, a doxorubicin (DXR) encapsulated in PEG immunoliposome, in patients with metastatic stomach cancer.* Ann Oncol 15(3): 517-525.

Matsumura, Y. and Maeda, H. **(1986)**. *A new concept for macromolecular therapeutics in cancer chemotherapy: mechanism of tumoritropic accumulation of proteins and the antitumor agent smancs.* Cancer Res 46(12 Pt 1): 6387-6392.

Mayer, L. D., Harasym, T. O., Tardi, P. G., Harasym, N. L., Shew, C. R.*, et al.* **(2006)**. *Ratiometric dosing of anticancer drug combinations: controlling drug ratios after systemic administration regulates therapeutic activity in tumor-bearing mice.* Mol Cancer Ther 5(7): 1854-1863.

Mayer, L. D. and Janoff, A. S. **(2007)**. *Optimizing combination chemotherapy by controlling drug ratios.* Mol Interv 7(4): 216-223.

Melero-Martin, J. M. and Dudley, A. C. **(2011)**. *Concise review: Vascular stem cells and tumor angiogenesis.* Stem Cells 29(2): 163-168.

Miller, M. L. and Ojima, I. **(2001)**. *Chemistry and chemical biology of taxane anticancer agents.* Chem Rec 1(3): 195-211.

Minotti, G., Menna, P., Salvatorelli, E., Cairo, G. and Gianni, L. **(2004)**. *Anthracyclines: molecular advances and pharmacologic developments in antitumor activity and cardiotoxicity.* Pharmacol Rev 56(2): 185-229.

Montana, M., Ducros, C., Verhaeghe, P., Terme, T., Vanelle, P.*, et al.* **(2011)**. *Albumin-bound paclitaxel: the benefit of this new formulation in the treatment of various cancers.* J Chemother 23(2): 59-66.

Morad, S. A., Madigan, J. P., Levin, J. C., Abdelmageed, N., Karimi, R.*, et al.* **(2013)**. *Tamoxifen magnifies therapeutic impact of ceramide in human colorectal cancer cells independent of p53.* Biochem Pharmacol 85(8): 1057-1065.

Moreira, J. N., Ishida, T., Gaspar, R. and Allen, T. M. **(2002)**. *Use of the post-insertion technique to insert peptide ligands into pre-formed stealth liposomes with retention of binding activity and cytotoxicity.* Pharm Res 19(3): 265-269.

Morimoto, K., Kim, S. J., Tanei, T., Shimazu, K., Tanji, Y.*, et al.* **(2009)**. *Stem cell marker aldehyde dehydrogenase 1-positive breast cancers are characterized by negative estrogen receptor, positive human epidermal growth factor receptor type 2, and high Ki67 expression.* Cancer Sci 100(6): 1062-1068.

Moura, V., Lacerda, M., Figueiredo, P., Corvo, M. L., Cruz, M. E.*, et al.* **(2012)**. *Targeted and intracellular triggered delivery of therapeutics to cancer cells and the tumor microenvironment: impact on the treatment of breast cancer.* Breast Cancer Res Treat 133(1): 61-73.

Nagamatsu, I., Onishi, H., Matsushita, S., Kubo, M., Kai, M.*, et al.* **(2014)**. *NOTCH4 Is a Potential Therapeutic Target for Triple-negative Breast Cancer.* Anticancer Research 34(1A): 69-80.

Nagata, T., Shimada, Y., Sekine, S., Hori, R., Matsui, K.*, et al.* **(2014)**. *Prognostic significance of NANOG and KLF4 for breast cancer.* Breast Cancer 21(1): 96-101.

Needham, D., Anyarambhatla, G., Kong, G. and Dewhirst, M. W. **(2000)**. *A new temperature-sensitive liposome for use with mild hyperthermia: characterization and testing in a human tumor xenograft model.* Cancer Res 60(5): 1197-1201.

Needham, D. and Dewhirst, M. W. **(2001)**. *The development and testing of a new temperature-sensitive drug delivery system for the treatment of solid tumors.* Adv Drug Deliv Rev 53(3): 285-305.

Nishi, M., Sakai, Y., Akutsu, H., Nagashima, Y., Quinn, G.*, et al.* **(2013)**. *Induction of cells with cancer stem cell properties from nontumorigenic human mammary epithelial cells by defined reprogramming factors.* Oncogene.

Niwa, H., Burdon, T., Chambers, I. and Smith, A. **(1998)**. *Self-renewal of pluripotent embryonic stem cells is mediated via activation of STAT3.* Genes & Development 12(13): 2048-2060.

Noda, K., Nishiwaki, Y., Kawahara, M., Negoro, S., Sugiura, T.*, et al.* **(2002)**. *Irinotecan plus cisplatin compared with etoposide plus cisplatin for extensive small-cell lung cancer.* N Engl J Med 346(2): 85-91.

O'Brien, M. E., Wigler, N., Inbar, M., Rosso, R., Grischke, E.*, et al.* **(2004)**. *Reduced cardiotoxicity and comparable efficacy in a phase III trial of pegylated liposomal doxorubicin HCl (CAELYX/ Doxil) versus conventional doxorubicin for first-line treatment of metastatic breast cancer.* Ann Oncol 15(3): 440-449.

Ohtsuka, M., Ishii, K., Kikuti, Y. Y., Warita, T., Suzuki, D.*, et al.* **(2006)**. *Construction of Mouse 129/ Ola BAC Library for Targeting Experiments Using E14 Embryonic Stem Cells.* Genes & Genetic Systems 81(2): 143-146.

Pan, G. and Thomson, J. A. **(2007)**. *Nanog and transcriptional networks in embryonic stem cell pluripotency.* Cell Res 17(1): 42-49.

Papahadjopoulos, D., Allen, T. M., Gabizon, A., Mayhew, E., Matthay, K.*, et al.* **(1991)**. *Sterically stabilized liposomes: improvements in pharmacokinetics and antitumor therapeutic efficacy.* Proc Natl Acad Sci U S A 88(24): 11460-11464.

Pastorino, F., Brignole, C., Loi, M., Di Paolo, D., Di Fiore, A.*, et al.* **(2013)**. *Nanocarrier-mediated targeting of tumor and tumor vascular cells improves uptake and penetration of drugs into neuroblastoma.* Front Oncol 3: 190.

Peer, D., Karp, J. M., Hong, S., Farokhzad, O. C., Margalit, R.*, et al.* **(2007)**. *Nanocarriers as an emerging platform for cancer therapy.* Nat Nanotechnol 2(12): 751-760.

Pesarrodona, M., Ferrer-Miralles, N., Unzueta, U., Gener, P., Tatkiewicz, W.*, et al.* **(2014)**. *Intracellular targeting of CD44 cells with self-assembling, protein only nanoparticles.* Int J Pharm 473(1-2): 286-295.

Petre, C. E. and Dittmer, D. P. **(2007)**. *Liposomal daunorubicin as treatment for Kaposi's sarcoma.* Int J Nanomedicine 2(3): 277-288.

Pinto, A. C., Moreira, J. N. and Simoes, S. **(2011)**. *Liposomal imatinib-mitoxantrone combination: formulation development and therapeutic evaluation in an animal model of prostate cancer.* Prostate 71(1): 81-90.

Poon, R. T. and Borys, N. **(2011)**. *Lyso-thermosensitive liposomal doxorubicin: an adjuvant to increase the cure rate of radiofrequency ablation in liver cancer.* Future Oncol 7(8): 937-945.

Porkka, K., Laakkonen, P., Hoffman, J. A., Bernasconi, M. and Ruoslahti, E. **(2002)**. *A fragment of the HMGN2 protein homes to the nuclei of tumor cells and tumor endothelial cells in vivo.* Proc Natl Acad Sci U S A 99(11): 7444-7449.

Prabhakar, U., Maeda, H., Jain, R. K., Sevick-Muraca, E. M., Zamboni, W.*, et al.* **(2013)**. *Challenges and key considerations of the enhanced permeability and retention effect for nanomedicine drug delivery in oncology.* Cancer Res 73(8): 2412-2417.

Quintana, E., Shackleton, M., Sabel, M. S., Fullen, D. R., Johnson, T. M.*, et al.* **(2008)**. *Efficient tumour formation by single human melanoma cells.* Nature 456(7222): 593-598.

Radzisheuskaya, A., Chia Gle, B., dos Santos, R. L., Theunissen, T. W., Castro, L. F.*, et al.* **(2013)**. *A defined Oct4 level governs cell state transitions of pluripotency entry and differentiation into all embryonic lineages.* Nat Cell Biol 15(6): 579-590.

Rae, J. M., Creighton, C. J., Meck, J. M., Haddad, B. R. and Johnson, M. D. **(2007)**. *MDA-MB-435 cells are derived from M14 melanoma cells--a loss for breast cancer, but a boon for melanoma research.* Breast Cancer Res Treat 104(1): 13-19.

Ramaswamy, S. **(2007)**. *Rational design of cancer-drug combinations.* N Engl J Med 357(3): 299-300.

Ranganathan, R., Madanmohan, S., Kesavan, A., Baskar, G., Krishnamoorthy, Y. R.*, et al.* **(2012)**. *Nanomedicine: towards development of patient-friendly drug-delivery systems for oncological applications.* Int J Nanomedicine 7: 1043-1060.

Reya, T., Morrison, S. J., Clarke, M. F. and Weissman, I. L. **(2001)**. *Stem cells, cancer, and cancer stem cells.* Nature 414(6859): 105-111.

Reyes-Reyes, E. M., Teng, Y. and Bates, P. J. **(2010)**. *A new paradigm for aptamer therapeutic AS1411 action: uptake by macropinocytosis and its stimulation by a nucleolin-dependent mechanism.* Cancer Res 70(21): 8617-8629.

Reynolds, J. G., Geretti, E., Hendriks, B. S., Lee, H., Leonard, S. C.*, et al.* **(2012)**. *HER2-targeted liposomal doxorubicin displays enhanced anti-tumorigenic effects without associated cardiotoxicity.* Toxicol Appl Pharmacol 262(1): 1-10.

Ricardo, S., Vieira, A. F., Gerhard, R., Leitao, D., Pinto, R.*, et al.* **(2011)**. *Breast cancer stem cell markers CD44, CD24 and ALDH1: expression distribution within intrinsic molecular subtype.* J Clin Pathol 64(11): 7.

Rios, A. C., Fu, N. Y., Lindeman, G. J. and Visvader, J. E. **(2014)**. *In situ identification of bipotent stem cells in the mammary gland.* Nature 506(7488): 322-327.

Saeki, T., Tsuruo, T., Sato, W. and Nishikawsa, K. **(2005)**. *Drug resistance in chemotherapy for breast cancer.* Cancer Chemother Pharmacol 56 Suppl 1: 84-89.

Santos, A., Sarmento-Ribeiro, A. B., de Lima, M. C., Simoes, S. and Moreira, J. N. **(2008)**. *Simultaneous evaluation of viability and Bcl-2 in small-cell lung cancer.* Cytometry A 73A(12): 1165-1172.

Sapra, P. and Allen, T. M. **(2003)**. *Ligand-targeted liposomal anticancer drugs.* Prog Lipid Res 42(5): 439-462.

Scheel, C. and Weinberg, R. A. **(2012)**. *Cancer stem cells and epithelial-mesenchymal transition: concepts and molecular links.* Semin Cancer Biol 22(5-6): 396-403.

Schepers, A. G., Snippert, H. J., Stange, D. E., van den Born, M., van Es, J. H.*, et al.* **(2012)**. *Lineage Tracing Reveals Lgr5+ Stem Cell Activity in Mouse Intestinal Adenomas.* Science.

Schmitt, F., Ricardo, S., Vieira, A. F., Dionisio, M. R. and Paredes, J. **(2012)**. *Cancer stem cell markers*

in breast neoplasias: their relevance and distribution in distinct molecular subtypes. Virchows Arch 460(6): 545-553.

Schroeder, A., Heller, D. A., Winslow, M. M., Dahlman, J. E., Pratt, G. W.*, et al.* **(2012)**. *Treating metastatic cancer with nanotechnology.* Nat Rev Cancer 12(1): 39-50.

Schuijers, J. and Clevers, H. **(2012)**. *Adult mammalian stem cells: the role of Wnt, Lgr5 and R-spondins.* EMBO J 31(12): 2685-2696.

Seveno, C., Loussouarn, D., Brechet, S., Campone, M., Juin, P.*, et al.* **(2012)**. *gamma-Secretase inhibition promotes cell death, Noxa upregulation, and sensitization to BH3 mimetic ABT-737 in human breast cancer cells.* Breast Cancer Res 14(3): R96.

Shaw, F. L., Harrison, H., Spence, K., Ablett, M. P., Simoes, B. M.*, et al.* **(2012)**. *A detailed mammosphere assay protocol for the quantification of breast stem cell activity.* J Mammary Gland Biol Neoplasia 17(2): 111-117.

Shi, H., Huang, Y., Zhou, H., Song, X., Yuan, S.*, et al.* **(2007)**. *Nucleolin is a receptor that mediates antiangiogenic and antitumor activity of endostatin.* Blood 110(8): 2899-2906.

Shi, J., Xiao, Z., Kamaly, N. and Farokhzad, O. C. **(2011)**. *Self-assembled targeted nanoparticles: evolution of technologies and bench to bedside translation.* Acc Chem Res 44(10): 1123-1134.

Shuen, A. Y. and Foulkes, W. D. **(2011)**. *Inherited mutations in breast cancer genes--risk and response.* J Mammary Gland Biol Neoplasia 16(1): 3-15.

Siegel, R., Naishadham, D. and Jemal, A. **(2013)**. *Cancer statistics, 2013.* CA Cancer J Clin 63(1): 11-30.

Simoes, S., Moreira, J. N., Fonseca, C., Duzgunes, N. and de Lima, M. C. **(2004)**. *On the formulation of pH-sensitive liposomes with long circulation times.* Adv Drug Deliv Rev 56(7): 947-965.

Singh, A. and Settleman, J. **(2010)**. *EMT, cancer stem cells and drug resistance: an emerging axis of evil in the war on cancer.* Oncogene 29(34): 4741-4751.

Siskind, L. J. **(2005)**. *Mitochondrial ceramide and the induction of apoptosis.* J Bioenerg Biomembr 37(3): 143-153.

Siskind, L. J. and Colombini, M. **(2000)**. *The lipids C2- and C16-ceramide form large stable channels. Implications for apoptosis.* J Biol Chem 275(49): 38640-38644.

Siskind, L. J., Feinstein, L., Yu, T., Davis, J. S., Jones, D.*, et al.* **(2008)**. *Anti-apoptotic Bcl-2 Family Proteins Disassemble Ceramide Channels.* J Biol Chem 283(11): 6622-6630.

Siskind, L. J., Kolesnick, R. N. and Colombini, M. **(2002)**. *Ceramide channels increase the permeability of the mitochondrial outer membrane to small proteins.* J Biol Chem 277(30): 26796-26803.

Siskind, L. J., Kolesnick, R. N. and Colombini, M. **(2006)**. *Ceramide forms channels in mitochondrial outer membranes at physiologically relevant concentrations.* Mitochondrion 6(3): 118-125.

Siskind, L. J., Mullen, T. D., Romero Rosales, K., Clarke, C. J., Hernandez-Corbacho, M. J.*, et al.* **(2010)**. *The BCL-2 protein BAK is required for long-chain ceramide generation during apoptosis.* J Biol Chem 285(16): 11818-11826.

Snippert, H. J., van der Flier, L. G., Sato, T., van Es, J. H., van den Born, M.*, et al.* **(2010)**. *Intestinal crypt homeostasis results from neutral competition between symmetrically dividing Lgr5 stem cells.* Cell 143(1): 134-144.

Srivastava, M. and Pollard, H. B. **(1999)**. *Molecular dissection of nucleolin's role in growth and cell proliferation: new insights.* FASEB J 13(14): 1911-1922.

Stadtfeld, M. and Hochedlinger, K. **(2010)**. *Induced pluripotency: history, mechanisms, and applications.* Genes Dev 24(20): 2239-2263.

Storck, S., Shukla, M., Dimitrov, S. and Bouvet, P. **(2007)**. *Functions of the histone chaperone nucleolin in diseases.* Subcell Biochem 41: 125-144.

Stover, T. and Kester, M. **(2003)**. *Liposomal delivery enhances short-chain ceramide-induced apoptosis of breast cancer cells.* J Pharmacol Exp Ther 307(2): 468-475.

Stover, T. C., Sharma, A., Robertson, G. P. and Kester, M. **(2005)**. *Systemic delivery of liposomal short-chain ceramide limits solid tumor growth in murine models of breast adenocarcinoma.* Clin Cancer Res 11(9): 3465-3474.

Stuart, H. T., van Oosten, A. L., Radzisheuskaya, A., Martello, G., Miller, A.*, et al.* **(2014)**. *NANOG amplifies STAT3 activation and they synergistically induce the naive pluripotent program.* Curr Biol 24(3): 340-346.

Stuelten, C. H., Mertins, S. D., Busch, J. I., Gowens, M., Scudiero, D. A.*, et al.* **(2010)**. *Complex display of putative tumor stem cell markers in the NCI60 tumor cell line panel.* Stem Cells 28(4): 649-660.

Suman, S., Das, T. P. and Damodaran, C. **(2013)**. *Silencing NOTCH signaling causes growth arrest in both breast cancer stem cells and breast cancer cells.* Br J Cancer 109(10): 2587-2596.

Suzuki, R., Takizawa, T., Kuwata, Y., Mutoh, M., Ishiguro, N.*, et al.* **(2008)**. *Effective anti-tumor activity of oxaliplatin encapsulated in transferrin-PEG-liposome.* Int J Pharm 346(1-2): 143-150.

Swaminathan, S. K., Roger, E., Toti, U., Niu, L., Ohlfest, J. R.*, et al.* **(2013)**. *CD133-targeted paclitaxel delivery inhibits local tumor recurrence in a mouse model of breast cancer.* J Control Release 171(3): 280-287.

Swenson, C. E., Bolcsak, L. E., Batist, G., Guthrie, T. H., Jr., Tkaczuk, K. H.*, et al.* **(2003)**. *Pharmacokinetics of doxorubicin administered i.v. as Myocet (TLC D-99; liposome-encapsulated doxorubicin citrate) compared with conventional doxorubicin when given in combination with cyclophosphamide in patients with metastatic breast cancer.* Anticancer Drugs 14(3): 239-246.

Takahashi, K., Tanabe, K., Ohnuki, M., Narita, M., Ichisaka, T.*, et al.* **(2007)**. *Induction of pluripotent stem cells from adult human fibroblasts by defined factors.* Cell 131(5): 861-872.

Takahashi, K. and Yamanaka, S. **(2006)**. *Induction of pluripotent stem cells from mouse embryonic and adult fibroblast cultures by defined factors.* Cell 126(4): 663-676.

Takebe, N., Harris, P. J., Warren, R. Q. and Ivy, S. P. **(2011)**. *Targeting cancer stem cells by inhibiting Wnt, Notch, and Hedgehog pathways.* Nat Rev Clin Oncol 8(2): 97-106.

Tardi, P., Johnstone, S., Harasym, N., Xie, S., Harasym, T.*, et al.* **(2009a)**. *In vivo maintenance of synergistic cytarabine:daunorubicin ratios greatly enhances therapeutic efficacy.* Leuk Res 33(1): 129-139.

Tardi, P. G., Dos Santos, N., Harasym, T. O., Johnstone, S. A., Zisman, N.*, et al.* **(2009b)**. *Drug ratio-dependent antitumor activity of irinotecan and cisplatin combinations in vitro and in vivo.* Mol Cancer Ther 8(8): 2266-2275.

Thomas, D. A., Kantarjian, H. M., Stock, W., Heffner, L. T., Faderl, S.*, et al.* **(2009)**. *Phase 1 multicenter study of vincristine sulfate liposomes injection and dexamethasone in adults with relapsed or refractory acute lymphoblastic leukemia.* Cancer 115(23): 5490-5498.

Thomas, D. A., Sarris, A. H., Cortes, J., Faderl, S., O'Brien, S.*, et al.* **(2006)**. *Phase II study of sphingosomal vincristine in patients with recurrent or refractory adult acute lymphocytic leukemia.* Cancer 106(1): 120-127.

Thomson, J. A., Itskovitz-Eldor, J., Shapiro, S. S., Waknitz, M. A., Swiergiel, J. J.*, et al.* **(1998)**. *Embryonic stem cell lines derived from human blastocysts.* Science 282(5391): 1145-1147.

Tonnesen, M. G., Feng, X. and Clark, R. A. **(2000)**. *Angiogenesis in wound healing.* J Investig Dermatol Symp Proc 5(1): 40-46.

Tran, M. A., Smith, C. D., Kester, M. and Robertson, G. P. **(2008)**. *Combining nanoliposomal ceramide with sorafenib synergistically inhibits melanoma and breast cancer cell survival to decrease tumor development.* Clin Cancer Res 14(11): 3571-3581.

Uchida, Y., Itoh, M., Taguchi, Y., Yamaoka, S., Umehara, H.*, et al.* **(2004)**. *Ceramide reduction and transcriptional up-regulation of glucosylceramide synthase through doxorubicin-activated Sp1 in drug-resistant HL-60/ADR cells.* Cancer Res 64(17): 6271-6279.

Ugrinova, I., Monier, K., Ivaldi, C., Thiry, M., Storck, S.*, et al.* **(2007)**. *Inactivation of nucleolin leads to nucleolar disruption, cell cycle arrest and defects in centrosome duplication.* BMC Mol Biol 8: 66.

Vallier, L., Mendjan, S., Brown, S., Chng, Z., Teo, A.*, et al.* **(2009)**. *Activin/Nodal signalling maintains pluripotency by controlling Nanog expression.* Development 136(8): 1339-1349.

Van Pham, P., Vu, N. B., Duong, T. T., Nguyen, T. T., Truong, N. H.*, et al.* **(2012)**. *Suppression of human breast tumors in NOD/SCID mice by CD44 shRNA gene therapy combined with doxorubicin treatment.* Onco Targets Ther 5: 77-84.

van Vlerken, L. E., Duan, Z., Seiden, M. V. and Amiji, M. M. **(2007)**. *Modulation of intracellular ceramide using polymeric nanoparticles to overcome multidrug resistance in cancer.* Cancer Res 67(10): 4843-4850.

Vares, G., Cui, X., Wang, B., Nakajima, T. and Nenoi, M. **(2013)**. *Generation of breast cancer stem cells by steroid hormones in irradiated human mammary cell lines.* PLoS One 8(10): e77124.

Varum, S., Rodrigues, A. S., Moura, M. B., Momcilovic, O., Easley, C. A. t.*, et al.* **(2011)**. *Energy metabolism in human pluripotent stem cells and their differentiated counterparts.* PLoS One 6(6): e20914.

Vazquez-Martin, A., Lopez-Bonetc, E., Cufi, S., Oliveras-Ferraros, C., Del Barco, S.*, et al.* **(2011)**. *Repositioning chloroquine and metformin to eliminate cancer stem cell traits in pre-malignant lesions.* Drug Resist Updat.

Visvader, J. E. **(2011)**. *Cells of origin in cancer.* Nature 469(7330): 314-322.

Visvader, J. E. and Lindeman, G. J. **(2008)**. *Cancer stem cells in solid tumours: accumulating evidence and unresolved questions.* Nat Rev Cancer 8(10): 755-768.

Visvader, J. E. and Lindeman, G. J. **(2012)**. *Cancer stem cells: current status and evolving complexities.* Cell Stem Cell 10(6): 717-728.

Wakayama, T., Rodriguez, I., Perry, A. C. F., Yanagimachi, R. and Mombaerts, P. **(1999)**. *Mice cloned from embryonic stem cells.* Proceedings of the National Academy of Sciences 96(26): 14984-14989.

Wang, A. Z., Langer, R. and Farokhzad, O. C. **(2012)**. *Nanoparticle delivery of cancer drugs.* Annu Rev Med 63: 185-198.

Welti, J., Loges, S., Dimmeler, S. and Carmeliet, P. **(2013)**. *Recent molecular discoveries in angiogenesis and antiangiogenic therapies in cancer.* J Clin Invest 123(8): 3190-3200.

Xu, L., Tang, W. H., Huang, C. C., Alexander, W., Xiang, L. M.*, et al.* **(2001)**. *Systemic p53 gene therapy of cancer with immunolipoplexes targeted by anti-transferrin receptor scFv.* Mol Med 7(10): 723-734.

Yang, A., Shi, G., Zhou, C., Lu, R., Li, H.*, et al.* **(2011)**. *Nucleolin maintains embryonic stem cell self-renewal by suppression of p53 protein-dependent pathway.* J Biol Chem 286(50): 43370-43382.

Yuan, F., Dellian, M., Fukumura, D., Leunig, M., Berk, D. A.*, et al.* **(1995)**. *Vascular permeability in a human tumor xenograft: molecular size dependence and cutoff size.* Cancer Res 55(17): 3752-3756.

Zhou, J., Wulfkuhle, J., Zhang, H., Gu, P., Yang, Y.*, et al.* **(2007)**. *Activation of the PTEN/mTOR/STAT3 pathway in breast cancer stem-like cells is required for viability and maintenance.* Proc Natl Acad Sci U S A 104(41): 16158-16163.

Zhuo, W., Luo, C., Wang, X., Song, X., Fu, Y.*, et al.* **(2010)**. *Endostatin inhibits tumour lymphangiogenesis and lymphatic metastasis via cell surface nucleolin on lymphangiogenic endothelial cells.* J Pathol 222(3): 249-260.

Zucker, D., Marcus, D., Barenholz, Y. and Goldblum, A. **(2009)**. *Liposome drugs' loading efficiency: A working model based on loading conditions and drug's physicochemical properties.* J Control Release.